# Prescribed fire in grassland butterfly habitat: targeting weather and fuel conditions to reduce risk to larvae and enhance post-burn habitat heterogeneity

Kathryn Courtney Hill

A thesis

submitted in partial fulfillment of the

requirements for the degree of

Master of Science

University of Washington

2015

Committee:

Jonathan D. Bakker, Chair

Peter W. Dunwiddie

Charles B. Halpern

Sarah T. Hamman

Program Authorized to Offer Degree:

School of Environmental and Forest Sciences

University of Washington

## Abstract

Prescribed fire in grassland butterfly habitat: targeting weather and fuel conditions to reduce risk to larvae and enhance post-burn habitat heterogeneity

Kathryn Courtney Hill

Chair of the Supervisory Committee:
Associate Professor Jonathan D. Bakker
School of Environmental and Forest Sciences

Prescribed burning is one of the primary tools used for habitat restoration in the fire-adapted prairies of the Pacific Northwest. Concerns about detrimental effects of burning on butterfly populations, however, can inhibit implementation of treatments. Burning in cool and humid conditions is likely to produce low-severity patches and result in lowered soil temperatures, which can be critical to survival of butterfly larvae. With these burning conditions, it may also be possible to enhance the heterogeneity of butterfly habitat, and thus achieve a secondary objective. In this study, twenty experimental plots were burned across a wide range of weather and fuel conditions to address the potential for meeting these two objectives. Overall risk to diapausing butterfly larvae – assessed by measuring subsurface soil temperatures and heat dosages – was lower when air temperature was less than 26 $^{o}$C, dead fuel moisture was greater than 8%, and relative humidity was higher than 54%, providing threshold recommendations for

habitat management using prescribed fire. Targeting moister burning conditions to leave some unburned or low-severity patches that can serve as insect refugia required at least a small amount of pre-existing fuel discontinuity. Post-burn habitat composition and structure were also influenced by burning conditions. In the first growing season post-burn, species richness increased slightly more when burns had occurred in mid-summer vs. late summer. Ordinations showed shifts in plant composition from perennials towards annuals, with somewhat larger shifts for plots burned in the afternoon. Geospatial analysis was used to assess the heterogeneity of vegetation height structure, which can help to buffer insect populations by producing fine-scale variability in thermal heat loading at ground level and providing a range of microclimates. This structural heterogeneity and microclimate availability increased following morning burns conducted in higher dead fuel moistures, and when burns occurred in little to no wind, highlighting the linkages between fuel continuity, fire spread, and vegetation response. This research provides regional recommendations for burning in sensitive butterfly habitat and contributes to a greater understanding of how fuel moisture and continuity during grassland burning can affect fine-scale heterogeneity of vegetation structure and microhabitat availability.

## TABLE OF CONTENTS

**List of Figures** ..... **iii**

**List of Tables** ..... **v**

**Acknowledgements** ..... **vi**

**Chapter 1: Effects of weather and fuel conditions during prescribed fires on burn severity, subsurface temperatures and heat dosage in South Puget Sound prairies** ..... **1**

**Introduction** ..... **1**

**Methods** ..... **3**

*Study Sites* ..... *3*

*Experimental Design* ..... *4*

*Prescribed Fires and Data Collection* ..... *5*

*Statistical Analysis* ..... *8*

**Results** ..... **10**

**Discussion** ..... **13**

**Figures** ..... **19**

**Tables** ..... **26**

**Chapter 2: Effects of weather and fuel conditions during prescribed fires on post-burn vegetation structure and composition in South Puget Sound prairies** ..... **29**

**Introduction** ..... **29**

**Methods** ..... **31**

*Study Sites* ..... *31*

*Experimental Design* ..... *32*

*Prescribed Fires and Fuels Data Collection* ..... *34*

*Vegetation Data Collection* ..... *36*

*Statistical Analysis* ..... *37*

Species diversity and composition ..... 39

Vegetation structure ..... 41

**Results** ..... **45**

Species diversity and composition ..... 45

Vegetation structure ..... 47

**Discussion** ..... **48**

**Figures** ..... **56**

**Tables** ..... **66**

**Literature Cited** ..... **67**

**Appendix A: Region and research plot maps for JBLM & Thurston County, WA** ..... **75**

**Appendix B: Sampling plot design** ..... **76**

**Appendix C: 'R' code used for all analyses** ..... **77**

**Appendix D: Burn weather and fuel data for each plot** ..... **85**

**Appendix E: Measured dead fuel moisture vs. fuel modeling tables** ..... **86**

**Appendix F: Data summary tables..... 87**
**Appendix G: Species list over all plots sampled for composition..... 91**
**Appendix H: Stresses for NMDS ordinations ..... 95**
**Appendix I: Semivariogram curves for vegetation height analysis..... 96**
**Appendix J: Semivariogram curves for bare or open ground analysis ..... 104**

**List of Figures**

Figure 1: Relationships of peak soil temperatures to air temperature and dead fuel moisture during a burn

Figure 2: Regression tree for quadrat-scale analysis of peak soil temperatures during a burn

Figure 3: Temperature-time duration curves for temperatures recorded by dataloggers within plots where a "100% lethal heat dosage" occurred during a burn

Figure 4: Box-and-whisker plot for the distribution of relative humidity during a burn based on whether a "100% lethal heat dosage" occurred

Figure 5: Regression tree for quadrat-scale analysis of total amount of "100% lethal heat dosage" occurring during a burn

Figure 6: Interaction plot for logit-transformed percent cover of unburned or low-severity areas within a plot as a function of percent bare or open ground and dead fuel moisture during a burn

Figure 7: Regression tree for quadrat-scale analysis of percent cover of unburned or low-severity areas

Figure 8: Schematic of different types of changes in heterogeneity and how they can be visually manifest

Figure 9: Change in species richness as a function of the Julian calendar day of burning

Figure 10: Change in Hill's $N_1$ diversity index as a function of pre-burn fuel loading

Figure 11: Bray-Curtis distance between pre- and post-burn species composition as a function of dead fuel moisture during a burn

Figure 12: Quadrat-scale Bray-Curtis distance between pre- and post-burn species composition as a function of relative humidity during a burn

Figure 13: Site-specific NMDS ordinations of pre- and post-burn species abundance data separated by time of burning (morning vs. afternoon)

Figure 14: NMDS ordination of pre- and post-burn functional group abundance data separated by time of burning (morning vs. afternoon)

Figure 15: Pre- to post-burn change in number of 2 cm height classes (under 30 cm) as a function of the Julian calendar day of burning

Figure 16: Box-and-whisker plot of the pre- to post-burn change in magnitude of spatial autocorrelation of vegetation height as a function of time of burning (morning vs. afternoon)

Figure 17: Pre- to post-burn change in magnitude of spatial autocorrelation of vegetation height as a function of dead fuel moisture during a burn

Figure 18: Pre- to post-burn change in Interspersion and Juxtaposition Index (IJI) of vegetation height as a function of wind speed during a burn

Figure 19: Post-burn percent cover of bare or open ground in a plot as a function of time of burning (morning vs. afternoon)

Figure 20: Pre- to post-burn change in coefficient of variation (CV) of litter depth as a function of air temperature during a burn

**List of Tables**

Table 1: Descriptions for substrate and vegetation severity classes, modified from the National Park Service Fire Monitoring Handbook

Table 2: Parameter estimates for multiple regression model of peak soil temperature as a function of air temperature and dead fuel moisture during a burn

Table 3: Split points and values for quadrat-scale regression tree analysis of peak soil temperatures during a burn

Table 4: Parameter estimates for Firth logistic regression model of "100%" lethal heat dosage" occurrence within a plot during a burn

Table 5: Split points and values for quadrat-scale regression tree analysis of total amount of "100% lethal heat dosage" occurring during a burn

Table 6: Parameter estimates for multiple regression model of logit-transformed percent cover of unburned or low-severity areas within a plot as a function of percent bare or open ground and dead fuel moisture during a burn

Table 7: Explanatory variables used in univariate multiple regression models for the given response variables in Chapter 2

**Acknowledgements**

I would like to thank my advisor, Jon Bakker, for always providing valuable advice and support throughout this process. I also thank my committee members, Peter Dunwiddie, Charlie Halpern, and Sarah Hamman, who each provided much insightful commentary and guidance during our meetings. My labmates in the Terrestrial Restoration Ecology Lab gave me a chance to bounce ideas around early on and let me be a part of some great ecology discussions at a certain pub in Ravenna. This research was funded by a National Science Foundation Graduate Research Fellowship under grant no. DGE-1256082. Both the Center for Natural Lands Management and Joint Base Lewis-McChord's Fish and Wildlife department also provided an enormous amount of resources, labor, and fire, fire, fire for this project. I am especially thankful to Mason McKinley and John Richardson for making this circus happen, and for making it fun. My colleague and friend Adam Martin has been the source of much insight and moral support along the way, while my good friends Allison Monat and Ralphie made life in Seattle much more bearable. Of course, my family has been supportive at each step and I thank them in every way possible. Finally, my husband (!) Chris Dinottia – otherwise known as the most patient person in the world – has been there for me through every up and down and has pulled me back from the edge more times than I can count; my thanks and love can not be expressed enough.

Dedicated to Neah.

# Chapter 1: Effects of weather and fuel conditions during prescribed fires on burn severity, subsurface temperatures and heat dosage in South Puget Sound prairies

## Introduction

Prescribed burning is one of the primary tools for habitat restoration in the fire-adapted prairies of the South Puget Sound region, as in many other grassland and shrubland ecosystems. Concerns about potentially detrimental effects of burning on current, newly introduced, or potential butterfly populations, however, can sometimes inhibit the implementation of consistent restoration treatments (Fimbel 2004; Hamman et al. 2011; Schultz et al. 2011). Conducting prescribed fires during cooler and more humid conditions is likely to leave a mosaic of unburned and low-severity patches and result in reduced soil temperatures, which can be important to survival of butterfly larvae that are in diapause during burning (Hamman et al. 2011; New 2014). By burning during these conditions, managers may be able to meet two separate habitat objectives: 1) leave critical unburned refuges for larvae in diapause and decrease overall risk from lethal temperatures (Bradstock et al. 2005); and 2) enhance aspects of vegetation structure considered desirable for butterfly habitat (e.g., variance in height and spatial dispersion of open cover; New 2014) in the post-burn growing season. This analysis focuses on the first objective through an assessment of response variables that evaluate overall risk to subsurface insects during prescribed fires.

Most studies that examine the effects of fire on insects do so by comparing abundance of species (or richness at higher taxonomic levels) pre- and post-treatment or in burned and unburned areas (Black et al. 2013), rather than quantifying insect thermal tolerance relative to

burn characteristics. Furthermore, most research on thermal tolerance is conducted in relation to control of agricultural or biological pests (Vermeire et al. 2004; New 2014).

Prairie and rangeland grasshoppers in North America are one notable exception to these generalities. Egg mortality has been studied in detail in relation to oviposition depth and associated temperatures during simulated burns of varying intensities (Branson and Vermeire 2007). Studies of several native and pest species generally conclude that only those with an oviposition depth of less than 1 cm would be susceptible to significant mortality from burning in areas of moderate fuel loads (Branson and Vermeire 2013). Specific temperature-depth-mortality models for the larval life stage are lacking for most butterfly species in Pacific Northwest prairies, although Schultz and Crone (1998) found significantly higher larval survivorship of Fender's blue butterfly (*Icaricia icarioides fenderi*) in unburned than in burned areas. As most prescribed fire managers appreciate, however, burned and unburned comparisons can be highly variable depending on weather and fuel conditions (New 2014), and increasingly refined burning programs are able to target specific conditions to meet habitat objectives.

Studies on the effects of conditions that vary continuously on soil temperatures during burning mainly examine fuel characteristics (e.g., fuel load or continuity) rather than weather characteristics, which are generally studied by simply contrasting season of burn (i.e. spring vs. autumn; Cochrane and Delphey 2002; Vermeire et al. 2004). In grassland, shrubland, and desert fires, lower surface or subsurface soil temperatures have been found in open areas or 'canopy gaps' than in areas with higher fuel loads (Davis et al. 1989; Brooks 2002; Wright and Clarke 2008). In addition, interruptions of effective fuel continuity from physical trampling (Shea et al. 1996) or high fuel moisture (Knapp and Keeley 2006) can reduce potential for fire spread and lead to patchier burns, potentially increasing organism survival (Paquin and Coderre 1997).

In this study, I experimentally burned South Puget Sound prairie plots under varying weather and fuel conditions and measured soil temperatures and burn severity, with the following research objectives: 1) determine the significant predictors of maximum subsurface soil temperatures and heat dosages during prescribed fire; and 2) determine the significant predictors of the percent cover of unburned or low-severity areas following these prescribed fires. Both objectives were intended to provide guidance to managers who are burning in sensitive butterfly habitat and desire to reduce the overall risk of larval mortality.

## Methods

### *Study Sites*

Study sites were in existing South Puget Sound prairie remnants on land owned by Joint Base Lewis-McChord (JBLM), Thurston County, and The Nature Conservancy (Appendix A). All of these areas are undergoing active restoration management, including regular prescribed fires. Historically, these prairies were maintained through several thousand years of anthropogenic burning by Native Americans, and thus have developed fire-adapted plant communities (Storm and Shebitz 2006). Ten prescribed burn units (Appendix A) were selected based on ease of access, feasibility for conducting research burns, similarity of burn history (1 – 2 burns at a 2 – 3 year frequency), and potential for butterfly habitat.

Eight burn units were located on JBLM land (47.0873º Latitude, -122.5707 Longitude) that is owned by the Department of Defense and managed in partnership with the Center for Natural Lands Management. Soils at these sites are a Spanaway gravelly sandy loam (NRCS 2015). A ninth burn unit was located on the Black River-Mima Prairie Glacial Heritage Preserve (GHP; 46.8658º Latitude, -123.0411º Longitude), a 459-ha preserve owned by Thurston County and

managed by the Center for Natural Lands Management. Soils are a well-drained mix of a Spanaway-Nisqually complex of gravelly sandy loam and loamy fine sand with Sultan silt loam (NRCS 2015). The tenth burn unit was located at Tenalquot Prairie (TQ; 46.9016º Latitude, -122.7309 Longitude), a 28-ha preserve owned by The Nature Conservancy and managed by the Center for Natural Lands Management. Soils are a Spanaway gravelly sandy loam (NRCS 2015). Vegetation on all ten burn units was generally short-statured bunchgrass prairie in various stages of restoration to native dominance; invasive species such as *Cytisus scoparius* (Scotch broom) were largely removed or limited in distribution on most sites.

From July to September (the primary prescribed fire season) 2014 at the nearest RAWS weather station in Chehalis, Washington, average air temperature ranged from 16.8 to 19.8ºC and average relative humidity (RH) ranged from 66.6 to 72.2%. Annual precipitation from 2004 to 2014 averaged 1117.8 mm, with an average for July – September of 79.4 mm (WRCC 2015).

*Experimental Design*

A pair of 26 x 37 m plots was placed within each of the ten burn units, for a total of twenty plots ($n$ = 20). For each pair in a given burn unit, plots were placed no more than 25 m apart to minimize potential variability in fuel loading or fuel type. Each plot was at least 20 m from the nearest road and at least 10 m from a mowed firebreak, which served as a control line during the burns.

Sampling quadrats within each plot were a subset of a larger project that used a layout designed for spatial analysis (see Chapter 2 and Appendix B). For this study, each plot contained 14 evenly spaced sampling quadrats arranged along 7 line transects (Appendix B; shaded quadrats). Transects were 26 m in length, spaced in a one-cycle 7/37 cyclic design (i.e., oriented

perpendicular to a 37-m baseline from the 0-, 1-, 6-, 10-, 17-, 23-, and 35-m marks). Along each transect, two 1-$m^2$ quadrats were spaced 13 m apart, with corners placed at either the 3- and 16-marks, or the 9- and 22-m marks, alternating for each consecutive transect (Appendix B; shaded quadrats). Each quadrat was further subdivided into sixteen 25 x 25 cm sub-quadrats; of these, seven were designated for assessing vegetation height, cover of bare or open ground, and burn severity (Appendix B; shaded sub-quadrats).

*Prescribed Fires and Data Collection*

Prescribed burns in all plots were conducted between 22 July and 22 September 2014, during the main prescribed fire season in this region (Hamman et al. 2011). To ensure data collection over a wide range of weather and fuel conditions, paired plots were burned either during relatively cool and humid morning hours or generally warmer and drier afternoon hours. To control for the potential confounding of time of year on fire behavior, both plots within a pair were burned on the same day (for most burn units). Due to logistical constraints, plots in two of the ten units were burned four days apart, during which there was little change in weather conditions or plant phenology.

Fuel loading was estimated from vegetation structural measurements in all quadrats prior to burning. Within each quadrat, seven 25 x 25 cm "sub-quadrats" were designated (Appendix B); a single estimate of total plant cover was assessed within this area. Height class, or herbaceous fuelbed depth, was visually assessed (at 10 cm resolution) using a meter stick at the corner of each quadrat. Height class, cover, and bulk density were used to estimate fuel loading (or biomass) in each quadrat with the equation $B = H * C * BD$, where B is biomass ($kg/m^2$), H is height-class midpoint (m), C is the total plant cover proportion in the seven sub-quadrats, and

BD is bulk density (approximated as 1.23 kg/$m^3$; Burgan and Rothermel 1984). Cover of bare or open ground was also assessed in each sub-quadrat (see Chapter 2), and the total percentage calculated at the plot scale. This cover category included open areas of bare ground, litter, rock, moss, and very low-statured (< 2 cm) vegetation, with minimal overhang of neighboring vegetation, and represented areas of low fuel continuity that could potentially inhibit fire spread.

An estimate of live fuel moisture within each quadrat was obtained prior to burning through visual assessment of the percent curing of the two main growth forms, grasses and forbs, using a modification of the Guide to Grassland Curing (NOAA 2008) that is based primarily on color and seed head formation. Percent curing of each growth form was then converted to a live fuel moisture percentage using standard fuel modeling tables (Scott and Burgan 2005).

Dead fuel moisture was estimated for each quadrat using a 1-hr fuel moisture stick made of small packets of straw ~12 cm in length tied with a plastic zip tie. At least 12 hr prior to burning, a packet was placed 10 cm outside of each quadrat and secured at ground level with a lawn staple. Immediately prior to ignition of each plot, the straw packets were removed and placed in airtight Whirlpaks; these were subsequently weighed, opened, and placed in a 60$^o$C drying oven for 48 hr and re-weighed. After correcting for the weight of the Whirlpak and zip tie, dead fuel moisture (% moisture content) was calculated as ([wet weight – dry weight] * 100) / dry weight (Pollet and Brown 2007). In three plots, dead fuel moisture was >30% due to excess rainwater or dew on the straw packets; for these cases, a value of 30% was used in the analyses, in accordance with fuel moisture models for dead fuels (Scott and Burgan 2005).

As the straw packets were removed from each quadrat directly prior to burning, an extended-range EL-USB-1-PRO temperature datalogger (Lascar Electronics Ltd. 2012) was buried in the same location, ~1 cm below the soil surface. Litter depth (cm) was recorded at each of these

locations. Each datalogger recorded the subsurface temperature (°C) every second from ignition time until all flames had self-extinguished. In two of the plots, dataloggers could not be used due to logistical problems, reducing the replication of soil temperature-based analyses to 18. In three plots where equipment melted under high heat, the number of functional dataloggers was reduced to 11 of 14 quadrats.

The type of ignition application was kept consistent across plots. To mimic the diversity of fire types (head, backing, and flanking) in both natural and prescribed burns, five point-source ignitions were applied in each plot within one minute of each other: one at the center and four along each half-diagonal of the rectangular plot, positioned halfway between the center and the corner (Appendix B). Drip torches were used to ignite the nearest fuel source using just enough fuel to light a circle of 50 cm in diameter. Mowed firebreaks surrounding the buffers of each plot were not lit until the nearest plot edge had completely burned, so that the behavior of the experimental plot fire was not influenced by interaction with the blackline fire ignited for control purposes.

Ambient air temperature (°C), relative humidity (%), and wind speed (m/s) were monitored during each burn using a Kestrel 4000 Weather Meter (Nielsen-Kellerman 2012), which was positioned 1.3 m above the ground on a tripod in a similar fuel type not more than 20 m from the edge of the plot. Each weather variable was recorded automatically every 30 seconds from ignition until all flames had self-extinguished.

Immediately following each prescribed fire, an assessment of burn severity was made at the 25 x 25 cm sub-quadrat scale within each quadrat. In each of the seven designated sub-quadrats (Appendix B), burn severity was scored visually using a modified version of the National Park Service Fire Effects Monitoring Handbook rating scale for vegetation in grassland fires (USDI

National Park Service 2003; Table 1). Values ranged from heavily (1), moderately (2), and lightly burned (3), to scorched (4) and unburned (5).

*Statistical Analysis*

I used generalized linear models to examine the plot-scale relationships of three response variables to weather and fuel conditions during the prescribed burns. Response variables were 1) the average maximum temperature reached at 1 cm depth; 2) whether or not a pre-defined 'lethal heat dosage' was reached; and 3) the percentage of sampling area that did not burn or burned at low-severity. Potential predictor variables included air temperature ($^{o}$C), relative humidity (%), wind speed (m/s), live fuel moisture (%), and dead fuel moisture (%) in each plot at the time of burning, as well as fuel loading (kg/m$^2$), litter depth (cm), cover of bare or open ground (%), burn duration (min), and the Julian calendar day of burning.

Analyses were conducted at the plot scale. Values of air temperature, relative humidity, and wind speed were each averaged over the time period of each burn. Fuel loading, litter depth, and dead fuel moisture were averaged across the 14 quadrats per plot; live fuel moisture was computed as a mean of the graminoid and forb values, each weighted by their respective percent cover in each quadrat, averaged across the 14 quadrats per plot. In addition to the means, I also considered the coefficient of variation (CV) of the variables measured at the quadrat scale (litter depth, fuel loading, and live and dead fuel moisture) as potential predictors.

To determine whether a '100% lethal heat dosage' occurred, the duration (seconds) of each temperature (to 0.1$^{o}$C) was plotted to produce a temperature-time curve for every quadrat. Curves were then compared to thermal death time (TDT) curves for insects – species-specific curves that describe lethality as a function of temperature and duration of heating. Because TDT

curves are lacking for many of the butterfly species in these prairies, here a '100% lethal heat dosage' was defined using the minimum TDT curve that resulted in 100% mortality from among the curves assembled by Rezende et al. (2014) for 17 insect species of various life stages representing temperate ecosystems. By choosing the minimum of these experimentally gathered curves, I used the most conservative assessment of 100% lethality, in lieu of having thermal tolerance data for the species in my system. Cover of unburned and low-severity areas within a plot was defined as the proportion of sub-quadrats ($n$ = 98) with a severity score of 5 (unburned) or 4 (scorched), expressed as a percentage. For analysis, a logit transformation (Warton and Hui 2011) was used.

Data were screened for potential outliers and predictors were screened for multicollinearity, which was strongest for air temperature and relative humidity. Separate stepwise regressions were then compared, using as predictors either air temperature or relative humidity with all other explanatory variables. Both forward and backward steps were allowed in an automatic process, with the lowest Akaike information criterion (AIC) used to assess the benefit of adding or deleting predictors; final models were adjusted manually to remove predictors with $p > 0.05$. Stepwise deletion was also done manually, by eliminating predictors with $p > 0.05$ beginning with the predictor with the highest $p$-value. The most parsimonious final model of the two methods was chosen. In addition, a principal components analysis (PCA) of the two correlated variables was attempted as a method to combine them into one predictor variable (Haugo et al. 2011), but using PCA scores from the first axis did not improve the fit of any of the final models, so the scores were not used further in the analysis.

Average maximum soil temperature and the logit-transformed percentage of unburned or low-severity areas were analyzed with linear models with normal error terms. Final models were

evaluated for constancy of variance, normal distribution of errors, and patterns in residuals. Appropriateness of a generalized additive model (GAM) instead of a linear model and significance of an interaction between main terms was also tested in these two analyses. The binary response variable of whether a 'lethal heat dosage' occurred in a plot was analyzed with a GLM using binomial errors. Finally, transformations of predictor variables were tried when appropriate to improve the fit of all final models.

For each response variable, I also explored patterns at the quadrat scale ($n$ = 243) to elucidate any relationships that may have been obscured when variables were averaged to the plot scale. I used all predictor variables in a regression tree analysis, which has few assumptions about the independence of observations. Cross-validation was used to determine the size of the optimal tree for each analysis, with the number of cross-validations equal to the number of observations and then using 100 repeats of this cross-validation procedure. Final tree sizes were selected manually based on those with the smallest cross-validated relative error (or within one standard error of that value). The response variable for the lethal heat dosage analysis here was the total area under the time-temperature curve that exceeded the thermal death time curve.

All analyses were conducted in R version 3.1.2 (R Core Team 2014), using the following packages: 'stats' version 3.1.2; 'car' version 2.0-24; 'mgcv' version 1.8-3; 'mvnormtest' version 0.1-9; 'mvpart' version 1.6-2; 'logistf' version 1.21; 'flux' version 0.3-0; and 'ggplot2' version 1.0.1 (see Appendix C).

**Results**

Prescribed burns were conducted between 22 July and 22 September 2014; the earliest burn was lit at 8:04 AM and the latest burn was lit at 5:16 PM. Burn durations ranged from 9 to 53

minutes (Appendix D). Air temperatures ranged from 14.4 to 32.0 ºC, relative humidity from 32.3 to 87.9%, and wind speed from 0.5 to 3.7 m/s (Appendix D). Dead fuel moisture computed from the change in weight of fine fuel sticks was moderately correlated ($r$ = 0.5) with fine fuel moisture estimated from published tables based on weather conditions, time of day, and time of year (Appendix E; NWCG 2014). The correlation was stronger ($r$ = 0.625) when two outlier values (likely representing recent precipitation events) were removed (Appendix E). Data summary tables for all of the following response variables are shown in Appendix F.

The optimal model predicting the average peak temperature at 1 cm depth in the soil included both air temperature (positive correlation) and dead fuel moisture (negative correlation) at the time of burning ($R^2_{adj}$ = 0.829, $p$ = < 0.001; Table 2). Plots of the relationships with the individual variables (Figures 1a,1b) show sharp thresholds in soil temperature when burning at air temperatures above ~26 ºC and dead fuel moistures below ~7%. The quadrat-scale regression tree analysis supports this distinction, splitting the dataset into two groups for dead fuel moisture less than or greater than 6.8% (Figure 2). The summary of the decision tree at each node, however, reveals that splitting the data on air temperature (at 26.1ºC) or relative humidity (at 52%) yields a very similar model fit as for dead fuel moisture (Table 3), thus all three variables provide similar predictions of target conditions for burning to produce lower soil temperatures. Wind speed was also important in the group of quadrats where dead fuel moisture was low (<6.8%), with higher soil temperatures (mean 50.5 ºC) occurring in wind speeds <1.9 m/s and lower soil temperatures (mean 42.0 ºC) occurring in wind speeds >=1.9 m/s (Figure 2). Soil temperatures were also more variable when dead fuel moistures were lower (Figure 1).

Based on data from Rezende et al. (2014), the slope of the minimum thermal death time (TDT) curve was 4 ºC/log[min], with a y-intercept (time = 1 min) of 48.8 ºC (Figure 3). Eight of

the eighteen plots had a lethal heat dosage (a temperature-time curve that crossed the TDT curve) in at least one quadrat. Where this occurred the lethal heat dosage varied from 0.1 to 27.7 $^{o}$C*log[min] (Figure 3), with the total combined lethal heat dosage across quadrats in a given plot varying from 0.1 to 67.6 $^{o}$C*log[min].

For the binary response variable of 100% lethal heat dosage occurrence, there was no optimal GLM due to a perfect separation of lethal and non-lethal dosages at a RH of 53.3% (Figure 4). A solution was found by using a penalized likelihood method of Firth logistic regression (Heinze and Schemper 2002) for the predictor variable of relative humidity to obtain a valid model ($p <$ 0.001 for likelihood ratio test; Table 4). The quadrat-scale regression tree analysis of the total lethal heat dosage (area under the curve that exceeded the TDT) had the first node split the data based on an air temperature of 28.1 $^{o}$C (Figure 5); higher air temperatures resulted in a greater lethal heat dosage (mean 3.0 $^{o}$C*log[min]) and lower air temperatures, a lower lethal heat dosage (mean 0.2 $^{o}$C*log[min]). However, a relative humidity value of 48.7% yielded a similar model fit (Table 5).

The optimal model for the logit-transformed cover of unburned or low-severity areas included dead fuel moisture, cover of bare or open ground, and an interaction effect between the two predictors ($R^2_{adj} = 0.779$, $p < 0.001$; Figure 6; Table 6). The results of the quadrat-level regression tree analysis showed a primary split on dead fuel moisture at 19.0% (Figure 7), with ~80% of quadrats at lower moisture. Among those, the next split was on cover of bare or open ground, at a value of 3.7%. A final split among quadrats with <3.7% bare or open ground was on wind speed (1.0 m/s), resulting in greater cover of unburned and low-severity areas (mean 21.2%; $n = 29$) under low wind speeds and less cover (mean 5.1%; $n = 127$) under greater wind

speeds (Figure 7). When dead fuel moisture was high (> 19.0%; $n$ = 48), the mean cover of unburned or low-severity areas was 62.8% (Figure 7).

**Discussion**

Subsurface soil temperatures during burning showed a clear relationship with both air temperature and dead fuel moisture, with a strong delineation into two distinct groups supported by both graphs of the raw data (Figure 1). A recent examination of an upper thermal limit (a temperature at which activity and movement is inhibited) across a wide array of terrestrial insects found an overall mean of 43.0 ºC (Hoffman et al. 2013). This value aligns well with the separation in mean soil temperatures observed here and supporting the associated threshold burning conditions under which risk of mortality for insect larvae is likely reduced. My results provide specific guidance on when to conduct prescribed burns in sensitive butterfly habitat in South Puget Sound prairies to avoid lethal soil temperatures for larvae, namely when temperatures are <26 ºC, relative humidity is >52%, and dead fuel moisture is >7%. Based on the relationship between moisture measured in this study and moisture estimated from tables, however (Appendix E), the prescription dead fuel moisture for fire managers would be better set at 8% or greater.

Other research in this system has produced different results. In a pilot study at nine sites with fewer sampling locations ($n$ = 5 to 12), maximum soil temperatures at the surface and 2 cm depth were best predicted by Julian calendar day and relative humidity (CNLM 2014). Several factors may account for this difference: the limited sample size, the greater depth of temperature measurements, and a narrower range of weather conditions (19.8 – 28.3 ºC air temperature and 42.4 – 68% RH vs. 14.4 – 32.0 ºC and 32.3 – 87.9% in this study). In contrast to studies of

burning in shrublands and deserts (Davis et al. 1989; Brooks 2002; Wright and Clarke 2008), neither litter depth nor fuel loading in my sites had a significant relationship with soil temperatures. This may reflect differences in methods of measurement (paint strips vs. temperature dataloggers) or differences in vegetation. Prairie grasslands support more uniform and continuous vegetation cover than do shrublands, which are characterized by distinct canopy gaps separating large shrubs. The importance of vegetation structure is supported by the much smaller range of maximum surface temperatures observed in grasslands than in shrublands (Neary et al. 1999). In addition, the plots in my study were established in potential butterfly habitat mostly free of large invasive shrubs and heavy fuel loads that can dramatically increase soil temperatures and heat dosages. A recent study that modeled peak soil temperatures during grassland fires from fuel and weather conditions found fuel load to be a much stronger predictor than weather conditions (Augustine et al. 2014); however, these sites had a much larger range of fuel loads and burned in a much narrower range of weather conditions than my sites.

In the current study, average peak soil temperatures were more variable when dead fuel moistures were lower (Figure 1). This likely reflects microsite variation that is amplified during drier and hotter burns; rocks or patches of dry organic matter may elevate local temperatures while other locations remain cooler. When fuels have more moisture these differences are likely muted, resulting in a more uniform distribution of temperatures.

Relative humidity was the best predictor of whether a 100% lethal heat dosage occurred within a plot (Table 4). These lethal heat dosages only occurred when RH was <54%, providing guidance for burn management decisions in sensitive habitat. Furthermore, quadrat-scale lethal heat dosages were reduced when air temperatures were <28 $^{o}$C (Figure 5), or RH was >49% (Table 5). This quadrat-scale analysis is able to take into account the quantitative amount of

'100% lethal' heat dosage at each datalogger, so could provide a more refined threshold for burning conditions than the binary response analysis at the plot scale.

The final model for explaining the cover of either unburned or low-severity areas was an interaction model between dead fuel moisture and cover of bare or open ground (Figure 6; Table 6), explaining 78% of the variation ($R^2_{adj} = 0.779$). When cover of bare or open ground was extremely low, higher dead fuel moistures did not result in greater cover of unburned areas. The idea behind burning in moist conditions to generate a "patchier" burn is that the increased fuel moisture effectively reduces fuel continuity and can increase patches of unburned areas that serve as insect refugia. Fuel continuity is a function of vegetation structure, including the horizontal and vertical spacing between patches of vegetation; in the absence of these spaces, increasing fuel moisture can effectively reduce continuity (Miller and Urban 2000) and increase burn patchiness (Knapp and Keeley 2006). This idea was not strongly supported by my results: increasing dead fuel moisture had a positive relationship with cover of unburned areas within a plot only when the pre-existing fuel structure included bare or open areas (Figure 6). Without these openings, high fuel moistures did not reduce continuity enough to leave unburned or low-consumption areas. In many habitat patches where butterflies such as the Taylor's checkerspot are present or will be reintroduced, bare or open ground of at least 10% is typically a high priority feature (Fimbel 2004), thus high continuity of fuels is unlikely to be a problem in these habitats.

In a typical prescribed fire in sensitive butterfly habitat in South Puget Sound prairies, leaving approximately 20 – 25% cover of unburned or low-severity areas would be a desirable objective (Cheryl Fimbel, personal communication, April 16, 2014). The results of both the plot-scale model and the quadrat-scale regression tree analysis can provide guidance toward this

objective. When burning in areas with at least a small amount of cover of bare or open ground (>2%), somewhat higher dead fuel moistures (7 – 15%) can help increase the cover of unburned or low-severity areas toward the target range (Figure 6). When burning in areas with extremely high fuel continuity (i.e., <3.7% bare or open ground), very light wind speeds (<1 m/s) can also help increase this unburned or low-severity cover (Figure 7). These results illustrate the complex interplay between high fuel moisture, low wind speed, and physical gaps in fuel, and how each can reduce the effective fuel continuity and fire spread.

This study shows that ideal target conditions for burning in potentially sensitive butterfly habitat in this region are an air temperature of less than 26ºC, relative humidity greater than 54%, dead fuel moisture greater than 8%, and wind speeds very light to still. Burning in light winds when fuel moistures are very low, however, likely increases the residence time of heating and can increase soil temperatures (Figure 2), thus the combination of conditions is important. Given the average burn-day conditions for the prescribed fire program in South Puget Sound prairies – 23 ºC, 56% RH (CNLM 2014) – these target conditions are not unreasonable to reach for summer burning. Specific burn objectives in butterfly habitat, such as moss and thatch reduction or promotion of a certain percentage of bare ground, may or may not be met in these conditions, however, and future work should map out the balance and overlap of these two goals.

Weather conditions during the prescribed fire season can change quickly over the day, especially if moisture from recent precipitation or humid mornings is evaporating rapidly in drier conditions. In these conditions there is the potential for a "tipping point"; initially the fuel moisture of extinction (Rothermel 1972) prohibits effective burning, but this can change rapidly once weather and fuel conditions pass a threshold, potentially rendering the pinpointing of recommended target conditions somewhat difficult. Indeed, this occurred on a few of the burn

days for this study: surface moisture prevented ignition for much of the morning, but once conditions changed there was a rush to implement the burn before it became too warm and dry. Thus, while the recommended target conditions may be a reasonable objective given the average burn-day conditions, the logistics of implementing a burn within a somewhat narrow range may require considerable planning and effort.

There were a few limitations of this study that can be addressed in future research. Measurements of live and dead fuel moisture can be refined further. Here, live fuel moisture was estimated from a visual assessment of curing percentage, but a more accurate estimate can be obtained through collection, drying, and weighing of live fuel samples (Pollet and Brown 2007); this method can better capture small changes in live fuel moisture due to precipitation events, in addition to normal seasonal senescence. On the other hand, my measurements of dead fuel moisture were likely more accurate than standard fuel moisture tables, but my method also accounted for external moisture from precipitation and dew. This is the probable reason that the correlation between my values and the table estimates was only moderate (Appendix E). A better examination of the effects of these different types of moisture might be to use a soil moisture meter probe (Voncina et al. 2014) to capture moisture from recent precipitation events and then estimate dead fuel moisture from moisture tables to capture fuel moisture in response to humidity and temperature. Moist soil can lower the absolute peak burn temperatures that occur at and below the surface (Wright and Clarke 2008), but it can also increase the depth to which a given peak temperature penetrates through increased thermal conductivity (DeBano et al. 1998). In addition, there is evidence that the lethal temperature thresholds for both plant roots and soil organisms are lower in moist soils, due to these effects of soil water on the transfer and storage of heat energy (DeBano et al. 1998). This would potentially affect the lethal thresholds given by

the TDT curves gathered by Rezende et al. (2014) (Figure 3), highlighting the dynamic nature of lethal temperatures and the need for larval mortality studies for the butterflies in this region.

The results of this study suggest that targeting specific weather and fuel conditions during prescribed burns in sensitive butterfly habitat of South Puget Sound prairies can mitigate mortality risk for soil-dwelling larvae by decreasing peak soil temperatures and lethal heat dosages and by increasing the "refuge" area left unburned or less severely burned. The most important determinants of these burn outcomes were ambient air temperature, dead fuel moisture, and relative humidity, with fuel structure (cover of bare or open ground) and wind speed also affecting fuel continuity. The recommended thresholds for conducting risk-reduced burns are within the normal range of weather patterns used for prescribed fires in the Sound Puget Sound burn program, but a closer examination of balancing specific burn objectives with risk reduction is warranted. Future research to refine strategies for reducing risk in these habitats should focus on more accurate measurements of fuel conditions, test how soil moisture affects larval mortality, and examine lethality thresholds and diapause locations of larvae of the endemic butterfly species in this system.

**Figures**

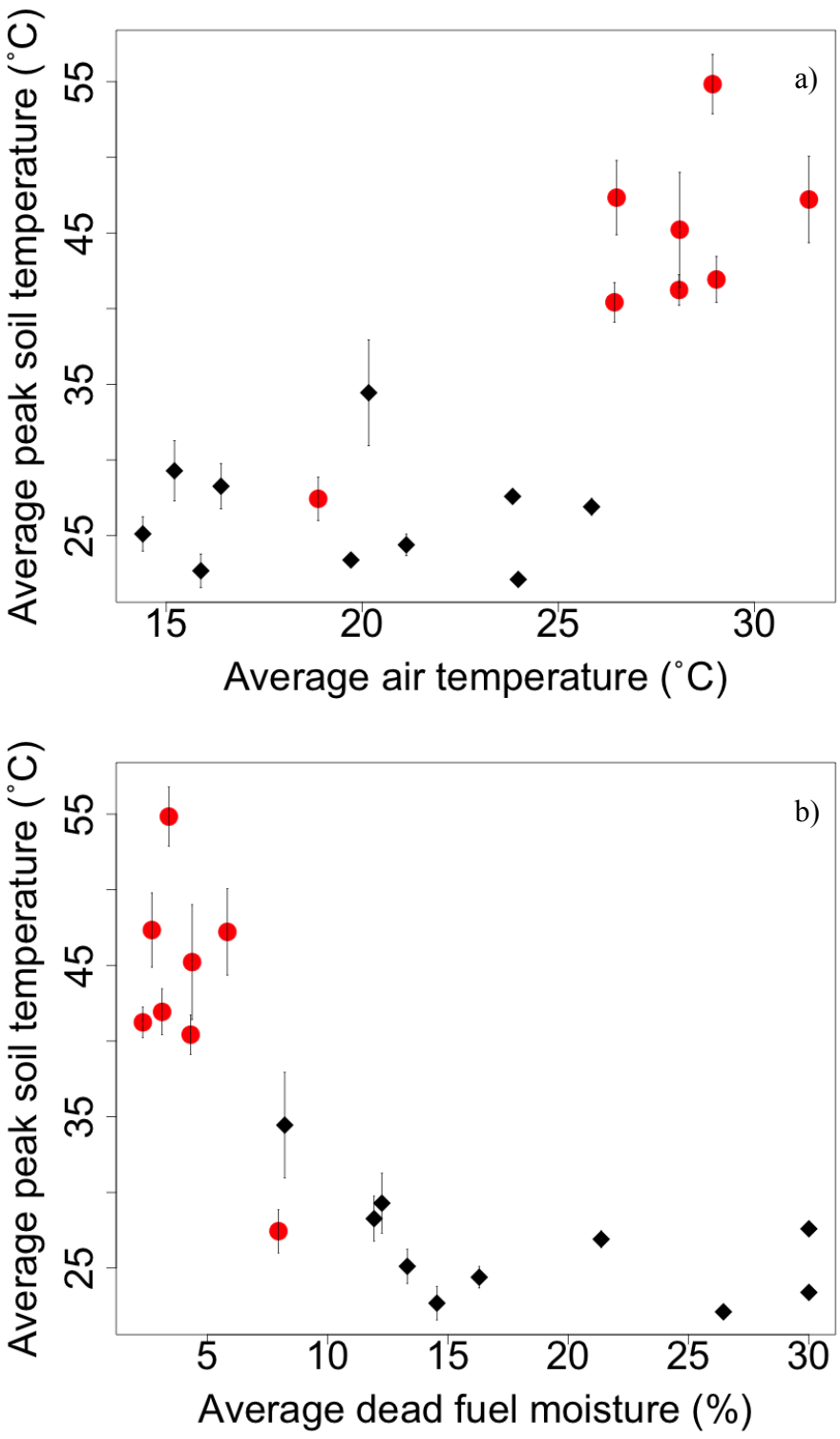


**Figure 1. Raw data for single predictor relationships of average peak soil temperature at 1cm depth with a) average air temperature and b) average dead fuel moisture at the time of the burn. Error bars represent standard error of the mean. Morning burns are black diamonds and afternoon burns are red circles.**

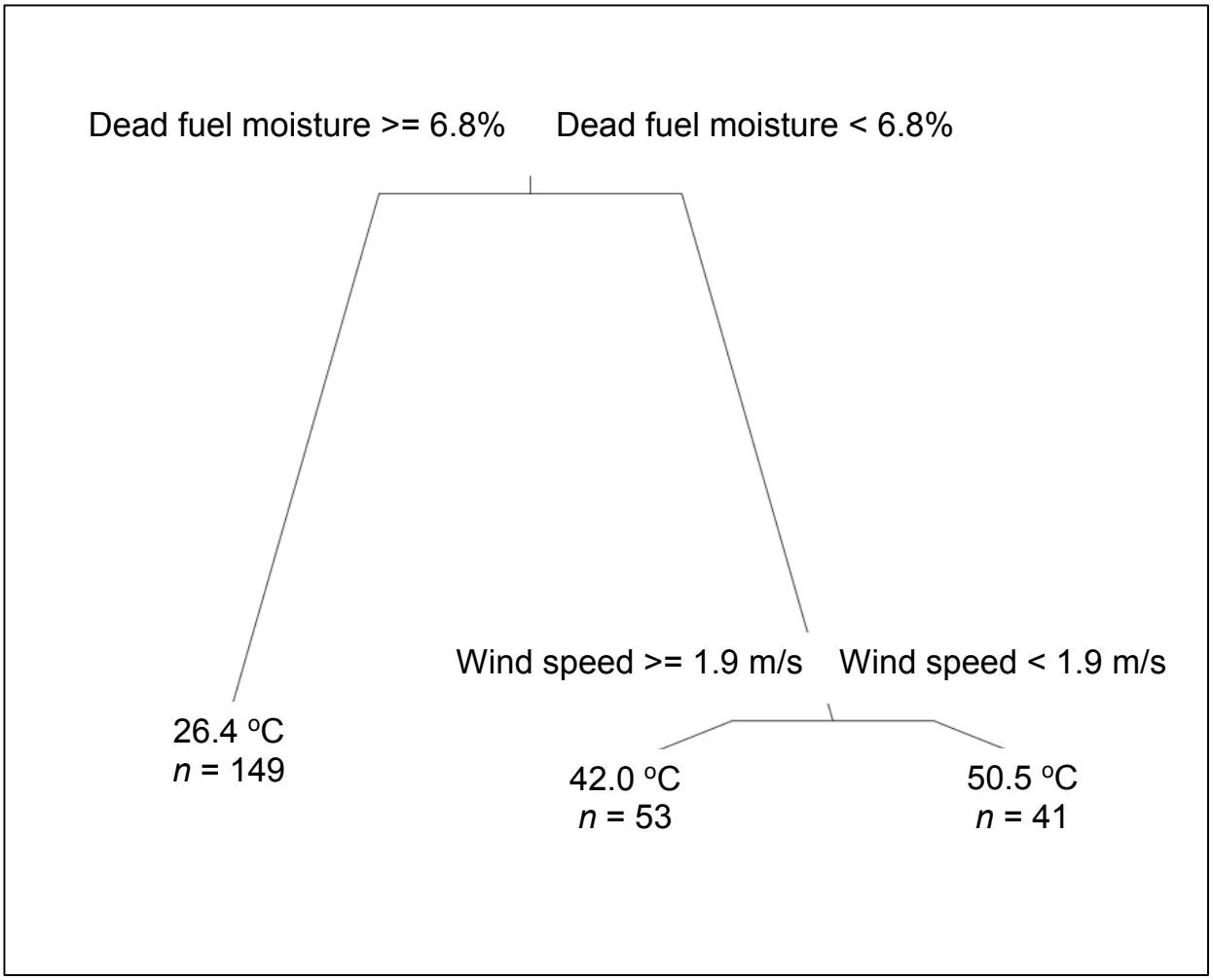


**Figure 2. Final regression tree for quadrat-level analysis of explanatory variables to classify the response (peak soil temperature at 1cm depth during the burn). Values that determine a split of a variable are indicated at each node; response mean for each group and number of observations in the group are indicated at each terminal node.**

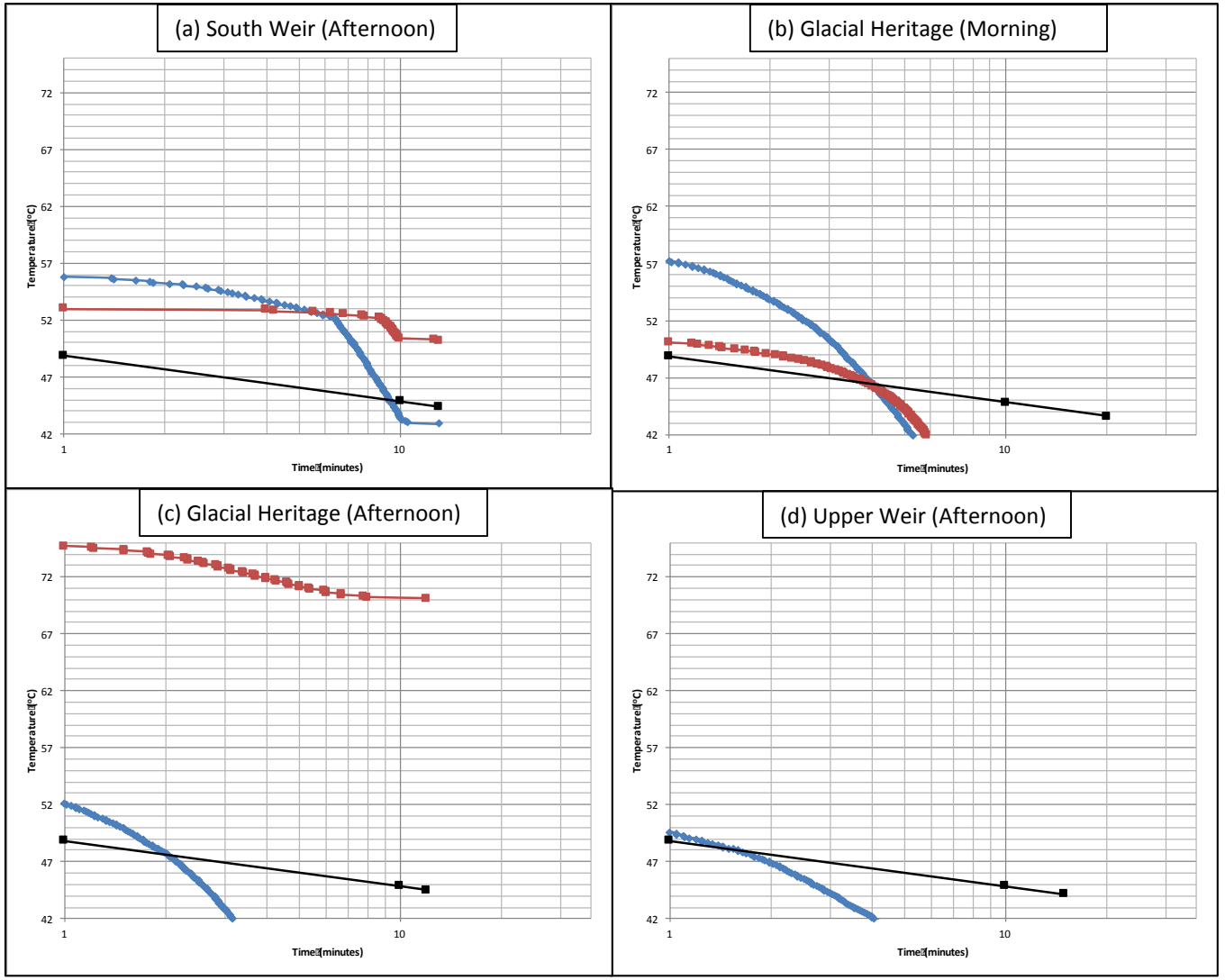


**Figure 3a – 3d. Temperature-time duration curves for each of the temperature dataloggers that recorded a lethal heat dosage (LHD); each graph represents a different research plot (LHD occurrences were only recorded in eight plots). Solid black lines are the minimum 100% lethal thermal death time (TDT) curve from experimental data gathered by Rezende et al. (2014). All curves are scaled to the duration of each burn. X-axes are logarithmic time (min) and y-axes are temperature (°C).**

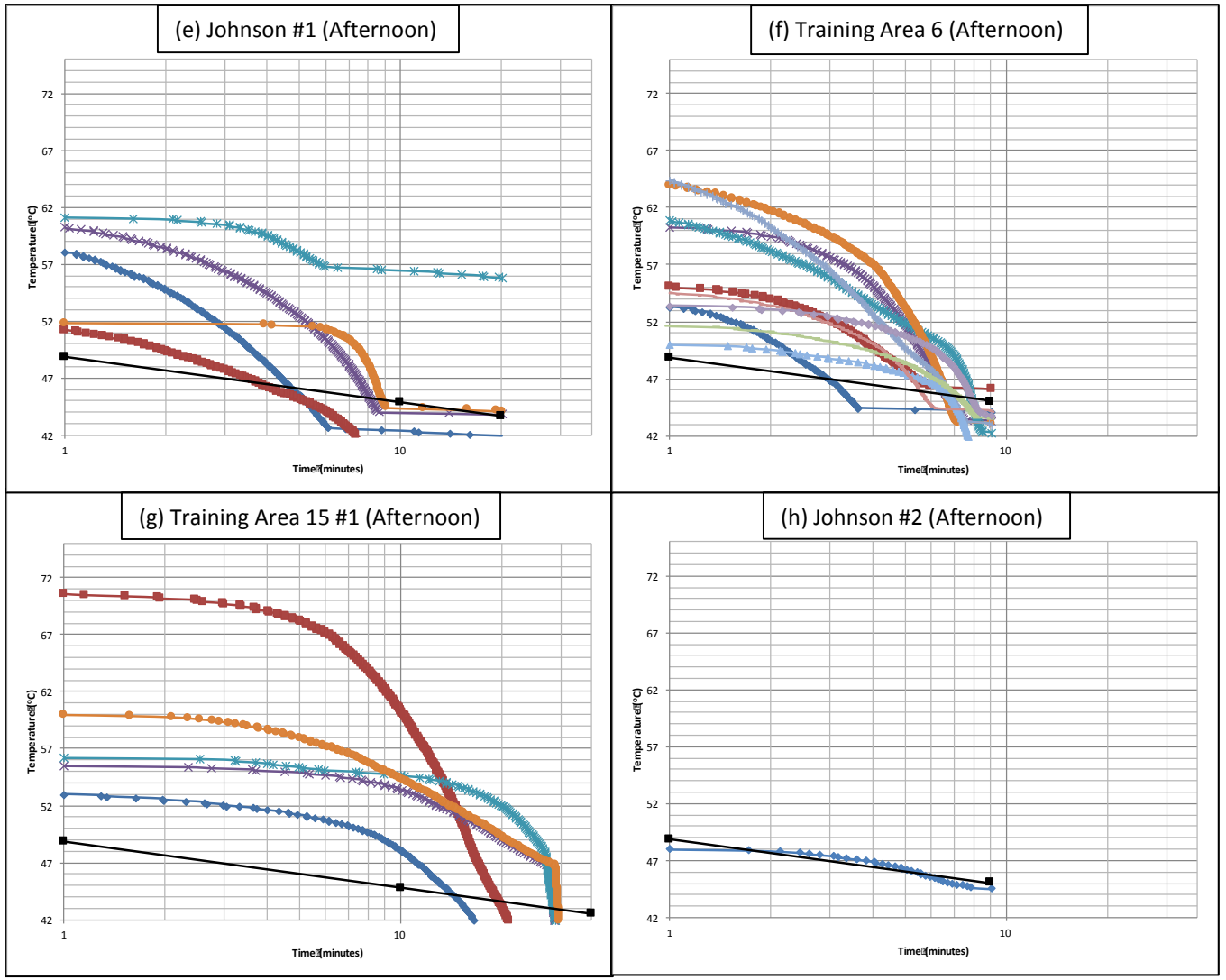


**Figure 3e -3h. Temperature-time duration curves for each of the temperature dataloggers that recorded a lethal heat dosage (LHD); each graph represents a different research plot (LHD occurrences were only recorded in eight plots). Solid black lines are the minimum 100% lethal thermal death time (TDT) curve from experimental data gathered by Rezende et al. (2014). All curves are scaled to the duration of each burn. X-axes are logarithmic time (min) and y-axes are temperature (°C).**

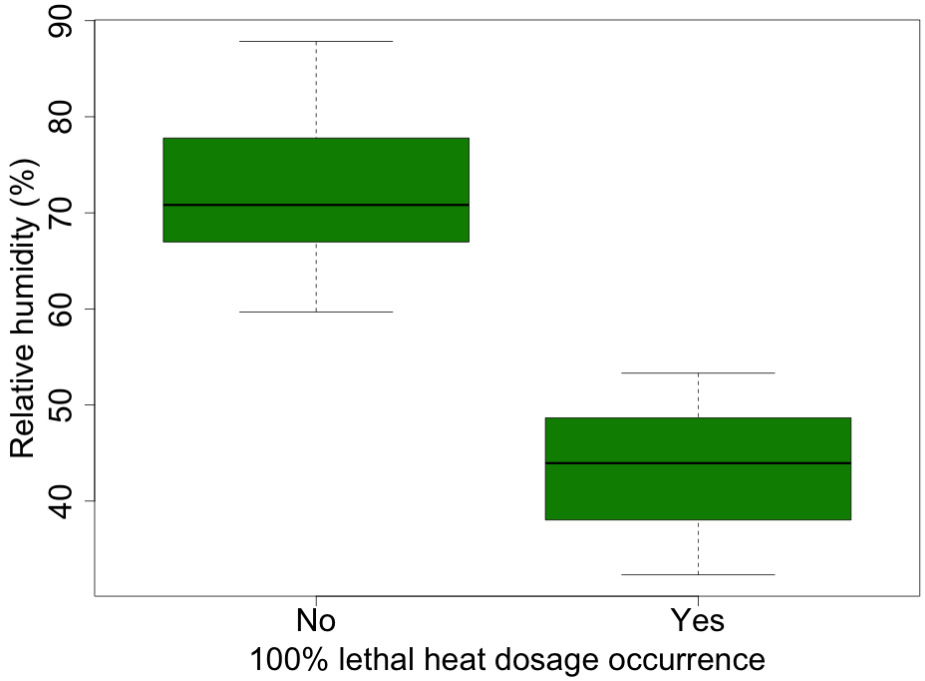


**Figure 4. Box-and-whisker plot of raw data for lethal heat dosage occurrence as a function of relative humidity at the time of the burn.**

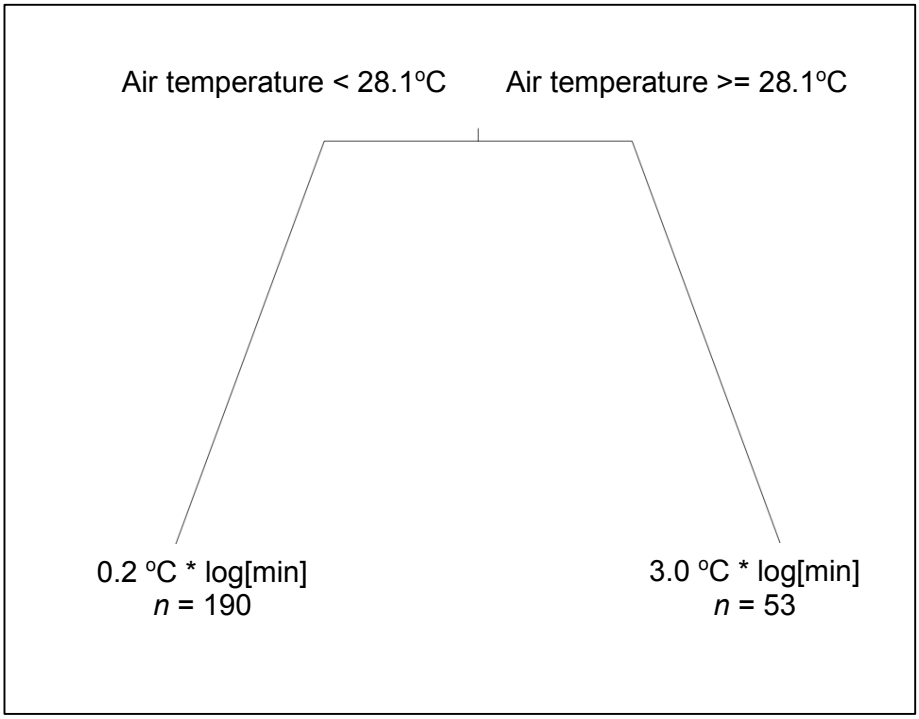


**Figure 5. Final regression tree for quadrat-level analysis of explanatory variables to classify the response (total amount of lethal heat dosage in °C*log[min] occurring during the burn). Values that determine a split of a variable are indicated at each node; response mean for each group and number of observations in the group are indicated at each terminal node**

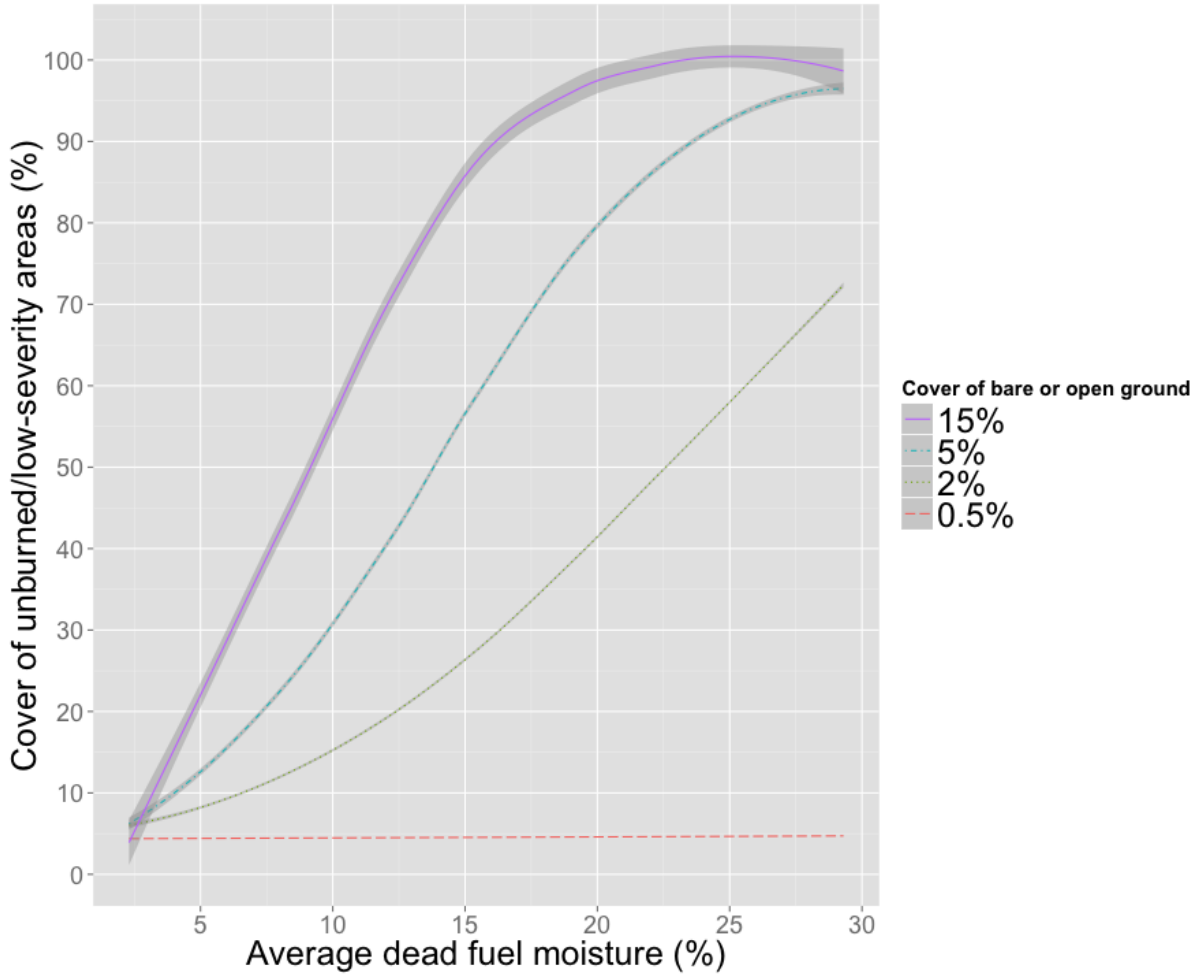


**Figure 6. Interaction plot for final model showing the relationship between percent cover of unburned or low-severity areas (assessed post-burn) and the average dead fuel moisture at the time of burning at different levels of the percent cover of bare or open ground.**

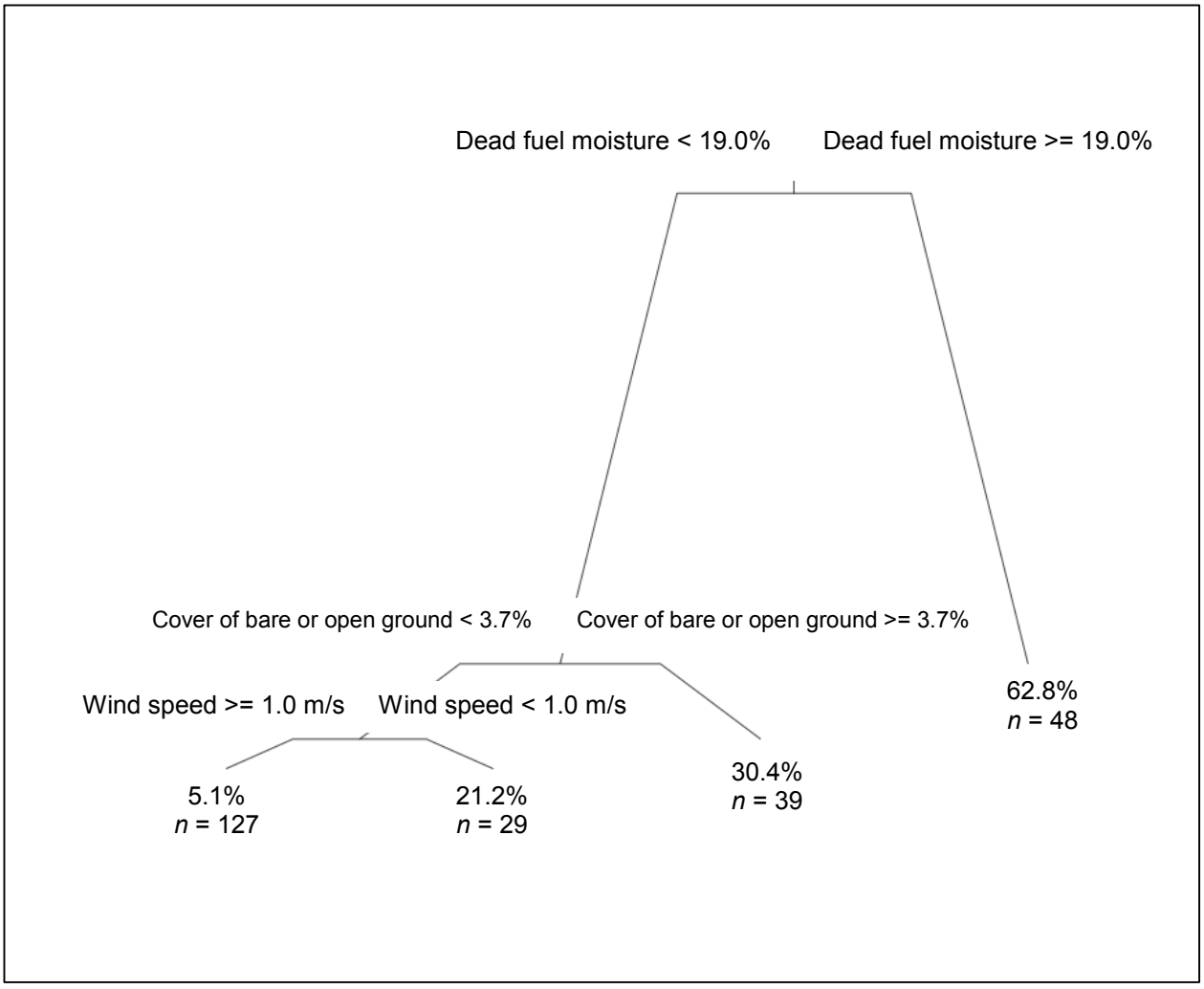


**Figure 7. Final regression tree for quadrat-level analysis of explanatory variables to classify the response (percent cover of unburned or low-severity areas assessed post-burn). Values that determine a split of a variable are indicated at each node; response mean for each group and number of observations in the group are indicated at each terminal node.**

## Tables

**Table 1.** Fire-severity class description, modified from National Parks Service Fire Effects Monitoring Handbook.

| | Substrate | Vegetation |
|---|---|---|
| **5 - Unburned** | Not burned | Not burned |
| **4 - Scorched** | Litter partially blackened; duff nearly unchanged; leaf structures unchanged | Foliage scorched |
| **3 - Lightly Burned** | Litter charred to partially consumed, but some plant parts are still discernible; charring may extend slightly into soil surface, but soil is not visibly altered; surface appears black (this soon becomes inconspicuous); burns may be spotty to uniform depending on the grass continuity | Grasses with approximately two inches of stubble; foliage and smaller twigs of associated species partially to completely consumed; some plant parts may still be standing; bases of plants are not deeply burned and are still recognizable |
| **2 - Moderately Burned** | Leaf litter consumed, leaving coarse, light gray or white colored ash immediately after the burn; ash soon disappears leaving bare mineral soil; charring may extend slightly into soil surface | Unburned grass stubble usually less than two inches tall, and mostly confined to an outer ring; for other species, foliage completely consumed, plant bases are burned to ground level and obscured in ash immediately after burning; burns tend to be uniform |
| **1 - Heavily Burned** | Leaf litter completely consumed, leaving a fluffy fine white ash, this soon disappears leaving bare mineral soil; charring extends to a depth of 1 cm (0.5 in) into the soil; this severity class is usually limited to situations where heavy fuel load on mesic sites has burned under dry conditions and low wind | No unburned grasses above the root crown; for other species, all plant parts consumed leaving some or no major stems or trunks, any left are deeply charred; this severity class is uncommon due to the short burnout time of grasses |

**Table 2.** Multiple linear regression model results for peak soil temperature (°C) at 1cm depth during a prescribed burn (averaged across a plot).

| | Coefficient | Standard error | *p*-value |
|---|---|---|---|
| Intercept | 17.337 | 5.533 | **0.007** |
| Average air temperature (°C) | 1.048 | 0.206 | **< 0.001** |
| Average dead fuel moisture (%) | -0.623 | 0.119 | **< 0.001** |
| $R^2_{adj}$ | 0.829 | | |
| F-statistic | 42.33 | | |
| *p*-value | **< 0.001** | | |

**Table 3.** Potential splits provided by explanatory variables at each non-terminal node of the quadrat-level regression analysis for peak soil temperature (°C) at 1cm depth during a prescribed burn, ranked by improvement to the fit of the tree; higher values of response variable occur when explanatory variables satisfy criteria in the 'Value' column. Shaded variables were used to split the dataset at each node.

| **Node 1: Primary splits** | **Value** | **Improvement** |
|---|---|---|
| Average dead fuel moisture (%) | < 6.784 | 0.635 |
| Average air temperature (°C) | > 26.140 | 0.620 |
| Average relative humidity (%) | < 52.010 | 0.620 |
| Average wind speed (m/s) | < 1.310 | 0.285 |
| Average live fuel moisture (%) | < 71.938 | 0.049 |
| **Node 3: Primary splits** | **Value** | **Improvement** |
| Average wind speed (m/s) | < 1.894 | 0.204 |
| Average air temperature (°C) | > 28.516 | 0.073 |
| Average relative humidity (%) | < 48.667 | 0.047 |
| Average fuel load (kg/m$^2$) | > 0.549 | 0.035 |
| Average live fuel moisture (%) | > 44.053 | 0.031 |

**Table 4.** Firth logistic regression model for the binary response variable 'lethal heat dosage occurrence' within a plot during a prescribed burn.

| | Coefficient | Standard error | *p*-value |
|---|---|---|---|
| Intercept | 14.739 | 6.961 | **< 0.001** |
| Average relative humidity (%) | -0.259 | 0.121 | **< 0.001** |
| Likelihood ratio test = 17.590 on 1 df, $p < 0.001$<br>Wald test = 4.609 on 1 df, $p = 0.032$ | | | |

**Table 5.** Potential splits provided by explanatory variables at each non-terminal node of the quadrat-level regression analysis for total amount of lethal heat dosage (°C * log[min]) during a prescribed burn, ranked by improvement to the fit of the tree; higher values of response variable occur when explanatory variables satisfy criteria in the 'Value' column. Shaded variables were used to split the dataset at each node.

| Node 1: Primary splits | Value | Improvement |
|---|---|---|
| Average air temperature (°C) | > 28.088 | 0.130 |
| Average relative humidity (%) | < 48.667 | 0.118 |
| Average dead fuel moisture (%) | < 5.705 | 0.099 |
| Average wind speed (m/s) | > 1.310 | 0.033 |
| Average live fuel moisture (%) | < 58.259 | 0.012 |

**Table 6.** Multiple linear regression model results for logit-transformed percent cover of unburned or low-severity areas (assessed post-burn).

| | Coefficient | Standard error | *p*-value |
|---|---|---|---|
| Intercept | -3.089 | 0.367 | **< 0.001** |
| Average dead fuel moisture (%) | 0.070 | 0.033 | **0.051** |
| log[cover bare or open ground (%)] | 0.002 | 0.304 | 0.996 |
| Interaction effect | 0.096 | 0.036 | **0.017** |
| $R^2_{adj}$ | 0.779 | | |
| F-statistic | 23.36 | | |
| *p*-value | **< 0.001** | | |

# Chapter 2: Effects of weather and fuel conditions during prescribed fires on post-burn vegetation structure and composition in South Puget Sound prairies

## Introduction

Habitat structure – the spatial configuration and arrangement of vegetation – can be a vital component of quality habitat for butterflies (Fimbel 2004; New 2014). In the initial stages of restoring butterfly habitat, composition is often the focus due to species' requirements for particular host and nectar plant species, but structural elements can also be manipulated to meet habitat objectives. In the prairies of the Pacific Northwest, prescribed fire is one of the primary tools for habitat restoration, but effects on habitat structure are not as well studied as effects on composition. Varying the type of prescribed fire, such as applying head and backing fires or burning under different weather conditions may be used to meet certain habitat goals, yet the specific effects of these applications on the spatial structure of vegetation are not well understood.

The importance of habitat structure for butterflies (and insect populations in general) has been studied in many grassland and meadow ecosystems (Kindvall 1996; Severns and Warren 2008; Bonebrake et al. 2010). While host and nectar plants can often be species-specific for prairie butterflies, certain structural elements, namely a mix of vegetation heights and patches of bare soil or low areas, may provide resources to diverse species (Fimbel 2004; Jerrentrup et al. 2014). The enhancement of habitat heterogeneity in terms of both structure and composition can buffer populations against environmental stochasticity (Oliver et al. 2010) and provide more diverse habitat for activities associated with multiple life stages, including ovipositing, feeding, basking, and roosting (Weiss et al. 1987; Hanski 2003; New 2014).

In the Pacific Northwest prairie-oak ecosystem, certain species of butterfly are state or federally listed as threatened or endangered due to habitat loss and degradation, including the Taylor's checkerspot (*Euphydryas editha taylori*) and the mardon skipper (*Polites mardon*). Several other endemic butterflies are considered species of concern; much of the current research on conservation and re-introduction of these species is centered on host plant requirements, growth rates and genetics of populations, and habitat preferences (Schultz et al. 2011). Meanwhile, habitat restoration of prairie remnants is ongoing, using combinations of herbicide, mowing, and prescribed fire; concerns about potentially detrimental effects of these activities on current or newly introduced butterfly populations, however, can sometimes inhibit the implementation of consistent restoration treatments (Hamman et al. 2011).

The effects of particular types of prescribed burns have mainly focused on burn severity and post-burn composition (Martin and Hamman 2014) rather than post-burn structure. It is often observed that burning under cooler or more humid conditions promotes structural heterogeneity due to incomplete or "patchy" burning. However, post-burn vegetation structure is usually not quantified, and the studies that have done so have mostly examined the effect of burn season rather than time-of-burn weather conditions (Gross and Romo 2010). The potential effects of burn season are also influenced by the phenology of dominant species, such that the relative importance of weather conditions (temperature and moisture) on post-burn spatial structure may be masked by the effect of season on fuel loads (de Angelis et al. 2012).

Conducting prescribed burns at specific times of year is one approach to lowering air temperatures and increasing moisture levels, but off-season and "shoulder" season burns can be difficult to implement and potentially detrimental to native species (Hamman et al. 2011). An alternative is to burn at different times of the day, because both temperature and relative

humidity (RH) can vary markedly over the day. Along with associated changes in fuel moisture, this variability in weather conditions during burning may affect post-burn habitat structure. In addition, burning in cooler and wetter conditions is likely to leave a larger mosaic of unburned and low-severity patches (see Chapter 1), which can be vital to survival of butterfly larvae that are in diapause during burning (Hamman et al. 2011; New 2014). Thus, by burning butterfly habitat earlier in the day within the primary fire season, restoration managers may be able to meet two habitat objectives: 1) leave critical unburned refuges for larvae in diapause; and 2) enhance structural characteristics in post-burn growing seasons that are considered desirable for butterfly habitat (e.g., a mix of tall and low vegetation and spatial dispersion of open patches).

The overall aim of this study was to determine whether prescribed burns conducted at different times of day with differing weather conditions (temperature, RH, and associated fuel moisture) have different effects on structural heterogeneity and compositional diversity of vegetation. My specific objective was to provide guidelines for refining burn plan prescriptions targeted toward improving the quality of butterfly habitat in this region, while contributing novel research on how fuel conditions during a burn can affect vegetation response. I hypothesized that burning under conditions of lower temperatures, higher relative humidity, and higher fuel moisture would result in plant communities with greater structural complexity (i.e., heterogeneity of vegetation height and spatial dispersion of bare or open patches), and higher species diversity.

## Methods

### *Study Sites*

Study sites were in existing South Puget Sound prairie remnants on land owned by Joint Base Lewis-McChord (JBLM) and The Nature Conservancy (Appendix A). All of these areas are

undergoing active restoration management, including regular prescribed fires. Historically, these prairies were maintained through several thousand years of anthropogenic burning by Native Americans, and thus have developed fire-adapted plant communities (Storm and Shebitz 2006). Eight prescribed burn units (Appendix A) were selected based on ease of access, feasibility for conducting research burns, similarity of burn history (1 – 2 burns at a 2 – 3 year frequency), and potential for butterfly habitat.

Seven burn units were located on JBLM land (47.0873º Latitude, -122.5707 Longitude) that is owned by the Department of Defense and managed in partnership with the Center for Natural Lands Management. The eighth burn unit was located at nearby Tenalquot Prairie (TQ; 46.9016º Latitude, -122.7309 Longitude), a 28-ha preserve owned by The Nature Conservancy and managed by the Center for Natural Lands Management. Soils at all eight burn units are a Spanaway gravelly sandy loam (NRCS 2015). Vegetation on all sites was generally short-statured bunchgrass prairie in various stages of restoration to native dominance; invasive species such as *Cytisus scoparius* (Scotch broom) were largely removed or limited in distribution on most sites.

From July to September (the primary prescribed fire season) 2014 at the nearest RAWS weather station in Chehalis, Washington, average air temperature ranged from 16.8 to 19.8ºC and average relative humidity (RH) ranged from 66.6 to 72.2%. Annual precipitation from 2004 to 2014 averaged 1117.8 mm, with an average for July – September of 79.4 mm (WRCC 2015).

*Experimental Design*

A pair of 26 x 37 m plots was placed within each of the eight burn units, for a total of sixteen plots ($n$ = 16). For each pair in a given burn unit, plots were placed no more than 25 m apart to

minimize potential variability in fuel loading or fuel type. Each plot was at least 20 m from the nearest road and at least 10 m from a mowed firebreak, which served as a control line during the burns.

Each plot consisted of cyclically separated quadrats arranged along line transects (Appendix B). A cyclic sampling design is often more efficient when geospatial analysis will be used to study spatial patterns, because the sample points (quadrats) are distributed such that an adequate (> ~30) number of pairs of points for each distance interval (e.g., 1-m separation, 2-m separation, etc.) is generated (Burrows et al. 2002). In these designs, a contiguous line of quadrats is divided into sections of a given length and within each section only certain quadrats are sampled (e.g., in a 3/7 cyclic design, three quadrats – the 1$^{st}$, 2$^{nd}$, and 4$^{th}$ – of each seven-quadrat section are sampled). For this study, seven transects, each 26 m in length, were spaced in a one-cycle 7/37 cyclic design (i.e., oriented perpendicular to a 37-m baseline from the 0-, 1-, 6-, 10-, 17-, 23-, and 35-m marks). Along each transect, eight 1-m$^2$ quadrats were spaced in a two-cycle 4/13 cyclic design, with corners placed at the 0-, 1-, 3-, 9-, 13-, 14-, 16-, and 22-m marks, resulting in a total of 56 quadrats in each plot (Appendix B).

Each quadrat was further subdivided into sixteen 25 x 25 cm sub-quadrats; of these, seven were designated for data collection on structural variables (Appendix B; shaded sub-quadrats). The spacing of the sub-quadrats within and among quadrats facilitated analyses over scales of less than one meter to tens of meters, representing the scales of response for butterflies and other insects over multiple life stages (Miskelly 2000). Finally, each of these seven sub-quadrats was subdivided into twenty-five 5 x 5 cm squares (Appendix B), the scale at which data were collected on presence/absence of plant cover.

Fourteen of the 56 quadrats in each plot were designated as "intensive" quadrats, in which I measured fuel load, litter depth, and live and dead fuel moisture, and sampled species composition data (see *Prescribed Fires and Fuels Data Collection*). The 14 quadrats were distributed as two quadrats spaced 13 m apart (either at the 3- and 16-m marks or the 9- and 22-m marks) on each of the seven transects (Appendix B; shaded quadrats).

*Prescribed Fires and Fuels Data Collection*

Prescribed burns in all plots were conducted between 22 July and 22 September 2014, during the main prescribed fire season in this region (Hamman et al. 2011). To ensure data collection over a wide range of weather and fuel conditions, paired plots were burned either during relatively cool and humid morning hours or generally warmer and drier afternoon hours. To control for the potential confounding of time of year on fire behavior, both plots within a pair were burned on the same day (for most burn units). Due to logistical constraints, plots in two of the ten units were burned four days apart, during which there was little change in weather conditions or plant phenology.

Fuel loading was estimated from vegetation structural measurements in the 14 "intensive" quadrats prior to burning. Within each quadrat, seven 25 x 25 cm "sub-quadrats" were designated (Appendix B); a single estimate of total plant cover was assessed within this area. Height class, or herbaceous fuelbed depth, was visually assessed (at 10 cm resolution) using a meter stick at the corner of each quadrat. Height class, cover, and bulk density were used to estimate fuel loading (or biomass) in each quadrat with the equation $B = H * C * BD$, where B is biomass ($kg/m^2$), H is height-class midpoint (m), C is the total plant cover proportion in the seven sub-quadrats, and BD is bulk density (approximated as 1.23 $kg/m^3$; Burgan and Rothermel

1984). In addition, one measurement of litter or moss depth (to mineral soil) was taken just outside the corner of each of these quadrats.

In the 14 "intensive" quadrats in each plot, an estimate of live fuel moisture was obtained prior to burning through visual assessment of the percent curing of the two main growth forms, grasses and forbs, using a modification of the Guide to Grassland Curing (NOAA 2008) that is based primarily on color and seed head formation. Percent curing of each growth form was then converted to a live fuel moisture percentage using standard fuel modeling tables (Scott and Burgan 2005).

Dead fuel moisture was estimated for the 14 "intensive" quadrats using a 1-hr fuel moisture stick made of small packets of straw ~12 cm in length tied with a plastic zip tie. At least 12 hr prior to burning, a packet was placed 10 cm outside of each quadrat and secured at ground level with a lawn staple. Immediately prior to ignition of each plot, the straw packets were removed and placed in airtight Whirlpaks; these were subsequently weighed, opened, and placed in a 60ºC drying oven for 48 hr and re-weighed. After correcting for the weight of the Whirlpak and zip tie, dead fuel moisture (% moisture content) was calculated as ([wet weight – dry weight] * 100) / dry weight (Pollet and Brown 2007). In two plots, dead fuel moisture was >30% due to excess rainwater or dew on the straw packets; for these cases, a value of 30% was used in the analyses, in accordance with fuel moisture models for dead fuels (Scott and Burgan 2005).

The type of ignition application was kept consistent across plots. To mimic the diversity of fire types (head, backing, and flanking) in both natural and prescribed burns, five point-source ignitions were applied in each plot within one minute of each other: one at the center and four along each half-diagonal of the rectangular plot, positioned halfway between the center and the corner (Appendix B). Drip torches were used to ignite the nearest fuel source using just enough

fuel to light a circle of 50 cm in diameter. Mowed firebreaks surrounding the buffers of each plot were not lit until the nearest plot edge had completely burned, so that the behavior of the experimental plot fire was not influenced by interaction with the blackline fire ignited for control purposes.

Ambient air temperature (°C), relative humidity (%), and wind speed (m/s) were monitored during each burn using a Kestrel 4000 Weather Meter (Nielsen-Kellerman 2012), which was positioned 1.3 m above the ground on a tripod in a similar fuel type not more than 20 m from the edge of the plot. Each weather variable was recorded automatically every 30 seconds from ignition until all flames had self-extinguished.

*Vegetation Data Collection*

All structural and species compositional data were collected in spring 2014 (pre-burn) and spring 2015 (the first growing season after burning); sampling occurred at approximately the same time of month each year in each plot, with some accommodations for earlier phenology in 2015. Plots within the same burn unit were sampled on the same day, or as close as possible in timing. Composition was measured for all plots in mid-spring (late April to mid-May), and structure was measured in late spring (late May to mid-June). Management and restoration activities, such as herbicide application, seeding, planting, or mowing, were prohibited within the plots between the burns and the spring 2015 data collection.

Data on species composition were collected only in the 14 "intensive" quadrats in each plot (Appendix B; shaded quadrats). Cover of each species was estimated to the nearest percent. Each plot was also systematically surveyed to record any additional species not present in the 14

sampling quadrats; the combination of data provided an estimate of plot-scale species richness. All vascular plants were identified using Hitchcock and Cronquist (1973).

Two components of vegetation structure were evaluated: variability in vertical height and horizontal distribution of bare or open ground. In all 56 quadrats per plot, maximum vegetation height was measured in one corner of each of the seven designated 25 x 25 cm sub-quadrats (Appendix B; shaded sub-quadrats) using a sward stick with a 2 x 1 cm plastic sleeve. The sleeve was lowered until it made contact with the vegetation, then the height was recorded. The plastic sleeve size was based on studies that have found the sward stick method with a 2-$cm^2$ area to be ideal for measuring the diversity of niches available to insects and spiders (Stewart et al. 2001; Suggitt et al. 2011).

Cover of bare or open ground was measured as presence/absence in all twenty-five 5 x 5 cm squares of each designated sub-quadrat for all 56 quadrats in a plot (total of 9800 squares; Appendix B). This cover category included open areas of bare ground, litter, rock, moss, and very low-statured (< 2 cm) vegetation, with minimal overhang of neighboring vegetation; resident butterflies use these ground-surface conditions for the same purposes (e.g., basking and accessing plant bases for ovipositing; Linders and Lewis 2013). The 5 x 5 cm sampling scale within the sub-quadrats represented the smallest patch size that would allow basking by butterflies (Cheryl Fimbel and R. Adam Martin, personal communication).

*Statistical Analysis*

I used linear models to examine the relationships of compositional or structural variables with weather and fuel conditions during the prescribed burns. Potential predictor variables included air temperature ($^oC$), relative humidity (%), wind speed (m/s), live fuel moisture (%),

and dead fuel moisture (%) in each plot at the time of burning, as well as fuel loading ($kg/m^2$), litter depth (cm), cover of bare or open ground (%), burn duration (min), and the Julian calendar day of burning (Table 7).

Analyses were conducted at the plot scale. Values of air temperature, relative humidity, and wind speed were each averaged over the time period of each burn. Fuel loading, litter depth, and dead fuel moisture were averaged across the 14 "intensive" quadrats per plot; live fuel moisture was computed as a mean of the graminoid and forb values, each weighted by their respective percent cover in each quadrat, averaged across the 14 "intensive" quadrats per plot. In addition to the means, I also considered the coefficient of variation (CV) of the variables measured at the quadrat scale (litter depth, fuel loading, and live and dead fuel moisture) as potential predictors.

Data were screened for potential outliers and predictors were screened for multicollinearity, which was strongest for air temperature and relative humidity. Separate stepwise regressions were then compared, using as predictors either air temperature or relative humidity with all other explanatory variables. Both forward and backward steps were allowed in an automatic process, with the Akaike information criterion (AIC) used to assess the benefit of adding or deleting predictors; final models were adjusted manually to remove predictors with $p > 0.05$. Stepwise deletion was also done manually, by eliminating predictors with $p > 0.05$ beginning with the predictor with the highest $p$-value. The most parsimonious final model of the two methods was chosen. In addition, a principal components analysis (PCA) of the two correlated variables was attempted as a method to combine them into one predictor variable (Haugo et al. 2011), but using PCA scores from the first axis did not improve the fit of any of the final models, so the scores were not used further in the analysis. All response variables were analyzed with linear models with normal error terms. Final models were evaluated for constancy of variance, normal

distribution of errors, patterns in residuals, and points with high leverage and large Cook's distance (greater than the median of the $F_{p,n-p}$ distribution where $p$ = the number of regression parameters and $n$ = the number of observations; McDonald 2002). Finally, transformations of predictor variables and use of generalized additive models were tried when appropriate to improve the fit of all final models.

Species diversity and composition

Responses were analyzed as the change from pre- to post-burn conditions (Allison 1990; Kelly and Price 2005). Response variables included 1) mean change in quadrat-scale species richness; 2) change in plot-scale species richness; 3) mean change in quadrat-scale Hill's $N_1$ species diversity index; and 4) change in beta richness (plot-scale richness divided by mean quadrat-scale richness). Species richness was analyzed at both the quadrat and plot scales to assess the multiple scales of response of butterflies and other insects. Hill's $N_1$ is calculated as the exponential of the Shannon diversity index $H$ (Hill 1973) and incorporates the proportional cover of species within each quadrat: ($H = -\sum_i^n p_i * \ln(p_i)$). $N_1$ is expressed in the same units as species richness, and is often described as "the equivalent number of equally common species" (Magurran 2004).

In addition to diversity, I assessed the Bray-Curtis distance between pre- and post-burn communities at both the plot and quadrat scales, using species abundance data. The plot-scale Bray-Curtis distance was calculated using average composition across the 14 "intensive" quadrats and the quadrat-scale Bray-Curtis distances were calculated for each quadrat and then averaged across the 14 quadrats. For both scales, Bray-Curtis distances were calculated after relativizing the columns (species) of the entire sampling unit-x-species abundance matrix by maxima and the rows (plots or quadrats) by total (McCune and Grace 2002). These data

adjustments allow all species (other than rare species) to contribute equally to differences between sampling units and equalizes the contribution of all sampling units. Prior to relativization, rare species (< 5% of plots or quadrats) were deleted from the matrix, as rare species may be poorly sampled and contribute little to overall composition (McCune and Grace 2002).

Species abundance data were also combined (summed) based on functional group (perennial / annual; forb / graminoid / woody) and origin (native / exotic), resulting in ten groups. The change in relative cover of groups (pre- to post-burn) was analyzed as a separate response variable with all predictor variables.

I used non-metric multidimensional scaling (NMDS) – a multivariate ordination of the quadrat-scale community data (McCune and Grace 2002) – for both the species and functional group abundance to facilitate interpretation of compositional responses and to visualize the community shifts. Separate NMDS ordinations were used for each site (burn unit) using both the pre- and post-burn species abundance data from the two plots ($n$ = 56). This reduced visual clutter and facilitated the comparisons of interest (morning vs. afternoon burns). For each site, I deleted rare species (< 5% of quadrats) from the quadrat-x-species abundance matrix and applied the same relativizations as used for the Bray-Curtis distance analysis. Three different dimensionalities ($k$ = 1, 2, and 3) were used in independent NMDS runs, with a maximum number of iterations set at 400 and the maximum number of repeat runs set at 40 for each of the three analyses. The Bray-Curtis distance measure was used for all runs. The best solution for each was used as the starting configuration for another ordination run to produce a final solution. Final dimensionality was based on a screeplot to assess stress as a function of dimensionality ($k$). A Shepard plot was used to assess the fit of the ordination point cloud to the original

dissimilarity matrix of the quadrat-x-species matrix. For each final ordination, quadrats were plotted in two dimensions (axes 1 and 2), and pre-burn quadrats were connected to post-burn quadrats with an arrow, to show change in composition in response to burning. Additionally, the average functional group abundance was calculated for each plot pre- and post-burn and an NMDS ($n$ = 32) was then conducted on the full set of plots x dates. Functional group scores were overlaid on the ordination and arrows were used to connect pre- to post-burn plots, to visualize functional group relationships to plots and functional group changes in response to burning.

Vegetation structure

Structural response variables were analyzed as the change from pre- to post-burn measurements (Allison 1990; Kelly and Price 2005). Variables for vegetation height were 1) change in coefficient of variation (CV; standard deviation divided by the mean) at both the quadrat and plot scales; 2) change in the average number of 2 cm maximum-height classes under 30 cm; 3) change in range of spatial autocorrelation; 4) change in magnitude of spatial autocorrelation; and 5) change in the interspersion and juxtaposition index (IJI) based on interpolation of height across each plot. Each of these variables has the potential to serve as a surrogate for microclimatic conditions at a particular scale through variability in vertical structure; this variability can help buffer insect populations against climatic extremes (Fimbel 2004; Oliver et al. 2010; Jerrentrup et al. 2014).

Overall variability of vegetation height (without a spatial component) was evaluated with the CV (standard deviation divided by the mean). In addition, the seven continuous height measurements within a quadrat were assigned to 2-cm height classes (i.e., 0 – 2 cm, 2 – 4 cm, etc.) and the mean number of different height classes among quadrats was calculated for each plot. A 2-cm interval was chosen as the minimum difference in height that might alter

microclimate for an organism the size of a larval insect (Eilers et al. 2013). Stewart et al. (2001) found a 30 ºC gradient in surface temperatures across a 40-cm range of sward heights during a summer period in which ambient air temperature varied by less than 2 ºC. Only height classes under 30 cm were evaluated, as vegetation heights greater than 30cm are generally not considered beneficial for some regional butterfly species, namely Taylor's checkerspot (Thurston County 2014).

When discussing spatial heterogeneity using geostatistics, it is important to outline an operational definition. 'Heterogeneity' can refer to many different aspects of structure depending upon the research objective (Li and Reynolds 1995) and it is often used to describe different trends. Here, I use an increase in heterogeneity to refer to a decrease in the scale and magnitude of spatial autocorrelation, as this decrease provides for more variation at a fine scale within the fixed size of the whole plot (Darrouzet-Nardi 2010; Figure 8). This fine-scale variation is of structural interest to a small organism in search of range of microclimates.

The spatial distribution of vegetation height was determined using geospatial statistics that express patterned variance on the cyclically spaced sampling points. A set of x-y spatial coordinates was assigned to each height measurement within a plot. I then created an empirical semivariogram, which plots semivariance – half the average squared difference of values from all pairs of sampling points separated by a given distance – against spatial separation. For each plot (both pre- and post-burn), a lag size of 0.25 m (the distance between sampling points) was used, and a stable semivariogram was constructed over 12 lags. A theoretical model was fit to the observed data and the range parameter (the spatial separation at which the semivariogram meets an upper asymptote) was calculated. The range describes the distance at which spatial autocorrelation exists among sampling points (i.e., an indication of autocorrelated patch size).

The magnitude of this spatial autocorrelation is further described by the sill and nugget parameters of the semivariogram model. The partial sill, which is the difference between the sill (maximum total variation) and the nugget (random variation), is divided by the sill and multiplied by 100 to represent the total height variation in a plot that is spatially structured (Li and Reynolds 1995; Dale 2003). A higher percentage of spatially structured variation indicates a greater magnitude of spatial autocorrelation of vegetation height (Darrouzet-Nardi 2010). Semivariograms that appeared to comprise mostly uncorrelated variance with a pure nugget effect were assumed to have autocorrelation at scales less than the spacing of sampling points here (25cm) and therefore undetectable by this sampling design; for analysis the range of these plots was assigned a value of zero (Welhan et al. 2002).

Ordinary kriging with the semivariogram model (Isaaks and Srivastava 1989) was used to create a height prediction map across each plot for both pre- and post-burn data. Cross-validation of each interpolation was performed to evaluate the validity of the model (i.e., that the root-mean-squared prediction error was close to the average estimated prediction standard error and the root-mean-square standardized was close to one; Haining 2003). The continuous prediction surface for each plot was then broken into 2 cm height classes to create a categorical map, and the "interspersion and juxtaposition index" (IJI) was calculated. The IJI is formatted somewhat similarly to a diversity index, and is calculated with the following equation, where $e_{ik}$ is equal to the total length of edge in a plot between height classes $i$ and $k$, and $m$ is the total number of height classes present in the plot:

$$\frac{-\sum_{k=1}^{m}\left[\left[\frac{e_{ik}}{\sum_{k=1}^{m} e_{ik}}\right] ln \left[\frac{e_{ik}}{\sum_{k=1}^{m} e_{ik}}\right]\right]}{\ln(m-1)} * (100)$$

The IJI is expressed as a percent. Low values of the IJI would represent plots in which height classes are distributed disproportionately and each class borders only a small number of other height classes. Higher values of the IJI would describe plots in which height classes are more equally adjacent to (e.g., more interspersed with) each other (McGarigal and Marks 1995).

The structural response variables for bare or open ground were 1) change in range of spatial autocorrelation and 2) change in edge to area ratio. The range of autocorrelation describes the patch size of these bare or open areas; larger open patches may provide less protection from predators. The edge to area ratio takes into account the shape complexity of open patches: greater patch edge for a given amount of open area would provide more opportunity for access to plant bases by ovipositing butterflies (Fimbel 2004) than patches with less edge.

The range of spatial autocorrelation in bare or open ground was calculated from a stable semivariogram, with a lag size of 5 cm (the spacing of sampling squares) over 12 lags. Indicator kriging (Fortin and Dale 2005) with the semivariogram model was used to create a probability map for the presence of open patches across each plot for both pre- and post-burn data. After cross-validation in the same manner as the spatial height prediction map, the open space probability map for each plot was parsed into a two-class (open or vegetated) categorical prediction map based on the actual cover of bare or open ground in a plot. Finally, the edge to area ratio of open patches was calculated for each plot prediction map.

The last structural component to be assessed was the change in variability of litter depth as a result of burning. Variability of litter depth was computed as the coefficient of variation (CV) of the 14 measurements in each plot, both pre- and post-burn.

Geospatial statistics using semivariogram analysis and kriging were calculated in ArcGIS 10.2 with the Geostatistical Analyst extension (ESRI 2013). Categorical prediction maps from

these analyses were exported into FRAGSTATS v4.1 (McGarigal et al. 2012) to calculate spatial pattern metrics. All other analyses were conducted in R version 3.1.2 (R Core Team 2014), using the following packages: 'stats' version 3.1.2; 'car' version 2.0-24; 'mgcv' version 1.8-3; 'mvnormtest' version 0.1-9; 'labdsv' version 1.6-1; 'vegan' version 2.2-1; and 'maptools' version 0.8-36 (see Appendix C).

**Results**

Prescribed burns were conducted between 22 July and 22 September 2014; the earliest burn was lit at 8:04 AM and the latest burn was lit at 5:16 PM. Burn durations ranged from 9 to 53 minutes (Appendix D). Air temperatures ranged from 14.4 to 32.0 $^{o}$C, relative humidity from 35.5 to 87.9%, and wind speed from 0.5 to 3.7 m/s (Appendix D). Dead fuel moisture computed from the change in weight of fine fuel sticks was moderately correlated ($r = 0.5$) with fine fuel moisture estimated from published tables based on weather conditions, time of day, and time of year (Appendix E; NWCG 2014). The correlation was stronger ($r = 0.625$) when two outlier values (likely representing recent precipitation events) were removed (Appendix E). Data summary tables for all of the following response variables are shown in Appendix F, while a complete plant species list is shown in Appendix G.

Species diversity and composition

Change in quadrat-scale richness was best predicted by the Julian calendar day of the burn: earlier burns resulted in a greater increase in richness (up to 3 species/quadrat; $p = 0.007$; Figure 9). The model accounted for 37% of the variation ($R^2_{adj} = 0.374$). No significant changes in species richness occurred at the plot scale. For quadrat-scale Hill's $N_1$ diversity, the only significant predictor was average fuel loading, with greater increases in diversity with lower fuel

loads ($p = 0.05$; Figure 10). This model accounted for only 19% of the variation ($R^2_{adj} = 0.187$). Change in beta richness was not related to any of the predictor variables.

For pre- to post-burn Bray-Curtis distance at the plot scale, average dead fuel moisture was the best predictor, with greater shifts in composition at lower dead fuel moistures ($R^2_{adj} = 0.562$, $p < 0.001$; Figure 11). At the quadrat scale, average relative humidity (RH) was the best predictor of the pre- to post-burn Bray-Curtis distance, with greater shifts in composition occurring at lower RH ($R^2_{adj} = 0.226$, $p = 0.036$; Figure 12).

None of the ten individual functional groups (native perennial graminoids, native annual graminoids, native perennial forbs, native annual forbs, native woody species, exotic perennial graminoids, exotic annual graminoids, exotic perennial forbs, exotic annual forbs, or exotic woody species) showed a significant change in relative percent cover in response to burning conditions. Ignoring origin (native/exotic) did not change this result, nor did abundance of natives or exotics as a whole significantly change with burning conditions.

For the NMDS ordinations of species data, three-dimensional solutions were chosen for all sites, with stresses from 0.128 to 0.178 (Appendix H), a range generally regarded as fair in quality of interpretability (McCune and Grace 2002). Ordinations showed greater changes in composition in plots burned in the afternoon than in the morning only at the two sites at Johnson Prairie (Figure 13d & 13h). NMDS ordination of functional group composition at the plot level resulted in a three-dimensional solution (stress of 0.117). Plots representing morning and afternoon burns generally shifted in the same direction, with somewhat larger shifts in afternoon burns (Figure 14). Functional group abundance tended to shift toward native and exotic annual forbs and away from exotic perennials (Figure 14).

Vegetation structure

I was unable to detect a relationship between change in CV of height at either the quadrat or the plot scale and weather or fuel conditions during the burn. Variation in distribution of heights was best predicted by the Julian calendar day of the burn, with earlier burns resulting in greater increases in the number of 2-cm height classes ($p = 0.008$; Figure 15). This model accounted for 37% of the variation ($R^2_{adj} = 0.366$).

In geostatistical analyses of vegetation height, there was no significant relationship between the change in the range of spatial autocorrelation of height (i.e., the *scale* of autocorrelation) and weather or fuel conditions during the burn. The change in magnitude of spatial autocorrelation of height was significantly different between morning and afternoon burns, with morning burns resulting in a greater decrease ($p = 0.046$; Figure 16). A relationship between this change in magnitude and continuous predictors was only detected when the two plots with excessively high dead fuel moistures (30%) were removed. Greater decreases in the magnitude of the spatial autocorrelation of height then resulted from burns with higher dead fuel moisture ($n = 14$; $p = 0.012$; Figure 17). This model accounts for 38% of the variation ($R^2_{adj} = 0.377$). Thus, here, the scope of inference was limited to conditions of dead fuel moistures of ~25% and lower. Semivariogram curves for vegetation height in each plot are shown in Appendix I.

Finally, the interspersion and juxtaposition index (IJI) showed a highly significant relationship with wind speed at the time of burning ($p < 0.001$; Figure 18). This model accounted for 74% of the variation ($R^2_{adj} = 0.740$). Plots burned under conditions of very little to no wind resulted in a greater increase in interspersion of height classes. For this analysis, one outlier plot that burned at a high wind speed (average 3.7 m/s) was removed (leaving $n = 15$) due to an excessively large Cook's distance, leverage, and residual in the model. Log transformation of

wind speed was attempted first, but this did not reduce the extreme influence of the data point on the relationship so it was removed from the analysis. Thus the overall range of inference for wind speed conditions was reduced to 0.5 to 2.2 m/s.

As expected, plots burned in the afternoon had more area of bare or open ground in the post-burn growing season than plots burned in the morning ($p = 0.042$; Figure 19). However, there was no change in the spatial distribution or complexity of bare or open ground in response to burning conditions. Neither the change in the range of spatial autocorrelation (scale of the patch size) nor the change in the edge to area ratio for bare or open ground was related to any of the predictors. Semivariogram curves for bare or open ground in each plot are shown in Appendix J.

The optimal model predicting the change in variability (CV) of litter depth was a generalized additive model with average air temperature at the time of burning as the predictor. The hump-shaped relationship showed greater increases in CV of litter depth at intermediate air temperatures ($p = 0.011$; Figure 20), with the model explaining 76.2% of the deviance in the change of litter depth CV following burning.

**Discussion**

While the availability of specific host and nectar plants for species of prairie butterflies is likely the most important factor affecting quality of habitat (Ehrlich and Hanski 2004), other general aspects of habitat quality such as compositional and structural heterogeneity can also be critical to population survival (Weiss et al. 1988; Miskelly 2000; Fimbel 2004). Species and functional diversity supports the general availability of resource plants, while heterogeneity in the vertical and horizontal structure of vegetation increases microclimatic variability and resource patch distribution (Oliver et al. 2010), potentially increasing insect species diversity

(Jerrentrup et al. 2014; New 2014). In this study, post-burn species diversity was primarily affected by timing of burning within the season and fuel load, and not by time-of-burn weather conditions. Weather conditions did, however, affect the magnitude of compositional change. Both timing within the burn season and particular time-of-burn fuel conditions influenced the structure of vegetation height and litter depth, within a given range of conditions.

The modest relationship between calendar day of burning and post-burn richness (Figure 9) tends to support studies in other systems in which richness increased more from growing season fires than dormant season fires (Biondini et al. 1989; Copeland et al. 2002; Knapp et al. 2007). In western Pacific Northwest grasslands, however, most of the growing season has passed before the prescribed fire season begins in earnest. Indeed, even the experimental fires in this study that occurred early in the burn season were too late to affect any dominant plant species. Thus the small increase in species richness after earlier burns is less likely to relate to plant phenology than to the additional time afforded before the onset of fall rains. More immediate rainfall following later-season burns may lead to larger nutrient losses from the system (Hamman et al. 2008), while the added solar warming of bare post-burn soils for earlier-season burns might encourage regrowth or stimulate species that might not otherwise "green up" before cooler temperatures set in (Copeland et al. 2002).

Change in alpha (quadrat-scale) diversity was most influenced by fuel loading at the time of the burn, with larger increases under lower fuel loads (Figure 10), although the relationship was weak ($R^2_{adj} = 0.187$). Fuel loading is an important aspect of fuel continuity, and when an area with high fuel continuity burns, it is likely to increase total consumption (Cheney et al. 1998; see Chapter 1). Reduced continuity where fuel loads are lower can thus fragment consumption; this

could leave areas of variable litter/thatch that may prevent dominance by a few species and thereby increase diversity (Hickman et al. 2004).

Richness and diversity changed only at the quadrat scale. This suggests that the processes that promote species establishment are operating at fine spatial scales. For example, reduced fuel continuity from lower fuel loads may only affect patchiness of burns at fine scales. Similarly, soil nutrients or warming after early-season burns may only prompt a change in distribution of species from coarse scales to finer scales, rather than allowing for new species to enter a plot.

Burn-day weather and fuel conditions appeared to have greater influence on composition than on richness or diversity. At the plot scale, a lower dead fuel moisture at the time of burning resulted in a greater change in composition between pre- and post-burn communities (Figure 11). At the quadrat scale, a somewhat weaker relationship emerged with lower RH during a burn producing larger community shifts (Figure 12). Previous studies of fire effects on community composition have focused either on fire intensity (Morrison 2002) or fire season (Biondini et al. 1989), which are likely to have similar effects as fire weather (i.e., more intense, hotter, or drier burns may stimulate greater change). In this study, larger shifts in composition with drier burn-day weather generally support these results of past studies, illustrating that timing of a burn, even over the course of a day, can influence community outcomes.

Depending upon management or restoration goals, the direction of these shifts in composition may be of interest; ordination of abundance data can help to visualize whether communities are changing in similar directions. Here, ordinations of each site by species (Figures 13a – 13h) and of all sites together by functional group (Figure 14) showed how time of burning (morning vs. afternoon) influenced compositional change. At most sites, quadrats generally moved in similar directions in ordination space (Figure 13). It is notable that the two

sites at Johnson Prairie, where morning and afternoon RH differed by >40 percentage points (Appendix D), experienced much larger changes in community composition in afternoon burns (Figure 13d, 13h), supporting the larger compositional changes found when burning at lower RH (Figure 12). For functional group composition (Figure 14), both morning- and afternoon-burned plots tended to shift in the same direction – away from exotic perennial forbs and toward both exotic and native annual forbs – but with somewhat larger shifts in afternoon-burned plots. Increased abundance of annuals post-burn is expected, as annuals are able to take over available growing space quickly (Trabaud 1987), indicating that afternoon-burned plots likely produced more of this available growing space.

Overall variation in height (CV) within plots or quadrats did not change with burning conditions. However, when height distributions were considered, there was a moderately strong relationship between the Julian calendar day of burning and the average number of height classes in a quadrat (Figure 15). Although the size of the effect was small (maximum change of 0.9), the number of sample points within a quadrat was also small (7), indicating that more sampling points within quadrats might be able to detect a greater effect. The additional soil moisture that is often present in patches of the prairie earlier in the burn season in the Pacific Northwest (Hamman et al. 2011) may be enough to help create a 'patchier' burn that could lead to this diversification of the height structure post-burn. Unfortunately, in addition to having fewer experimental burns during the later part of the burn season, soil moisture measurements were not taken in this study. Future work on fire effects should consider this factor as a potential predictor of changes in vegetation structure than can be affected by the spatial pattern of a burn.

There were no significant changes in the scale of vegetation patches of similar height in response to burning conditions. However, the magnitude of the spatial autocorrelation of

vegetation height was influenced by the time of day of burning (Figure 16) and, specifically, by the average dead fuel moisture, within a somewhat limited range of moisture conditions (Figure 17). The two plots that were removed from the dataset for this analysis due to high leverage had high fuel moistures that would likely not produce fire effects strong enough to meet ecological objectives (e.g., thatch consumption). Without these outlier plots, the magnitude or intensity of autocorrelation of vegetation height decreased more when burning under higher fuel moistures (Figure 17). This suggests that the higher moistures in this range may fragment fuel consumption and severity within a burn enough to increase the heterogeneity and distribution of the post-burn vegetation height structure.

To my knowledge, few studies have examined this effect of burning conditions on the vertical structure of grassland vegetation. However, others have examined the influence of different grazing systems on the spatial distribution of vegetation types using variogram analysis. Harris et al. (2003) found that grazed areas of rangelands in Utah had both a greater range (scale) and magnitude (intensity) of autocorrelation of photosynthetic vegetation cover, indicating a potentially homogenizing effect of grazing. In my study, the increase in heterogeneity of height structure via a decrease in magnitude of autocorrelation highlights the potential for using particular burning conditions (i.e., morning burns with higher dead fuel moistures) to promote a vegetation canopy that provides more diverse microclimates for small organisms at a fine scale (see Figure 8).

Finally, I found a strong relationship between average wind speed and the post-burn interspersion and juxtaposition index (IJI) of height classes (Figure 18). Greater interspersion and juxtaposition of patches of differing height can enhance the local diversity of microhabitats at fine scales (McGarigal and Marks 1995). The strong relationship with wind (decreasing IJI

with increasing wind) across a small range of speeds (0.5 – 2.2 m/s) could possibly be due to the spatial complexity of fire types that results when burning with little wind. In these conditions, flame fronts are more likely to shift between head, backing, and flanking fires due to local thermal activity rather than a prevailing wind (Cheney et al. 1998). The resulting mosaic of fuel consumption may contribute to the structural heterogeneity of vegetation height that emerges in the following growing season. While the effect size (up to a 9 percentage point change) is somewhat small, the strength of the relationship presents a fascinating connection between burning conditions and post-burn vegetation structure.

In this study, only the total amount of bare or open ground, and not its spatial distribution, was influenced by burning conditions (Figure 19). Hotter and drier burns will generally promote more complete fuel consumption (Knapp et al. 2005), increasing the total bare ground, but this effect may be counteracted by the positive effect on vegetation resulting from an increase in growing space. However, the increases in bare or open ground with drier afternoon burns indicates that other mechanisms may keep those spaces open, such as increased pocket gopher activity in response to regrowth of vegetation (Spencer et al. 1985), or drier soils following afternoon burns inhibiting spring growth. The lack of changes in spatial distribution of bare or open ground (i.e., patch size or edge-to-area ratio) suggests that the influence of patchier consumption in burns conducted in higher fuel moisture conditions does not extend to this structural component in the post-burn growing season. It is likely that many factors in combination affect the shape and distribution of bare ground in the intervening time period.

The expectation that the variability in litter and thatch depth following fire should be higher in cooler or more humid burns also relates to the patchy nature of fuel consumption in these conditions. The resulting variability in litter depth can provide a more diverse array of

microhabitats for larval insects during times of climatic stress. Here, a more complex association with burning conditions emerged. A hump-shaped relationship between CV of litter depth and air temperature during burning was the best model (Figure 20), aligning in the form of the intermediate disturbance hypothesis (Connell 1978). The coolest burns effected little change in the litter and thatch, whereas the hottest burns decreased variability by maximizing consumption. Burns conducted at moderate air temperatures (18 – 25 $^{o}$C) appeared to increase overall variation by promoting a mosaic of consumption.

In combination, compositional and structural outcomes suggest that burning under intermediate or moderate conditions (air temperature, relative humidity, fuel moisture, or wind) can enhance habitat heterogeneity. In this study, the conditions sampled focused on the typical range in which prescribed burns are conducted, including some more extreme high moisture conditions on the edge of what is reasonable to burn in to obtain adequate fire effects. Compositional heterogeneity was most influenced by the time of year of burning, while compositional change was most affected by the localized weather conditions during the burn. Structural heterogeneity was also affected by the time of year of burning (for diversity of potential microclimates) and by daily weather conditions (for the spatial distribution and interspersion of this variation). Given that site selection for this study was based on potential for butterfly habitat (i.e., free of shrubs, low structure, moderate native component), the generalizability of these results may not extend to other types of habitats.

One limitation of this study is that it includes only one year of post-burn vegetation data and one year of experimental burns. Multiple years of measurement would provide a more comprehensive picture of how compositional and structural heterogeneity changes over time (Gross and Romo 2010) and the persistence of initial effects. Because prairies in this region are

typically burned every 2 – 3 years, 1 – 2 years of spring growing season data may be sufficient. Interannual variability in both the burn season conditions and post-burn season (i.e., autumn) weather can also have an influence on spring vegetation response (Lesica and Martin 2003), thus experimentally burning in different years may help elucidate how longer-term weather patterns combine with day-of-burn conditions to affect composition and structure of prairie vegetation.

A prairie restoration matrix generally consists of a combination of treatments including prescribed fire, herbicide, and seeding or planting of native species (Stanley et al. 2011). This study examined the specific effects of prescribed fire independent of the interactions with other management efforts, but the combination of these actions has the potential to influence the compositional and structural heterogeneity of vegetation responses and should be examined in future research. As invasives are removed and the native seed bank is replenished, however, other treatments may lessen in importance while fire remains critical as a habitat maintenance strategy (Hamman et al. 2011) and a fundamental ecological process (Storm and Shebitz 2006).

For land and fire managers, habitat restoration and enhancement for particular species or groups of butterflies via seeding or planting of host and nectar species is a primary objective; when these plants are present, the promotion of beneficial habitat structure is a secondary objective (Fimbel 2004). Here, I show that 1) targeting more specific conditions for burn prescriptions can enhance habitat heterogeneity that benefits threatened populations, and 2) these targets are within the range of burn conditions used in western Washington prairies. I also provide support for the concept that "patchier" burns under mild conditions can have quantifiable effects on the post-burn vegetation in the following year, highlighting important links in grasslands among moisture conditions, fuel continuity, spatial patterns of consumption, and habitat structure.

## Figures

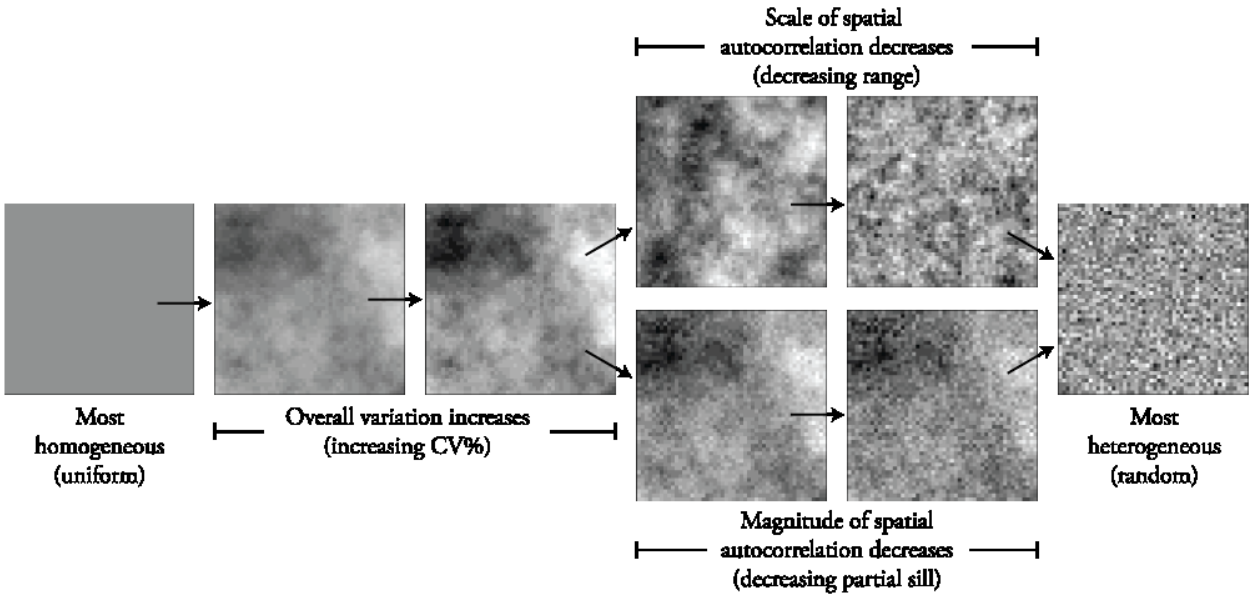


**Figure 8. Example of how changes in different aspects of spatial heterogeneity (overall variation, scale of autocorrelation, and magnitude of autocorrelation) can manifest visually; image created and copyrighted by Anthony Darrouzet-Nardi 2009.**

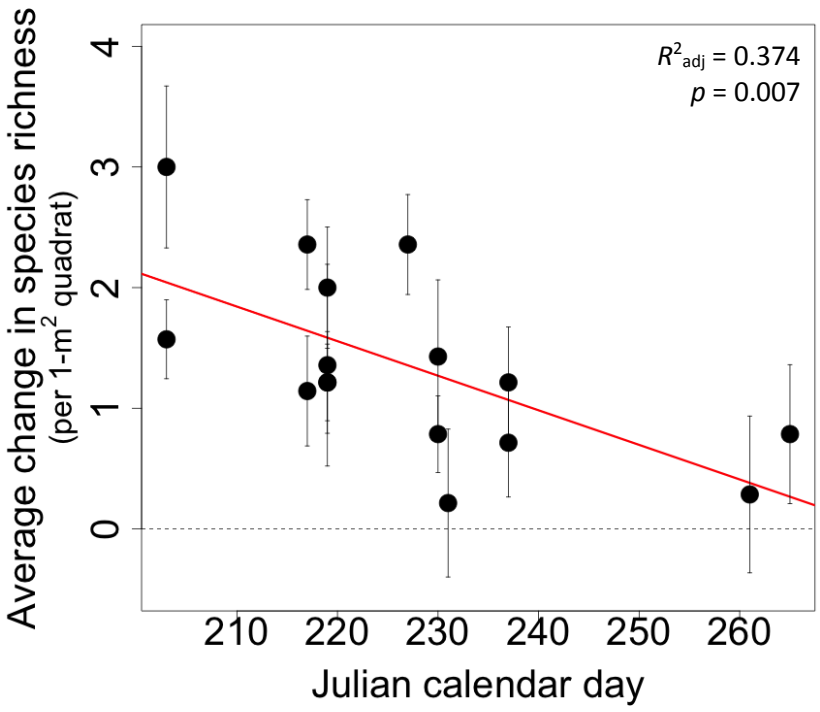


**Figure 9. Mean change in species richness at the 1-m² scale as a function of the day of the year a plot was burned. Error bars represent standard error of the mean.**

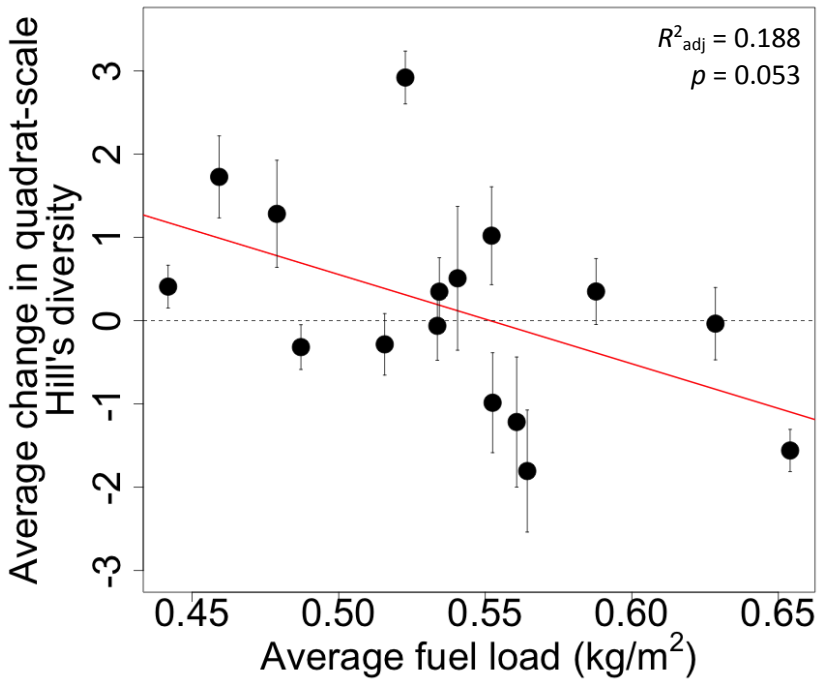


**Figure 10. Mean change in Hill's $N_1$ diversity index at the 1-m² scale as a function of the average estimated fuel loading prior to burning. Error bars represent standard error of the mean.**

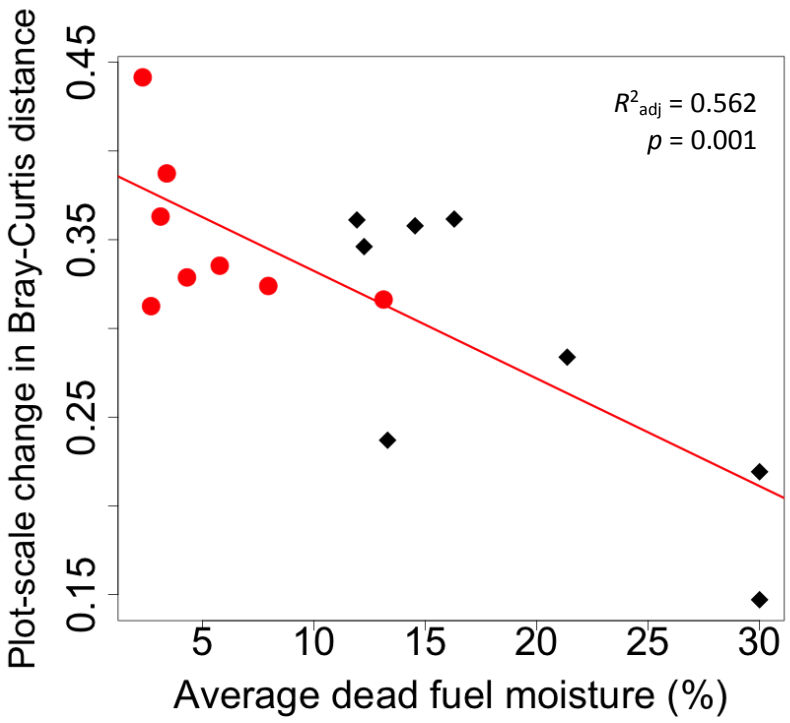


**Figure 11. Bray-Curtis distance between pre- and post-burn communities for average plot composition as a function of the average dead fuel moisture during burning. Morning burns are black diamonds and afternoon burns are red circles.**

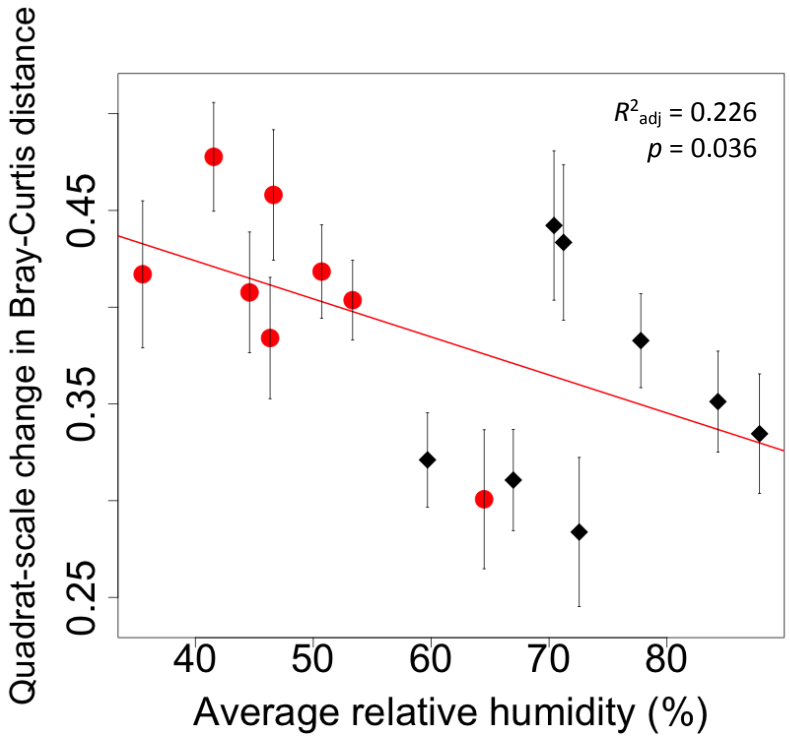


**Figure 12. Average Bray-Curtis distance between pre- and post-burn communities at the 1-m² scale as a function of the average relative humidity during burning. Error bars represent standard error of the mean. Morning burns are black diamonds and afternoon burns are red circles.**

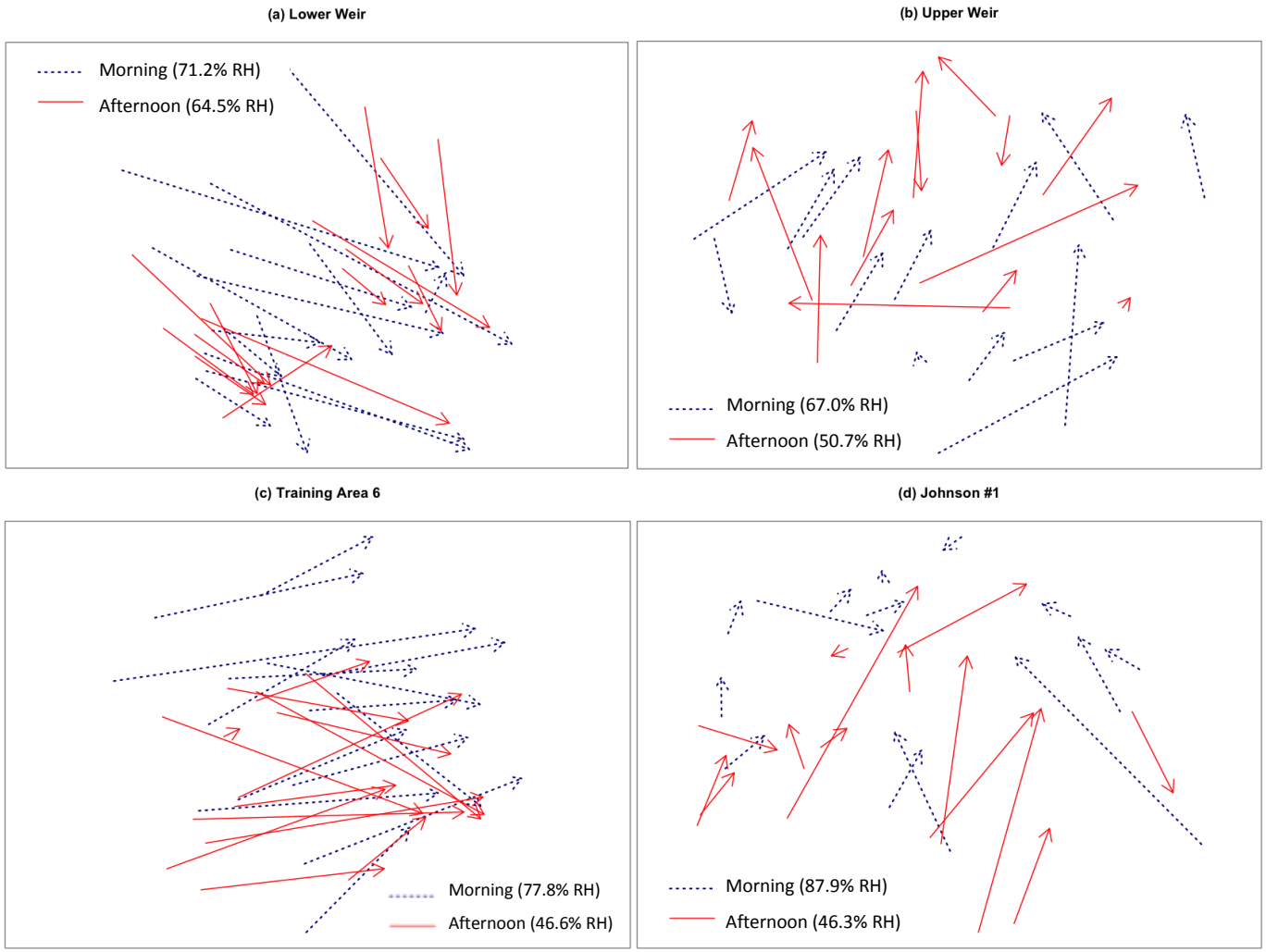


**Figure 13a – 13d. First two dimensions of non-metric multidimensional scaling (NMDS) ordinations of quadrat-scale species abundance data at each site. Arrows display the pre- to post-burn change of each quadrat across ordination space, with blue dashed lines showing morning burns and red solid lines showing afternoon burns. Relative humidity (RH) during burning shown for each plot.**

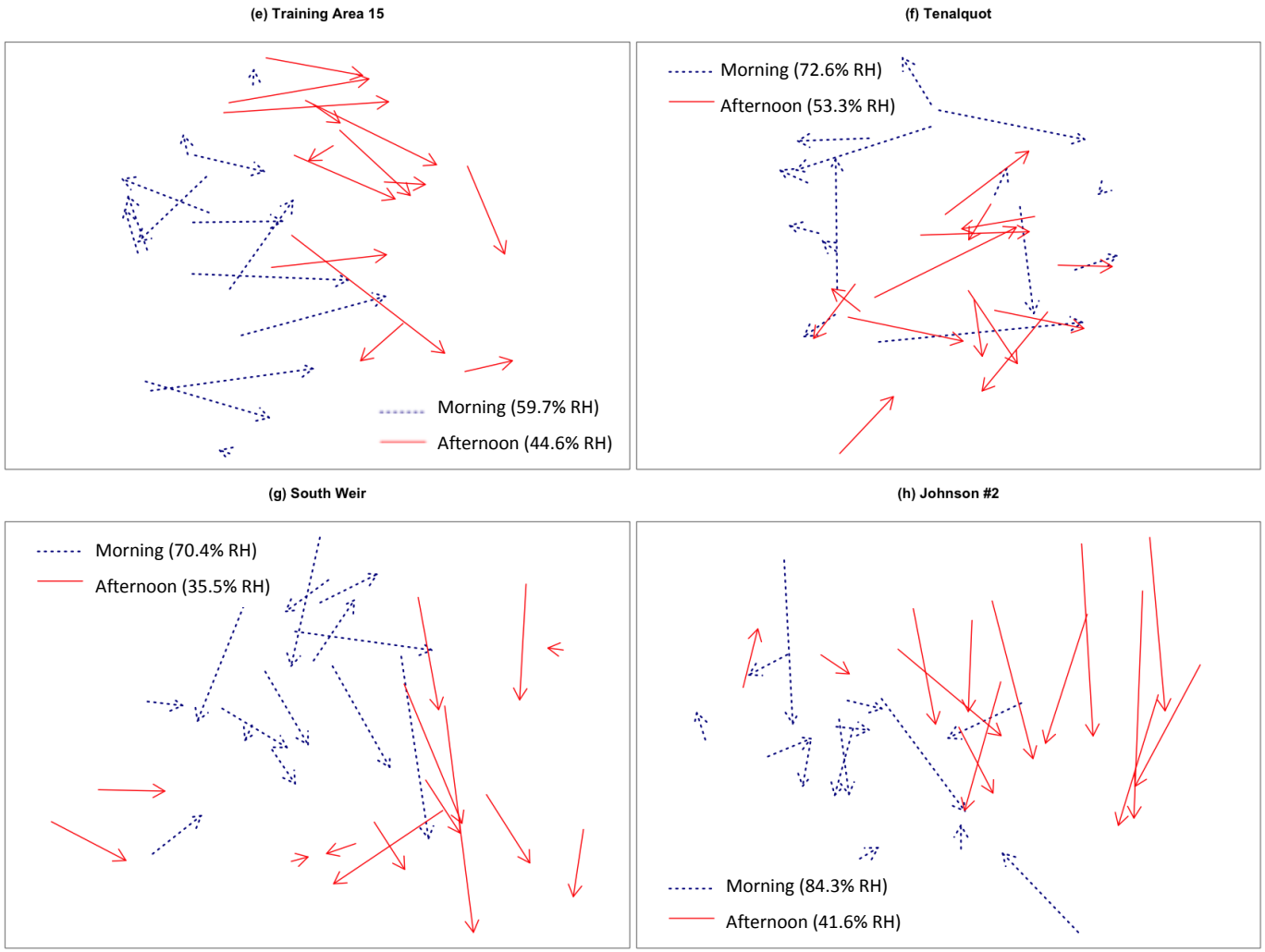


**Figure 13e – 13h. First two dimensions of non-metric multidimensional scaling (NMDS) ordinations of quadrat-scale species abundance data at each site. Arrows display the pre- to post-burn change of each quadrat across ordination space, with blue dashed lines showing morning burns and red solid lines showing afternoon burns. Relative humidity (RH) during burning shown for each plot.**

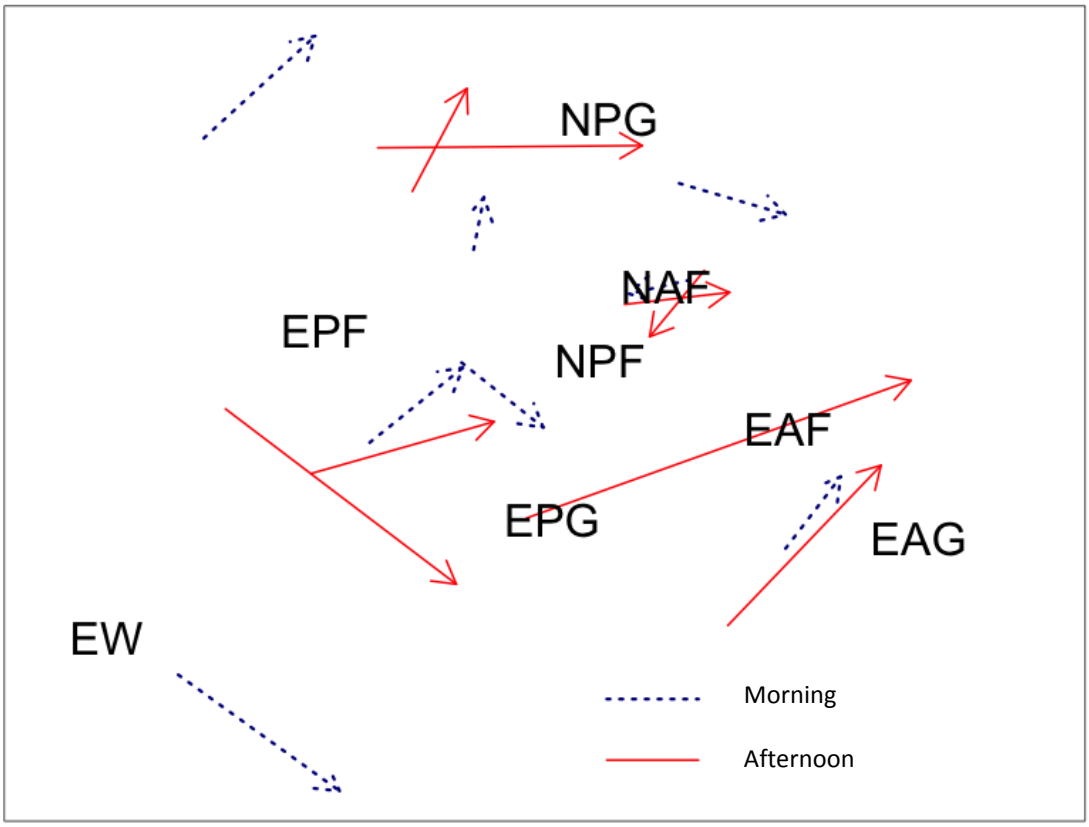


**Figure 14. First two dimensions of non-metric multidimensional scaling (NMDS) ordination of plot-scale average functional group (by origin) abundance data. Arrows display the pre- to post-burn change of each plot across ordination space, with blue dashed lines showing morning burns and red solid lines showing afternoon burns. NPG = native perennial graminoids; NPF = native perennial forbs; NAF = native annual forbs; EPG = exotic perennial graminoids; EPF = exotic perennial forbs; EAF = exotic annual forbs; EAG = exotic annual graminoids; EW = exotic woody shrubs.**

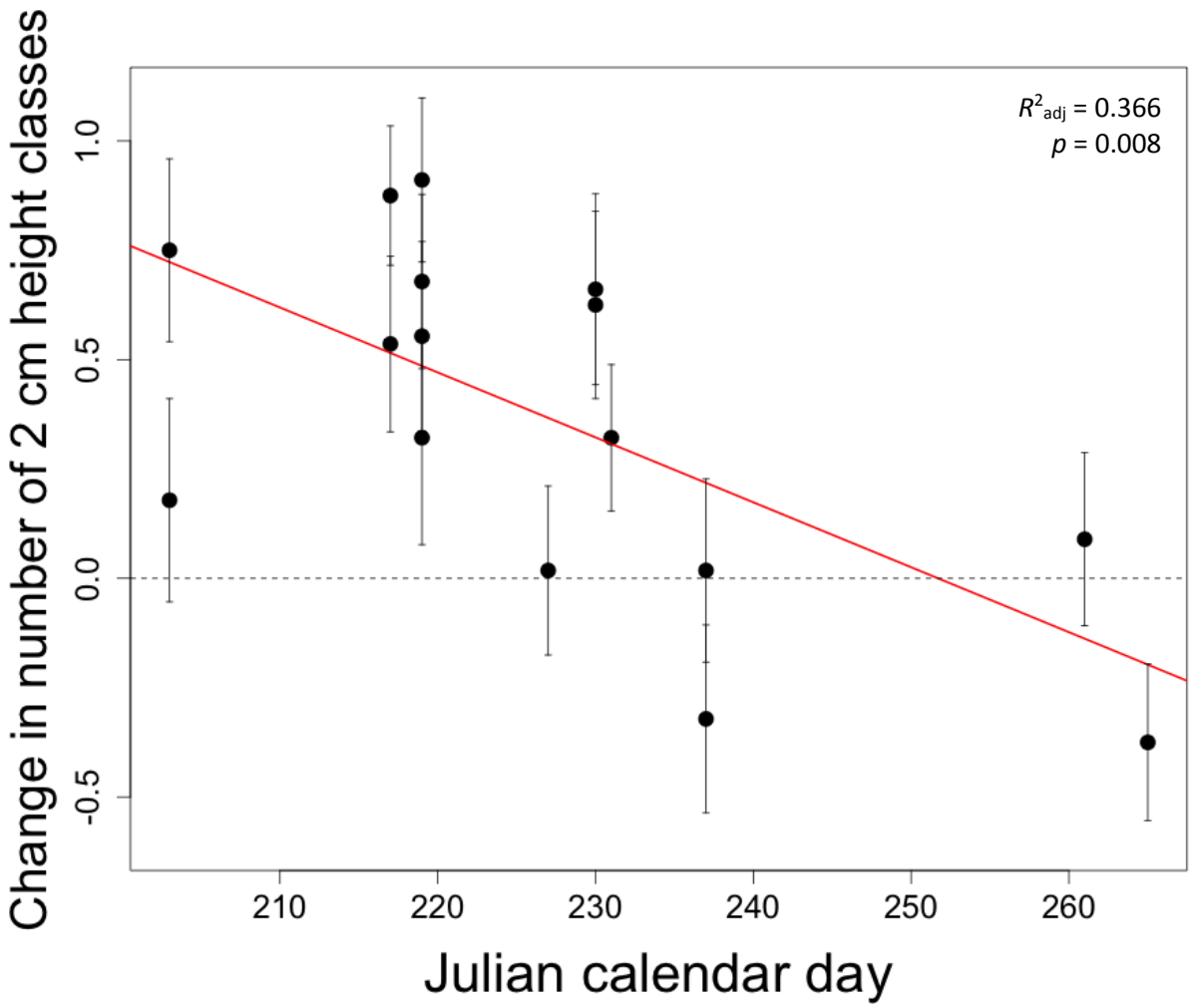


**Figure 15. Average change in the number of 2 cm height classes (under 30 cm) at the 1-m² scale as a function of the day of the year in which an area was burned. Error bars represent standard error of the mean.**

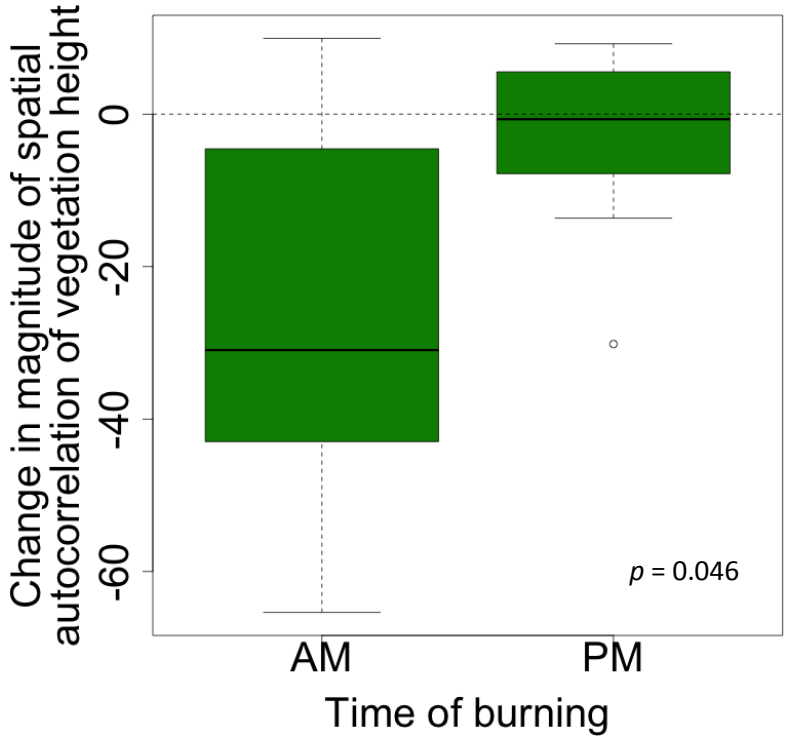


**Figure 16. Box-and-whisker plot of the change in the magnitude of spatial autocorrelation of vegetation height as a function of the time of day of burning.**

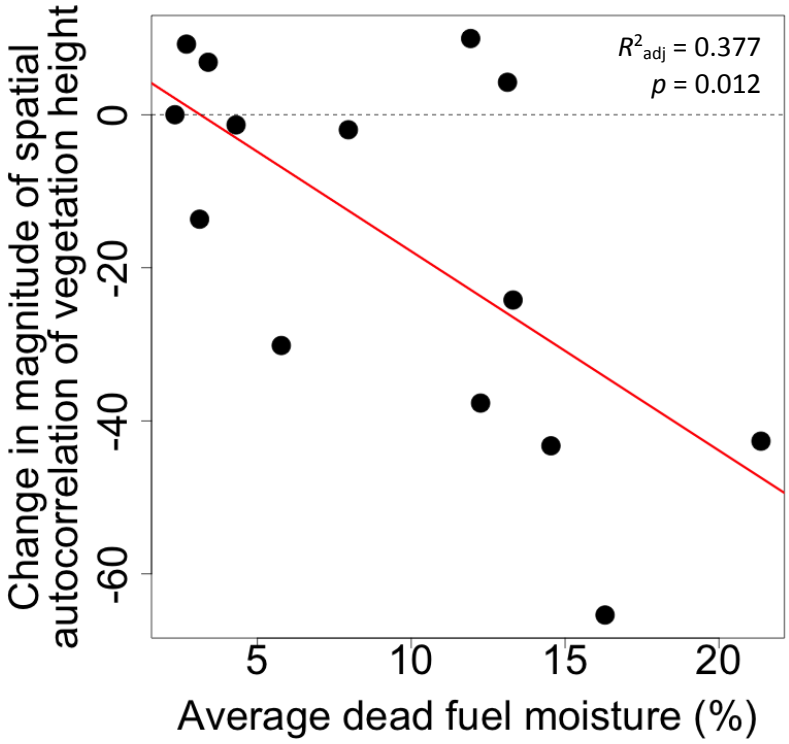


**Figure 17. Change in the magnitude of spatial autocorrelation of vegetation height as a function of the average dead fuel moisture prior to burning.**

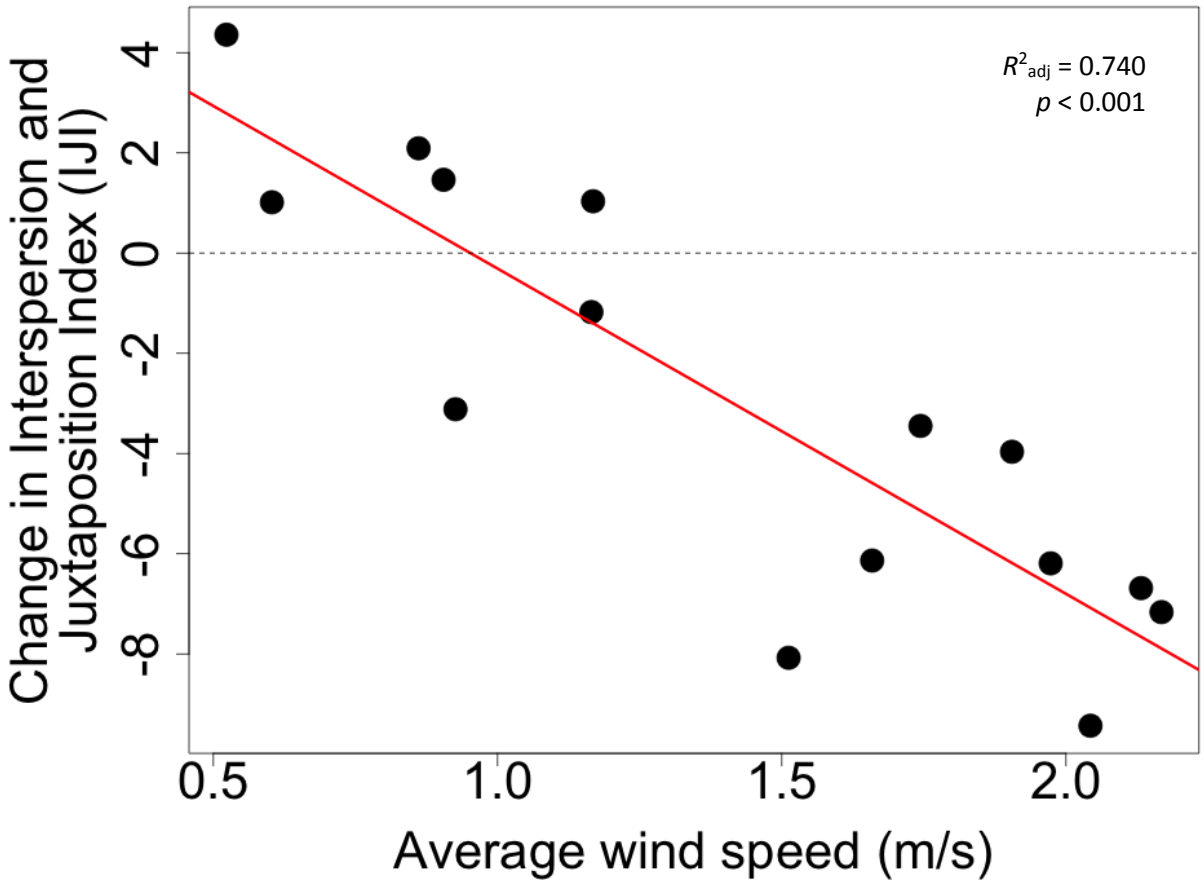


**Figure 18. Change in the interspersion and juxtaposition index (IJI) for 2 cm vegetation height classes within a plot as a function of the average wind speed during burning.**

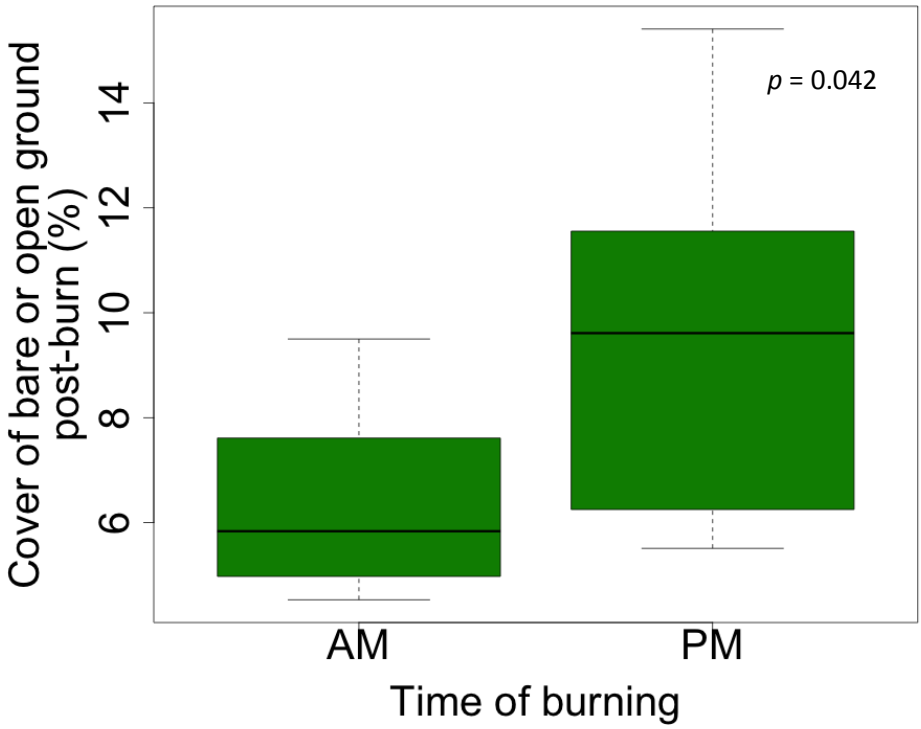


**Figure 19. Distribution of the post-burn percent cover of bare or open ground for morning-burned and afternoon-burned plots.**

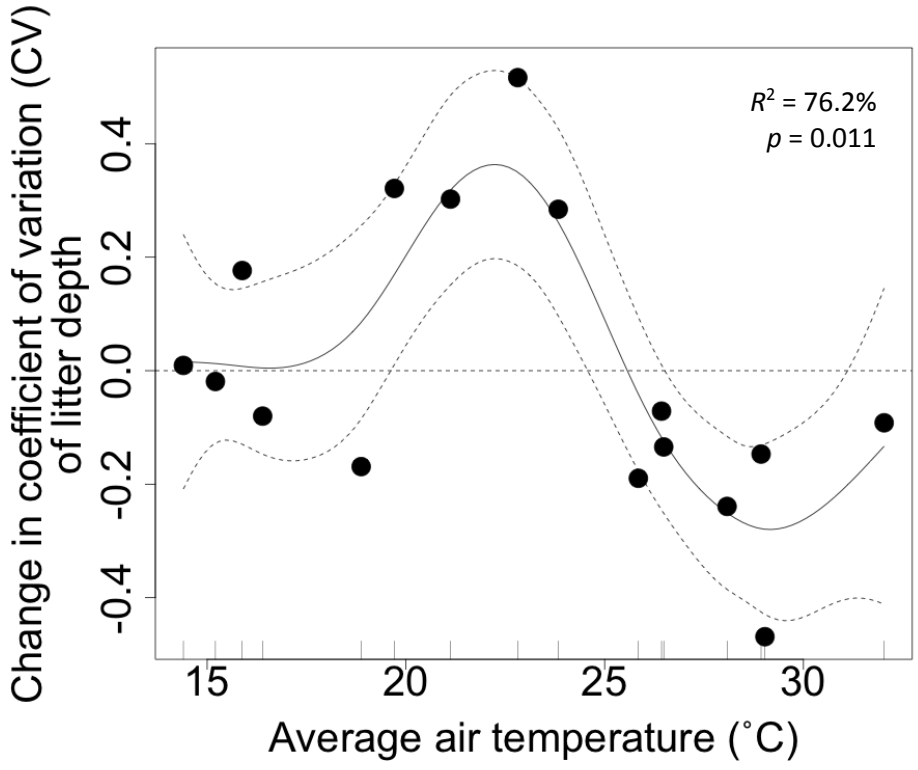


**Figure 20. Generalized additive model for the change in the coefficient of variation (CV) of litter depth within a plot as a function of the average air temperature during burning.**

## Tables

**Table 7.** Summary of explanatory and response variables used in univariate multiple regression models

| **Explanatory Variables** | |
|---|---|
| Average air temperature (°C) | |
| Average relative humidity (%) | |
| Average wind speed (m/s) | |
| Average and CV of live fuel moisture (%) | |
| Average and CV of dead fuel moisture (%) | |
| Average and CV of fuel loading (kg/m$^2$) | |
| Average and CV of litter depth (cm) | |
| Cover of bare or open ground (%) | |
| Burn duration (min) | |
| Julian calendar day | |
| **Response Variables – Diversity and composition** | |
| Mean change in quadrat-scale species richness & change in plot-scale species richness | |
| Mean change in quadrat-scale Hill's $N_1$ species diversity index | |
| Change in beta richness | |
| Pre- to post-burn Bray-Curtis distance for average species composition | |
| Average pre- to post-burn Bray-Curtis distance for species composition | |
| Average change in relative percent cover of all ten functional groups | |
| **Response Variables – Vegetation structure** | **Interpretation** |
| Change in coefficient of variation (CV) of vegetation height (at plot and quadrat scale) | Positive change ⇒ increase in variability of microclimates |
| Change in average number of 2 cm vegetation height classes in a quadrat (under 30 cm) | Positive change ⇒ increase in variability of microclimates |
| Change in range of spatial autocorrelation of vegetation height | Negative change ⇒ increase in variability of microclimates |
| Change in magnitude of spatial autocorrelation of vegetation height | Negative change ⇒ increase in variability of microclimates |
| Change in the Interspersion and Juxtaposition Index (IJI) of vegetation height | Positive change ⇒ increase in variability of microclimates |
| Change in range of spatial autocorrelation of bare or open ground | Negative change ⇒ increase in edge complexity |
| Change in edge-to-area ratio of bare or open ground | Positive change ⇒ increase in edge complexity |
| Change in coefficient of variation (CV) of litter depth | Positive change ⇒ increase in variability of microclimates |

**Literature Cited**

Allison, P. D. 1990. Change scores as dependent variables in regression analysis. Sociological Methodology **20**:93-114.

Augustine, D. J., J. D. Derner, and D. P. Smith. 2014. Characteristics of burns conducted under modified prescriptions to mitigate limited fuels in a semi-arid grassland. Fire Ecology **10**:36-47.

Biondini, M. E., A. A. Steuter, and C. E. Grygiel. 1989. Seasonal fire effects on the diversity patterns, spatial distribution and community structure of forbs in the Northern Mixed Prairie, USA. Vegetatio **85**:21-31.

Black, S. H., C. Fallon, R. Hatfield, and C. Mazzacano. 2013. Controlled burning and Mardon skipper: summary of Mardon skipper Coon Mountain burn site occupancy study 2009-2013. Final report to US Forest Service, Oregon Zoo and US Fish and Wildlife Service. Xerces Society, Portland, Oregon.

Bonebrake, T. C., C. L. Boggs, J. M. McNally, J. Ranganathan, and P. R. Ehrlich. 2010. Oviposition behavior and offspring performance in herbivorous insects: consequences of climatic and habitat heterogeneity. Oikos **119**:927-934.

Bradstock, R. A., M. Bedward, A. M. Gill, and J. S. Cohn. 2005. Which mosaic? A landscape ecological approach to evaluating interactions between fire regimes, habitats and animals. Wildlife Research **32**:409-423.

Branson, D. H., and L. T. Vermeire. 2007. Grasshopper egg mortality mediated by oviposition tactics and fire intensity. Ecological Entomology **32**:128-134.

Branson, D. H., and L. T. Vermeire. 2013. Heat dosage and oviposition depth influence egg mortality of two common rangeland grasshopper species. Rangeland Ecology and Management **66**:110-113.

Brooks, M. L. 2002. Peak fire temperatures and effects on annual plants in the Mojave Desert. Ecological Applications **12**:1088-1102.

Burgan, R. E., and R. C. Rothermel. 1984. BEHAVE: fire behavior prediction and fuel modeling system – FUEL subsystem. Gen. Tech. Rep. INT-167. Ogden, UT: U.S. Department of Agriculture, Forest Service, Intermountain Forest and Range Experiment Station.

Burrows, S. N., S. T. Gower, M. K. Clayton, D. S. Mackay, D. E. Ahl, J. M. Norman, and G. Diak. 2002. Application of geostatistics to characterize leaf area index (LAI) from flux tower to landscape scales using a cyclic sampling design. Ecosystems **5**:667-679.

Cheney, N. P., J. S. Gould, and W. R. Catchpole. 1998. Prediction of fire spread in grasslands. International Journal of Wildland Fire **8**:1-13.

CNLM (Center for Natural Lands Management). 2014. Puget Sound Ecological Fire Program 2014 Summary Report. Olympia, Washington.

Cochrane, J. F., and P. Delphey. 2002. Status assessment and conservation guidelines: Dakota Skipper, *Hesperia dacotae* (Skinner) (Lepidoptera: Hesperiidae), Iowa, Minnesota, North Dakota, South Dakota, Manitoba and Saskatchewan. United States Fish and Wildlife Service, Minneapolis.

Connell, J. H. 1978. Diversity in tropical rain forests and coral reefs. Science **199**:1302-1310.

Copeland, T. E., W. Sluis, and H. F. Howe. 2002. Fire season and dominance in an Illinois tallgrass prairie restoration. Restoration Ecology **10**:315-323.

Dale, M. R. T. 2003. Spatial pattern analysis in plant ecology. Cambridge University Press, Cambridge, United Kingdom.

Darrouzet-Nardi, A. 2010. Landscape heterogeneity of differently aged soil organic matter constituents at the forest-alpine tundra ecotone, Niwot Ridge, Colorado, U.S.A. Arctic, Antarctic, and Alpine Research **42**:179-187.

Davis, F. W., M. I. Borchert, and D. C. Odion. 1989. Establishment of microscale vegetation pattern in maritime chaparral after fire. Vegetatio **84**:53-67.

de Angelis, A., S. Bajocco, and C. Ricotta. 2012. Phenological variability drives the distribution of wildfires in Sardinia. Landscape Ecology **27**:1535-1545.

DeBano, L. F., D. G. Neary, and P. F. Ffolliott. 1998. Fire's effects on ecosystems. John Wiley & Sons, New York.

Eilers, S., L. B. Pettersson, and E. Ockinger. 2013. Micro-climate determines oviposition site selection and abundance in the butterfly *Pyrgus armoricanus* at its northern range margin. Ecological Entomology **38**:183-192.

Erlich, P. R., and I. Hanski. 2004. On the wings of checkerspots: a model system for population biology. Oxford University Press, Oxford, United Kingdom.

ESRI (Environmental Systems Research Institute). 2013. ArcGIS Desktop: Release 10.2. Redlands, CA, USA.

Fimbel, C. 2004. Habitat enhancement for rare butterflies on Fort Lewis prairies. The Nature Conservancy Report, Olympia, WA, USA.

Fortin, M., and M. Dale. 2005. Spatial analysis: a guide for ecologists. Cambridge University Press, Cambridge, United Kingdom.

Gross, D. V., and J. T. Romo. 2010. Burning history, time of burning, and year effects on plant community structure and heterogeneity in Fescue Prairie. Botany **88**:1-12.

Haining, R. 2003. Spatial data analysis: theory and practice. Cambridge University Press, Cambridge, United Kingdom.

Hamman, S. T., I. C. Burke, and E. E. Knapp. 2008. Soil nutrients and microbial activity after early and late season prescribed burns in a Sierra Nevada mixed conifer forest. Forest Ecology and Management **256**:367-374.

Hamman, S. T., P. W. Dunwiddie, J. L. Nuckols, and M. McKinley. 2011. Fire as a restoration tool in Pacific Northwest prairies and oak woodlands: challenges, successes, and future directions. Northwest Science **85**:317-328.

Hanski, I. 2003. Biology of extinctions in butterfly metapopulations. Pages 557-602 in C. L. Boggs, W. B. Watt, and P. R. Ehrlich, editors. Butterflies, ecology and evolution, taking flight. University of Chicago Press, Chicago, USA.

Harris, A. T., G. P. Asner, and M. E. Miller. 2003. Changes in vegetation structure after long-term grazing in pinyon-juniper ecosystems: integrating imaging spectroscopy and field studies. Ecosystems **6**:368-383.

Haugo, R. D., C. B. Halpern, and J. D. Bakker. 2011. Landscape context and long-term tree influences shape the dynamics of forest-meadow ecotones in mountain ecosystems. Ecosphere **2**:art91.

Heinze, G., and M. Schemper. 2002. A solution to the problem of separation in logistic regression. Statistics in Medicine **21**:2409-2419.

Hickman, K. R., D. C. Hartnett, R. C. Cochran, and C. E. Owensby. 2004. Grazing management effects on plant species diversity in tallgrass prairie. Rangeland Ecology and Management **57**:58-65.

Hill, M. O. 1973. Diversity and evenness: a unifying notation and its consequences. Ecology **54**:427-432.

Hitchcock, C. L., and A. Cronquist. 1973. Flora of the Pacific Northwest. University of Washington Press, Seattle, WA, USA.

Hoffman, A. A., S. L. Chown, and S. Clusella-Trullas. 2013. Upper thermal limits in terrestrial ectotherms: how constrained are they? Functional Ecology **27**:934-949.

Isaaks, E. H., and R. M. Srivastava. 1989. An introduction to applied geostatistics. Oxford University Press, New York, NY, USA.

Jerrentrup, J. S., N. Wrage-Monnig, K. U. Rover, and J. Isselstein. 2014. Grazing intensity affects insect diversity via sward structure and heterogeneity in a long-term experiment. Journal of Applied Ecology **51**:968-977.

Kelly, C., and T. D. Price. 2005. Correcting for regression to the mean in behavior and ecology. The American Naturalist **166**:700-707.

Kindvall, O. 1996. Habitat heterogeneity and survival in a bush cricket metapopulation. Ecology **77**:207-214.

Knapp, E. E., J. E. Keeley, E. A. Ballenger, and T. J. Brennan. 2005. Fuel reduction and coarse woody debris dynamics with early season and late season prescribed fire in a Sierra Nevada mixed conifer forest. Forest Ecology and Management **208**:383-397.

Knapp, E. E., and J. E. Keeley. 2006. Heterogeneity in fire severity within early season and late season prescribed burns in a mixed-conifer forest. International Journal of Wildland Fire **15**:37-45.

Knapp, E. E., D. W. Schwilk, J. M. Kane, and J. E. Keeley. 2007. Role of burning season on initial understory vegetation response to prescribed fire in a mixed conifer forest. Canadian Journal of Forest Research **37**:11-22.

Lascar Electronics Ltd. 2012. EL-USB-1-PRO. Lascar Electronics Ltd., Salisbury, United Kingdom.

Lesica, P., and B. Martin. 2003. Effects of prescribed fire and season of burn on recruitment of the invasive exotic plant, *Potentilla recta*, in a semiarid grassland. Restoration Ecology **11**:516-523.

Li, H., and J. F. Reynolds. 1995. On definition and quantification of heterogeneity. Oikos **73**:280-284.

Linders, M., and K. Lewis. 2013. Captive rearing and translocation of Taylor's checkerspot butterfly (*Euphydryas editha taylori*): South Puget Sound, Washington, 2012 – 2013. 2013 Annual Report to the US Fish and Wildlife Service, Joint Base Lewis-McChord Fish and Wildlife Program and JBLM-ACUB Technical Review Committee, 17 December 2013.

Magurran, A. E. 2004. Measuring biological diversity. Blackwell Science Ltd., Oxford, UK.

Martin, R. A., and S. T. Hamman. Ignition patterns influence fire effects and plant communities in Pacific Northwest prairies. Manuscript submitted for publication.

McCune, B., and J. B. Grace. 2002. Analysis of ecological communities. MjM Software Design, Gleneden Beach, OR, USA.

McDonald, B. 2002. A teaching note on Cook's distance – a guideline. Research Letters in the Information and Mathematical Sciences **3**:127-128.

McGarigal, K., and B. J. Marks. 1995. FRAGSTATS: spatial pattern analysis program for quantifying landscape structure. U.S. Forest Service General Tech. Report PNW-GTR-351.

McGarigal, K., S. A. Cushman, and E. Ene. 2012. FRAGSTATS v4: spatial pattern analysis program for categorical and continuous maps. University of Massachusetts, Amherst, USA.

Miller, C., and D. L. Urban. 2000. Connectivity of forest fuels and surface fire regimes. Landscape Ecology **15**:145-154.

Miskelly, J. W. 2000. Habitat requirements and conservation of the butterflies *Euchloe ausonides insulanus* (Pieridae) and *Euphydryas editha taylori* (Nymphalidae) in southwestern British Columbia. Unpublished master's thesis, University of Victoria, British Columbia.

Morrison, D. A. 2002. Effects of fire intensity on plant species composition of sandstone communities in the Sydney region. Austral Ecology **27**:433-441.

Neary, D. G., C. C. Klopatek, L. F. DeBano, and P. F. Ffolliott. 1999. Fire effects on belowground sustainability: a review and synthesis. Forest Ecology and Management **122**:51-71.

New, T. R. 2014. Insects, fire, and conservation. Springer International Publishing, Switzerland.

Nielsen-Kellerman. 2012. Kestrel 4000 Weather & Environmental Meter. Nielsen-Kellerman, 21 Creek Circle, Boothwyn, PA 19061.

NOAA (National Oceanic and Atmospheric Administration). 2008. Guide to Grassland Curing Observations for National Weather Grassland Fire Danger Forecast Indices (GFDI).

NRCS (Natural Resources Conservation Service). 2015. Web Soil Survey. URL http://websoilsurvey.nrcs.usda.gov/app/HomePage.htm [accessed on 1 June 2015]

NWCG (National Wildfire Coordinating Group). 2014. Incident Response Pocket Guide (IRPG).

Oliver, T., D. B. Roy, J. K. Hill, T. Brereton, and C. D. Thomas. 2010. Heterogeneous landscapes promote population stability. Ecology Letters **13**:473-484.

Paquin, P., and D. Coderre. 1997. Deforestation and fire impact on edaphic insect larvae and other macroarthropods. Environmental Entomology **26**:21-30.

Pollet, J., and A. Brown. 2007. Fuel Moisture Sampling Guide. Bureau of Land Management, Utah State Office, Salt Lake City, UT, USA.

R Core Team. 2014. R: a language and environment for statistical computing. R Foundation for Statistical Computing, Vienna, Austria. URL http://www.R-project.org/.

Rezende, E. L., L. E. Castaneda, and M. Santos. 2014. Tolerance landscapes in thermal ecology. Functional Ecology **28**:799-809.

Rothermel, R. C. 1972. A mathematical model for predicting fire spread in wildland fuels. Res. Pap. INT-115. Ogden, UT: U.S. Department of Agriculture, Intermountain Forest and Range Experiment Station. 40 p.

Schultz, C. B., and E. E. Crone. 1998. Burning prairie to restore butterfly habitat: a modeling approach to management tradeoffs for the Fender's blue. Restoration Ecology **6**:244-252.

Schultz, C. B., E. Henry, A. Carleton, T. Hicks, R. Thomas, A. Potter, M. Collins, M. Linders, C. Fimbel, S. Black, H. E. Anderson, G. Diehl, S. Hamman, R. Gilbert, J. Foster, D. Hays, D. Wilderman, R. Davenport, E. Steel, N. Page, P. L. Lilley, J. Heron, N. Kroeker, C. Webb, and B. Reader. 2011. Conservation of prairie-oak butterflies in Oregon, Washington, and British Columbia. Northwest Science **85**:361-388.

Scott, J. H., and R. E. Burgan. 2005. Standard fire behavior fuel models: a comprehensive set for use with Rothermel's surface fire spread model. Gen. Tech. Rep. RMRS-GTR-153. Fort Collins, CO: USDA, Forest Service, Rocky Mountain Research Station. 72 p.

Severns, P. M., and A. D. Warren. 2008. Selectively eliminating and conserving exotic plants to save an endangered butterfly from local extinction. Animal Conservation **11**:476-483.

Shea, R. W., B. W. Shea, J. B. Kauffman, D. E. Ward, C. I. Haskins, and M. C. Scholes. 1996. Fuel biomass and combustion factors associated with fires in savanna ecosystems of South Africa and Zambia. Journal of Geophysical Research **101**:23,551-23,568.

Spencer, S. R., G. N. Cameron, B. D. Eshelman, L. C. Cooper, and L. R. Williams. 1985. Influence of pocket gopher mounds on a Texas coastal prairie. Oecologia **66**:111-115.

Stanley, A. G., P. W. Dunwiddie, and T. N. Kaye. 2011. Restoring invaded Pacific Northwest prairies: management recommendations from a region-wide experiment. Northwest Science **85**:233-246.

Stewart, K. E. J., N. A. D. Bourn, and J. A. Thomas. 2001. An evaluation of three quick methods commonly used to assess sward height in ecology. Journal of Applied Ecology **38**:1148-1154.

Storm, L., and D. Shebitz. 2006. Evaluating the purpose, extent, and ecological restoration applications of indigenous burning practices in southwestern Washington. Ecological Restoration **24**:256-268.

Suggitt, A. J., P. K. Gillingham, J. K. Hill, B. Huntley, W. E. Kunin, D. B. Roy, and C. D. Thomas. 2011. Habitat microclimates drive fine-scale variation in extreme temperatures. Oikos **120**:1-8.

Thurston County Resource Stewardship Department. 2014. Thurston County prairie habitat assessment methodology: species and habitat risk and asset prioritization (SHARP) model documentation. Version 1.00. Olympia, WA, USA.

Trabaud, L. 1987. The role of fire in ecological systems. SPB Academic Publishers, The Hague, The Netherlands.

USDI National Park Service. 2003. Fire Monitoring Handbook. Fire Management Program Center, National Interagency Fire Center, Boise, ID.

Vermeire, L. T., R. B. Mitchell, S. D. Fuhlendorf, and D. B. Wester. 2004. Selective control of rangeland grasshoppers with prescribed fire. Journal of Rangeland Management **57**:29-33.

Voncina, A., M. Ferlan, K. Eler, F. Batic, and D. Vodnik. 2014. Effects of fire on carbon fluxes of a calcareous grassland. International Journal of Wildland Fire **23**:425-434.

Warton, D. I., and F. K. C. Hui. 2011. The arcsine is asinine: the analysis of proportions in ecology. Ecology **92**:3-10.

Weiss, S. B., R. R. White, D. D. Murphy, and P. R. Ehrlich. 1987. Growth and dispersal of larvae of the checkerspot butterfly *Euphydryas editha*. Oikos **50**:161-166.

Weiss, S. B., D. D. Murphy, and R. R. White. 1988. Sun, slope, and butterflies: topographic determinants of habitat quality for *Euphydryas editha*. Ecology **69**:1486-1496.

Welhan, J.A., T. M. Clemo, and E. L. Gego. 2002. Stochastic simulation of aquifer heterogeneity in a layered basalt aquifer system, eastern Snake River Plain, Idaho. Geological Society of America Special Papers **353**:225-247.

WRCC (Western Regional Climate Center). 2015. URL http://www.wrcc.dri.edu/ [accessed 18 April 2015]

Wright, B. R., and P. J. Clarke. 2008. Relationships between soil temperatures and properties of fire in feathertop spinifex (*Triodia schinzii* (Henrard) Lazarides) sandridge desert in central Australia. The Rangeland Journal **30**:317-325.

## Appendix A: Region and research plot maps for JBLM & Thurston County, WA


*Plots at Glacial Heritage and southern plots at Training Area 15 were not included in analyses of Chapter 2 due to post-burn management interference*

## Appendix B: Sampling plot design

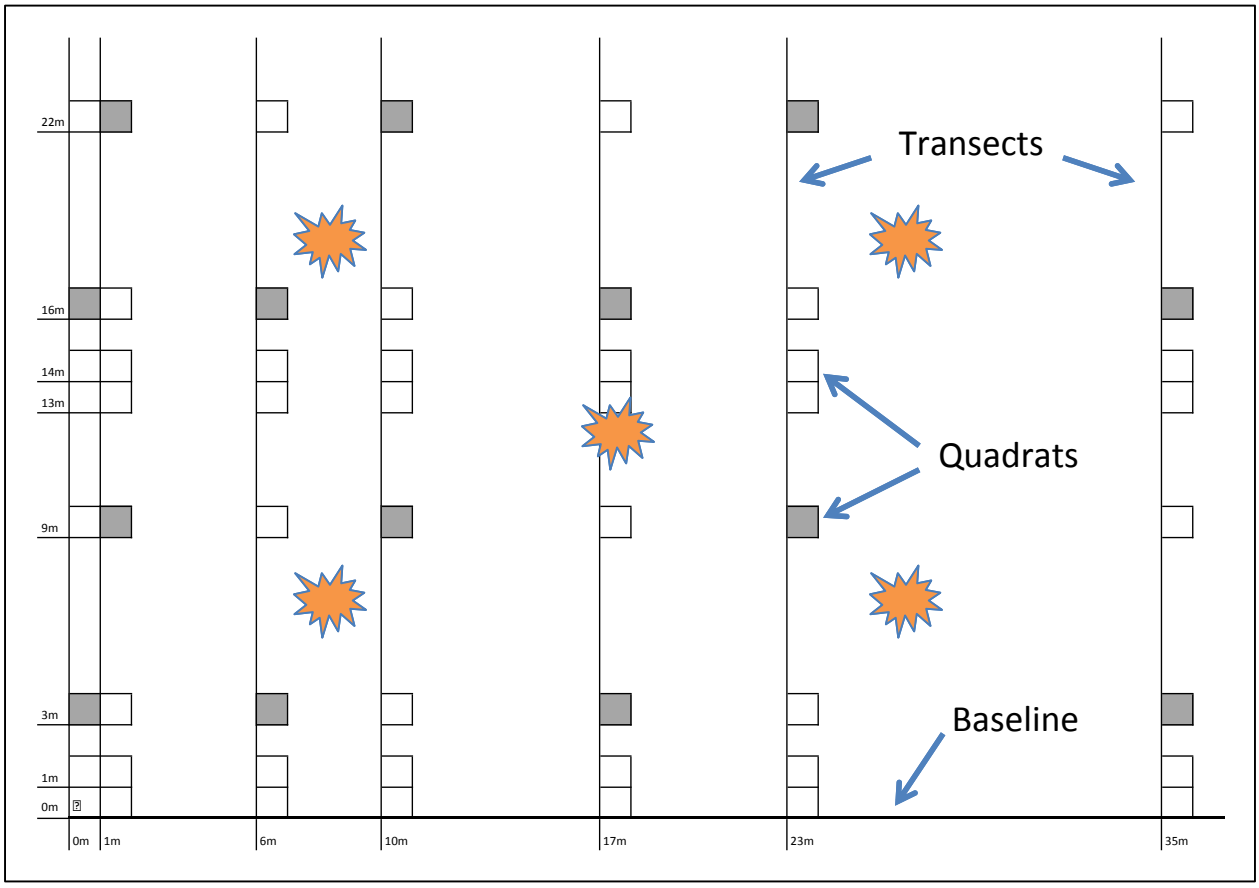


Shaded quadrats within the plot indicate 'intensive' data collection, including species composition, substrate cover, live fuel moisture, dead fuel moisture, fuel loading, litter depth, subsurface soil temperature, post-burn severity (see below), and photo documentation. Orange stars indicate ignition points during the burn.

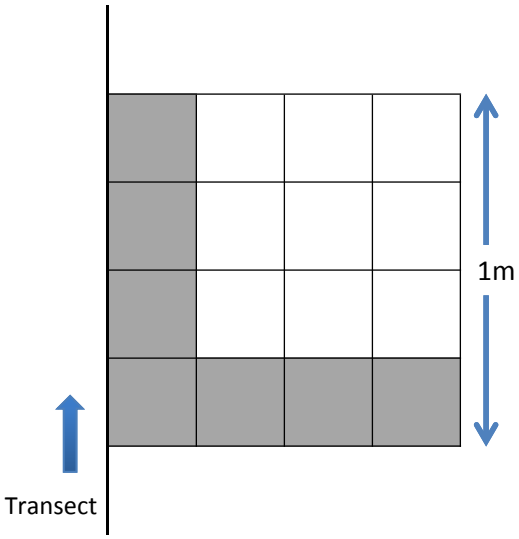


Within every 1-m$^2$ quadrat, seven 25cm x 25cm 'sub-quadrats' were designated for sampling of 1) vegetation height and 2) the number of 5cm x 5cm squares that were bare or open. In the 14 'intensive' quadrats, post-burn severity was also assessed within the seven sub-quadrats.

## Appendix C: 'R' code used for all analyses

Chapter 1 – soil temperatures

```
attach(Temperatures)
dotchart(AvgTemp, main = "TEMP", group = BurnUnit) #data distributions
dotchart(AvgRH, main = "RH", group = BurnUnit)
dotchart(AvgWind, main = "WIND", group = BurnUnit)
dotchart(AvgLiveFuel, main = "LIVEFUEL", group = BurnUnit)
dotchart(CVLiveFuel, main = "CVLIVEFUEL", group = BurnUnit
dotchart(AvgDeadFuel, main = "DEADFUEL", group = BurnUnit)
dotchart(CVDeadFuel, main = "CVDEADFUEL", group = BurnUnit)
dotchart(AvgFuelLoad, main = "FUELLOAD", group = BurnUnit)
dotchart(CVFuelLoad, main = "CVFUELLOAD", group = BurnUnit)
dotchart(julian, main = "BURNDAY", group = BurnUnit)
dotchart(length, main = "BURNLENGTH", group = BurnUnit)
dotchart(PercentOpenCover, main = "POC", group = BurnUnit)
dotchart(LitterDepth, main = "LITTER", group = BurnUnit)
dotchart(CVLitterDepth, main = "CVLITTER", group = BurnUnit)
dotchart(AvgPeakTemp, main = "PEAKTEMP", group = BurnUnit)
correlations = cbind(AvgTemp, AvgRH, AvgWind, AvgLiveFuel, CVLiveFuel, AvgDeadFuel, CVDeadFuel,
          AvgFuelLoad, CVFuelLoad, julian, length, PercentOpenCover, LitterDepth, CVLitterDepth,
          AvgPeakTemp) #general relationships
panel.cor <- function(x, y, digits=2, prefix="", cex.cor) #correlation matrix function
 {
  usr <- par("usr"); on.exit(par(usr))
  par(usr = c(0, 1, 0, 1))
  r <- abs(cor(x, y))
  txt <- format(c(r, 0.123456789), digits=digits)[1]
  txt <- paste(prefix, txt, sep="")
  if(missing(cex.cor)) cex <- 0.8/strwidth(txt)

  test <- cor.test(x,y)
  Signif <- symnum(test$p.value, corr = FALSE, na = FALSE,
               cutpoints = c(0, 0.001, 0.01, 0.05, 0.1, 1),
               symbols = c("***", "**", "*", ".", " "))

  text(0.5, 0.5, txt, cex = cex * r)
  text(.8, .8, Signif, cex=cex, col=2)
 }
pairs(correlations, lower.panel = panel.smooth, upper.panel = panel.cor)
library(car) #multicollinearity
full = lm(AvgPeakTemp ~ AvgTemp + AvgRH + AvgWind + AvgLiveFuel + CVLiveFuel + AvgDeadFuel +
          CVDeadFuel + AvgFuelLoad + CVFuelLoad + julian + length + PercentOpenCover + LitterDepth +
          CVLitterDepth)
vif(full)
burnunit = lm(AvgPeakTemp ~ AvgTemp + AvgRH + AvgWind + AvgLiveFuel + CVLiveFuel + AvgDeadFuel +
          CVDeadFuel + AvgFuelLoad + CVFuelLoad + julian + length + PercentOpenCover + LitterDepth +
          CVLitterDepth + BurnUnit) #effect of burn unit
```

```
anova(burnunit, full)
null = lm(AvgPeakTemp ~ 1) #stepwise model selection
fulltemp = lm(AvgPeakTemp ~ AvgTemp + AvgWind + AvgLiveFuel + CVLiveFuel + AvgDeadFuel +
        CVDeadFuel + AvgFuelLoad + CVFuelLoad + julian + length + PercentOpenCover + LitterDepth +
        CVLitterDepth)
fullrh = lm(AvgPeakTemp ~ AvgRH + AvgWind + AvgLiveFuel + CVLiveFuel + AvgDeadFuel + CVDeadFuel +
        AvgFuelLoad + CVFuelLoad + julian + length + PercentOpenCover + LitterDepth + CVLitterDepth)
step(null, scope=list(upper = fulltemp, lower = null), direction = 'both', trace = TRUE)
step(null, scope=list(upper = fullrh, lower = null), direction = 'both', trace = TRUE)
final = lm(AvgPeakTemp ~ AvgTemp + AvgDeadFuel)
alt = lm(AvgPeakTemp ~ AvgRH + AvgDeadFuel)
AIC(final, alt) #compare temp and RH models
plot(final) #patterns in residuals and leverage
ncvTest(final) #constancy of variance
qqp = qqnorm(final$residuals) #normal probability plot
cor(qqp$x, qqp$y)
library(mgcv) #try a generalized additive model
tempgam = gam(AvgPeakTemp ~ s(AvgTemp, k = 4) + s(AvgDeadFuel, k = 4))
plot(tempgam)
e.tempgam = resid(tempgam)
fit.tempgam = fitted(tempgam)
plot(fit.tempgam, e.tempgam)
anova(final, tempgam)
int = lm(AvgPeakTemp ~ AvgTemp*AvgDeadFuel) #try interaction term
summary(int)
temp2 = AvgTemp^2 #try transformed predictors
df2 = AvgDeadFuel^(1/2)
transx = lm(AvgPeakTemp ~ temp2 + df2)
summary(transx)
expl.data <- Temperatures[, c("AvgTemp", "AvgRH")] #try PCA for correlated temp and RH
expl <- t(expl.data)
library(mvnormtest) #multivariate normality
mshapiro.test(expl)
expl.PCA <- princomp(expl.data, cor = TRUE)
summary(expl.PCA, loadings = TRUE)
plot(expl.PCA)
pcfull = lm(AvgPeakTemp ~ expl.PCA$scores[,1] + AvgWind + AvgLiveFuel + CVLiveFuel + AvgDeadFuel +
        CVDeadFuel + AvgFuelLoad + CVFuelLoad + julian + length + PercentOpenCover + LitterDepth +
        CVLitterDepth)
step(null, scope=list(upper = pcfull, lower = null), direction = 'both', trace = TRUE)
pcfinal = lm(AvgPeakTemp ~ expl.PCA$scores[,1] + AvgDeadFuel)
par(mar = c(5.1, 7.5, 2.5, 2.1)) #final plots
plot(AvgPeakTemp ~ AvgTemp, ann = FALSE, ylim = c(22,57), pch = c(18,19)[as.numeric(Temperatures$ampm)],
        cex = 2.5, cex.axis = 2.5, col = Temperatures$ampm)
segments(AvgTemp, AvgPeakTemp - sem, AvgTemp, AvgPeakTemp + sem)
epsilon = 0.02
segments(AvgTemp - epsilon, AvgPeakTemp - sem, AvgTemp + epsilon, AvgPeakTemp - sem)
segments(AvgTemp - epsilon, AvgPeakTemp + sem, AvgTemp + epsilon, AvgPeakTemp + sem)
title(ylab = "Average peak soil temperature (˚C)", cex.lab = 2.5, line = 4)
```

```
title(xlab = "Average air temperature (˚C)", cex.lab = 2.5, line = 3.8)
plot(AvgPeakTemp ~ AvgDeadFuel, ann = FALSE, ylim = c(22,57), pch =
        c(18,19)[as.numeric(Temperatures$ampm)], cex = 2.5, cex.axis = 2.5, col = Temperatures$ampm)
segments(AvgDeadFuel, AvgPeakTemp - sem, AvgDeadFuel, AvgPeakTemp + sem)
epsilon = 0.02
segments(AvgDeadFuel - epsilon, AvgPeakTemp - sem, AvgDeadFuel + epsilon, AvgPeakTemp - sem)
segments(AvgDeadFuel - epsilon, AvgPeakTemp + sem, AvgDeadFuel + epsilon, AvgPeakTemp + sem)
title(ylab = "Average peak soil temperature (˚C)", cex.lab = 2.5, line = 4)
title(xlab = "Average dead fuel moisture (%)", cex.lab = 2.5, line = 3.8)
detach(Temperatures)
library(mvpart) #regression tree analysis
env = Quadrat[,c("AvgTemperature", "AvgRH", "AvgWindSpeed", "CornerLitterDepth", "FuelLoad",
        "LiveFuelMoisture", "DeadFuelMoisture", "Percent.Open.Cover")]
peaktemp = mvpart(Quadrat[,"PeakBurnTemp"] ~ ., data = env, xv = "pick", xvmult = 100, all.leaves = TRUE,
        control = rpart.control(xval = 243))
plot(peaktemp, branch = 0.5, margin = 0.1)
text(peaktemp, use.n = TRUE, cex = 1.5)
```

Chapter 1 – lethal heat dosages

```
attach(LHD) #see 'Chapter 1 – soil temperatures' for data exploration, model selection, and diagnostics
library(logistf) #Firth logistic regression for final model
finallhd = logistf(BinaryLHD ~ AvgRH)
summary(finallhd)
lethal = LHD$BinaryLHD
lethal[lethal==0] = "No"
lethal[lethal==1] = "Yes"
par(mar = c(5.1, 5.1, 2.5, 2.1)) #final plot
boxplot(LHD$AvgRH ~ lethal, xlab = "100% lethal heat dosage occurrence", ylab = "Relative humidity
        (%)", col = "green4", cex.lab = 2.0, cex.axis = 2.0)
detach(LHD)
library(flux) #total lethal heat dosage by quadrat
attach(QuadratAUC) #calculate total area under time-temperature curve
X2.28 = auc(X2.28.x, X2.28.y) #repeated for every quadrat with LHD (not shown)
QAUC = c(X2.28, X2.44, X3.12, X3.48, X4.48, X4.51, X6.12, X8.32, X8.39, X8.44, X8.48, X8.51, X10.19,
        X10.23, X10.28, X10.32, X10.35, X10.39, X10.44, X10.48, X10.51, X10.55, X12.23, X12.32, X12.35,
        X12.39, X12.51, X16.23)
detach(QuadratAUC)
attach(TDTAUC) #calculate area under TDT curve
T2.28 = auc(X2.28.x, X2.28.y) #repeated for every quadrat with LHD (not shown)
TAUC = c(T2.28, T2.44, T3.12, T3.48, T4.48, T4.51, T6.12, T8.32, T8.39, T8.44, T8.48, T8.51, T10.19, T10.23,
        T10.28, T10.32, T10.35, T10.39, T10.44, T10.48, T10.51, T10.55, T12.23, T12.32, T12.35, T12.39,
        T12.51, T16.23)
detach(TDTAUC)
LethalAUC = QAUC – TAUC #calculate heat dosage over the 100% lethal threshold
write.csv(LethalAUC, "LethalAUC") #add in zeroes for quadrats without LHD (not shown)
lethalhd = mvpart(Quadrat[,"LethalAUC"] ~ ., data = env, xv = "pick", xvmult = 100, all.leaves = TRUE, control =
        rpart.control(xval = 243)) #regression tree analysis
plot(lethalhd, branch = 0.5, margin = 0.1)
text(lethalhd, use.n = TRUE, cex = 1.5)
```

Chapter 1 – cover of unburned/low-severity areas

```
attach(Severity) #see 'Chapter 1 – soil temperatures' for data exploration, model selection, and diagnostics
logpoc = log(PercentOpenCover)
finalsev = lm(logitsev ~ AvgDeadFuel*logpoc)
library(ggplot2) #creating interaction plot
z1a = seq(2.3,30)
z2a = c(-0.7,0.7,1.6,2.7)
newdfa = expand.grid(AvgDeadFuel = z1a, logpoc = z2a)
pa = ggplot(data=transform(newdfa, ypa = inv.logit(predict(finalsev, newdfa))*100), aes(y=ypa, x = AvgDeadFuel,
        color=factor(logpoc), linetype=factor(logpoc))) + stat_smooth(method=loess)
pa + scale_colour_discrete(name = "Cover of bare or open ground", breaks = c("2.7","1.6","0.7","-0.7"), labels =
        c("15%","5%","2%","0.5%")) + scale_linetype_manual(values = c("longdash", "dotted", "dotdash",
        "solid"), name = "Cover of bare or open ground", breaks = c("2.7","1.6","0.7","-0.7"), labels =
        c("15%","5%","2%","0.5%")) + labs(x = "Average dead fuel moisture (%)", y = "Cover of unburned/low
        severity areas (%)") + theme(axis.text = element_text(size = 18), axis.title = element_text(size=25),
        legend.text = element_text(size = 25), legend.title = element_text(size = 15)) +
        scale_x_continuous(breaks=seq(0,30,5)) + scale_y_continuous(breaks = seq(0,100,10))
detach(Severity)
severity = mvpart(Quadrat[,"VSeverity"] ~ ., data = env, xv = "pick", xvmult = 100, all.leaves = TRUE, control =
        rpart.control(xval = 243)) #regression tree analysis
plot(severity, branch = 0.5, margin = 0.1)
text(severity, use.n = TRUE, cex = 1)
```

Chapter 2 – species richness and diversity

```
attach(Composition) #see 'Chapter 1 – soil temperatures' for data exploration, model selection, and diagnostics
finalqrich = lm(dQuadRichness ~ julian)
finaldiv = lm(dHillsDiversity ~ AvgFuelLoad)
par(mar = c(5.1, 7.5, 2.5, 2.1)) #final plots
plot(dQuadRichness ~ julian, ann = FALSE, pch = 19, cex = 2.5, cex.axis = 2.5, ylim = c(-0.5,4))
abline(finalqrich$coeff, col = "red", lwd = 3)
segments(julian, dQuadRichness - semq, julian, dQuadRichness + semq)
epsilon = 0.2
segments(julian - epsilon, dQuadRichness - semq, julian + epsilon, dQuadRichness - semq)
segments(julian - epsilon, dQuadRichness + semq, julian + epsilon, dQuadRichness + semq)
title(ylab = "Average change in species richness", cex.lab = 2.5, line = 5.5)
title(ylab = expression(paste("(per 1-",m^2, " quadrat)")), cex.lab = 2, line = 3.2)
title(xlab = "Julian calendar day", cex.lab = 2.5, line = 3.8)
abline(h = 0, lty = 2)
plot(dHillsDiversity ~ AvgFuelLoad, ann = FALSE, pch = 19, cex = 2.5, cex.lab = 2.5, cex.axis = 2.5, ylim = c(
        3,3.5))
abline(finaldiv$coeff, col = "red", lwd = 2)
segments(AvgFuelLoad, dHillsDiversity - semd, AvgFuelLoad, dHillsDiversity + semd)
epsilon2 = 0.0005
segments(AvgFuelLoad - epsilon2, dHillsDiversity - semd, AvgFuelLoad + epsilon2, dHillsDiversity - semd)
segments(AvgFuelLoad - epsilon2, dHillsDiversity + semd, AvgFuelLoad + epsilon2, dHillsDiversity + semd)
title(ylab = "Average change in quadrat-scale", cex.lab = 2.5, line = 5.5)
title(ylab = "Hill's diversity", cex.lab = 2.5, line = 3.5)
title(xlab = expression(paste("Average fuel load (kg/",m^2,")")), cex.lab = 2.5, line = 3.8)
```

```
abline(h = 0, lty = 2)
detach(Composition)
```

Chapter 2 – compositional change

```
library(labdsv) #delete rare species (found in <5% of plots)
Plot.no.Average <- vegtab(taxa = PlotAverage, minval = (.05*nrow(PlotAverage))) #average plot composition
library(vegan) #relativize species by maxima and plots by totals
Plot.no.Average.wis <- wisconsin(Plot.no.Average)
PlotAverage.dis <- vegdist(Plot.no.Average.wis, method = "bray") #create Bray-Curtis distance matrix
PlotAverage.dis.x <- as.matrix(PlotAverage.dis)
write.csv(PlotAverage.dis.x, "PlotAverageDist.csv") #export Bray-Curtis distances between plots
Quadrats.no <- vegtab(taxa = Quadrats, minval = (.05*nrow(Quadrats))) #delete rare species for quadrats
Quadrats.no.wis <- wisconsin(Quadrats.no) #relativize species by maxima and quadrats by totals
Quadrats.dis <- vegdist(Quadrats.no.wis, method = "bray") #create Bray-Curtis distance matrix
Quadrats.dis.x <- as.matrix(Quadrats.dis)
write.csv(Quadrats.dis.x, "QuadratsDist.csv") #export Bray-Curtis distances between quadrats
#organize data in "PlotAverageDist.csv" and "QuadratsDist.csv" spreadsheets (not shown)
#keep only the distances between pairs of pre- and post-burn plots and quadrats (not shown)
attach(BCDist) #see 'Chapter 1 – soil temperatures' for data exploration, model selection, and diagnostics
finalbcplot = lm(BCPlotAvg ~ AvgDeadFuel)
finalbcquad = lm(AvgQuadBC ~ AvgRH)
par(mar = c(5.1, 6.5, 4.1, 2.1)) #final plots
plot(BCPlotAvg ~ AvgDeadFuel, ann = FALSE, pch = c(18,19)[as.numeric(BCDist$ampm)], cex = 2.5,
        cex.axis = 2.5, col = BCDist$ampm)
abline(finalbcplot$coeff, col = "red", lwd = 3)
title(xlab = "Average dead fuel moisture (%)", cex.lab = 2.5, line = 3.8)
title(ylab = "Plot-scale change in Bray-Curtis distance", cex.lab = 2.3, line = 4.2)
plot(AvgQuadBC ~ AvgRH, ann = FALSE, pch = c(18,19)[as.numeric(BCDist$ampm)], cex = 2.5, cex.lab =
        2.5, cex.axis = 2.5, ylim = c(0.24,0.51), col = BCDist$ampm)
abline(finalbcquad$coeff, col = "red", lwd = 2)
segments(AvgRH, AvgQuadBC - sema, AvgRH, AvgQuadBC + sema)
epsilon = 0.1
segments(AvgRH - epsilon, AvgQuadBC - sema, AvgRH + epsilon, AvgQuadBC - sema)
segments(AvgRH - epsilon, AvgQuadBC + sema, AvgRH + epsilon, AvgQuadBC + sema)
title(ylab = "Quadrat-scale change in Bray-Curtis distance", cex.lab = 2.2, line = 4.2)
title(xlab = "Average relative humidity (%)", cex.lab = 2.5, line = 3.8)
detach(BCDist)
#NMDS ordinations of species abundance for each site (burn unit)
Lower.no.Weir <- vegtab(taxa = LowerWeir, minval = (.05*nrow(LowerWeir))) #delete rare species
Lower.no.Weir.wis <- wisconsin(Lower.no.Weir) #relativize species by maxima and quadrats by totals
z1LW <- metaMDS(comm = Lower.no.Weir.wis, autotransform = FALSE, k = 1, maxit = 400, trymax = 40, pc =
        TRUE) #k = 1 dimension
z1LW <- metaMDS(comm = Lower.no.Weir.wis, autotransform = FALSE, k = 1, previous.best = z1LW, maxit =
        400, trymax = 40, pc = TRUE) #re-run starting with previous best solution
z2LW <- metaMDS(comm = Lower.no.Weir.wis, autotransform = FALSE, k = 2, maxit = 400, trymax = 40, pc =
        TRUE) #k = 2 dimensions
z2LW <- metaMDS(comm = Lower.no.Weir.wis, autotransform = FALSE, k = 2, previous.best = z2LW, maxit =
        400, trymax = 40, pc = TRUE) #re-run starting with previous best solution
```

```
z3LW <- metaMDS(comm = Lower.no.Weir.wis, autotransform = FALSE, k = 3, maxit = 400, trymax = 40, pc =
        TRUE) #k = 3 dimensions
z3LW <- metaMDS(comm = Lower.no.Weir.wis, autotransform = FALSE, k = 3, previous.best = z3LW, maxit =
        400, trymax = 40, pc = TRUE) #re-run starting with previous best solution
dim <- c(1,2,3) #plot a screeplot for stress to compare dimensions k
stressLW <- c(z1LW$stress, z2LW$stress, z3LW$stress)
plot(dim, stressLW, type = "o", xlab = "Dimensions (k)", ylab = "Stress", ylim = c(0,0.5), pch = 19)
stressplot(z3LW, lwd = 5) #make a Shepard plot to evaluate fit of best solution

plot(z3LW, display = "sites", type = "n", xaxt = "n", xlab = "", yaxt = "n", ylab = "") #plot the ordination
ordiarrows(z3LW, groups = SiteInfo$Levels, order.by = SiteInfo$Replicates, show.groups = c(1:14), col = "blue4",
        lwd = 3, lty = 3) #successional arrows from pre- to post-burn quadrats
ordiarrows(z3LW, groups = SiteInfo$Levels, order.by = SiteInfo$Replicates, show.groups = c(15:28), col = "red",
        lwd = 2)
legend(x = "topleft", bty = "n", cex = 1, lty = c(3,1), lwd = c(3,2), col = c("blue4", "red"), legend =
        c("Morning (71.2% RH)", "Afternoon (64.5% RH)"))
title(main = "(a) Lower Weir")
#repeated for every site (not shown)
#NMDS ordination of average functional group abundance using all plots
FGAverage.wis <- wisconsin(FGAverage) #relativize functional groups by maxima and plots by totals
z1FG <- metaMDS(comm = FGAverage.wis, autotransform = FALSE, k = 1, maxit = 400, trymax = 40, pc =
        TRUE) #k = 1 dimension
z1FG <- metaMDS(comm = FGAverage.wis, autotransform = FALSE, k = 1, previous.best = z1FG, maxit =
        400, trymax = 40, pc = TRUE) #re-run starting with previous best solution
z2FG <- metaMDS(comm = FGAverage.wis, autotransform = FALSE, k = 2, maxit = 400, trymax = 40, pc =
        TRUE) #k = 2 dimensions
z2FG <- metaMDS(comm = FGAverage.wis, autotransform = FALSE, k = 2, previous.best = z2FG, maxit =
        400, trymax = 40, pc = TRUE) #re-run starting with previous best solution
z3FG <- metaMDS(comm = FGAverage.wis, autotransform = FALSE, k = 3, maxit = 400, trymax = 40, pc =
        TRUE) #k = 3 dimensions
z3FG <- metaMDS(comm = FGAverage.wis, autotransform = FALSE, k = 3, previous.best = z3FG, maxit =
        400, trymax = 40, pc = TRUE) #re-run starting with previous best solution
stressFG <- c(z1FG$stress, z2FG$stress, z3FG$stress) #plot a screeplot for stress to compare dimensions k
plot(dim, stressFG, type = "o", xlab = "Dimensions (k)", ylab = "Stress", ylim = c(0,0.5), pch = 19)
stressplot(z3FG, lwd = 5) #make a Shepard plot to evaluate fit of best solution
par(mar = c(2.1, 2.1, 2.1, 2.1))
plot(z3FG, display = "sites", type = "n", xaxt = "n", xlab = "", yaxt = "n", ylab = "") #plot the ordination
ordiarrows(z3FG, groups = PlotSiteInfo$Levels, order.by = PlotSiteInfo$Replicates, show.groups =
        c(1,5,7,9,13,15,17,19), col = "blue4", lwd = 3, lty = 3) #successional arrows from pre- to post-burn plots
ordiarrows(z3FG, groups = PlotSiteInfo$Levels, order.by = PlotSiteInfo$Replicates, show.groups =
        c(2,6,8,10,14,16,18,20), col = "red", lwd = 2)
legend(x = "bottomright", bty = "n", cex = 1, lty = c(3,1), lwd = c(3,2), col = c("blue4", "red"), legend =
        c("Morning", "Afternoon"))
sp = wascores(x = z3FG$points, w = FGAverage.wis, expand = TRUE)
library(maptools) #overlay location at which each functional group is most abundant
pointLabel(sp, rownames(sp), cex = 2)
```

Chapter 2 – vegetation height structure

```
attach(Height.Class) #see 'Chapter 1 – soil temperatures' for data exploration, model selection, and diagnostics
change = lm(AvgdHC2cm ~ julian)
par(mar = c(5.1, 5.1, 2.5, 2.1)) #final plots
plot(AvgdHC2cm ~ julian, ann = FALSE, pch = 19, cex = 1.5, cex.lab = 1.5, cex.axis = 1.5, ylim = c(-0.6,1.1))
abline(change$coeff, col = "red", lwd = 2)
segments(julian, AvgdHC2cm - semc, julian, AvgdHC2cm + semc)
epsilon = 0.2
segments(julian - epsilon, AvgdHC2cm - semc, julian + epsilon, AvgdHC2cm - semc)
segments(julian - epsilon, AvgdHC2cm + semc, julian + epsilon, AvgdHC2cm + semc)
title(ylab = "Change in number of 2 cm height classes", cex.lab = 2.3, line = 3.0)
title(xlab = "Julian calendar day", cex.lab = 2.5, line = 3.8)
abline(h = 0, lty = 2)
detach(Height.Class)
RangeSH30 = RangeSH[-3,] #spatial autocorrelation – remove plots with dead fuel moisture of 30%
RangeSH30 = RangeSH30[-8,]
attach(RangeSH30) #see 'Chapter 1 – soil temperatures' for data exploration, model selection, and diagnostics
var.test(dSH. ~ ampm) #categorical predictor
t.test(dSH. ~ ampm)
par(mar = c(5.1, 7.5, 2.5, 2.1))
boxplot(dSH. ~ ampm, col = "green4", cex.lab = 2.5, cex.axis = 2.5)
title(ylab = "Change in magnitude of spatial", cex.lab = 2.5, line = 5.5)
title(ylab = "autocorrelation of vegetation height", cex.lab = 2.5, line = 3.5)
title(xlab = "Time of burning", cex.lab = 2.5, line = 3.8)
abline(h = 0, lty = 2)
magnitude = lm(dSH. ~ AvgDeadFuel) #continuous predictor
par(mar = c(5.1, 7.5, 2.5, 2.1))
plot(dSH. ~ AvgDeadFuel, ann = FALSE, pch = 19, cex = 2.5, cex.axis = 2.5)
abline(magnitude$coeff, col = "red", lwd = 3)
title(xlab = "Average dead fuel moisture (%)", cex.lab = 2.5, line = 3.8)
title(ylab = "Change in magnitude of spatial", cex.lab = 2.5, line = 5.5)
title(ylab = "autocorrelation of vegetation height", cex.lab = 2.5, line = 3.5)
abline(h = 0, lty = 2)
detach(RangeSH30)
Fragstats2 = Fragstats[-4,] #remove plot with high wind speed (3.7m/s)
attach(Fragstats2) #see 'Chapter 1 – soil temperatures' for data exploration, model selection, and diagnostics
iji = lm(dIJI ~ AvgWind) #IJI of height
par(mar = c(5.1, 7.5, 2.5, 2.1))
plot(dIJI ~ AvgWind, ann = FALSE, pch = 19, cex = 2.5, cex.axis = 2.5)
abline(iji$coeff, col = "red", lwd = 3)
title(ylab = "Change in Interspersion and", cex.lab = 2.5, line = 5.5)
title(ylab = "Juxtaposition Index (IJI)", cex.lab = 2.5, line = 3.5)
title(xlab = "Average wind speed (m/s)", cex.lab = 2.5, line = 3.8)
abline(h = 0, lty = 2)
detach(Fragstats2)
```

Chapter 2 – bare or open ground and litter depth

```
attach(BareGround) #see 'Chapter 1 – soil temperatures' for data exploration, model selection, and diagnostics
bg = aov(POC2015 ~ time)
par(mar = c(5.1, 7.5, 2.5, 2.1))
boxplot(POC2015 ~ time, col = "green4", cex.lab = 2.5, cex.axis = 2.5)
title(ylab = "Cover of bare or open ground", cex.lab = 2.5, line = 5.5)
title(ylab = "post-burn (%)", cex.lab = 2.5, line = 3.5)
title(xlab = "Time of burning", cex.lab = 2.5, line = 3.8)
detach(BareGround)
attach(LitterDepth) #see 'Chapter 1 – soil temperatures' for data exploration, model selection, and diagnostics
centtemp = AvgTemp - mean(AvgTemp)
litter = lm(dCVLitterDepth ~ centtemp + I(centtemp^2))
littergam = gam(dCVLitterDepth ~ s(AvgTemp)) #try a generalized additive model
plot(littergam)
e.littergam = resid(littergam)
fit.littergam = fitted(littergam)
plot(fit.littergam, e.littergam)
anova(litter, littergam)
par(mar = c(5.1, 7.5, 2.5, 2.1))
plot.gam(littergam, residuals = T, ann = FALSE, pch = 19, cex = 2.5, cex.lab = 2.5, cex.axis = 2.5)
title(ylab = "Change in coefficient of variation (CV)", cex.lab = 2.5, line = 5.5)
title(ylab = "of litter depth", cex.lab = 2.5, line = 3.5)
title(xlab = "Average air temperature (˚C)", cex.lab = 2.5, line = 3.8)
abline(h = 0, lty = 2)
detach(LitterDepth)
```

## Appendix D: Burn weather and fuel data for each plot

| Plot | Burn Unit | Burn Date | Ignition Time | Burn Length (min) | Average air temperature (°C) | Average relative humidity (%) | Average wind speed (m/s) | Average live fuel moisture (%) | Average dead fuel moisture (%) | Average fuel loading ($kg/m^2$) | Average litter depth (cm) | Cover of bare or open ground (%) |
|---|---|---|---|---|---|---|---|---|---|---|---|---|
| 1 | South Weir | 8/25/2014 | 0900 | 28 | 21.1 | 70.4 | 0.6 | 58.4 | 16.3 | 0.65 | 2.7 | 1.6 |
| 2 | South Weir | 8/25/2014 | 1505 | 13 | 29.0 | 35.5 | 2.2 | 60.3 | 3.1 | 0.55 | 1.8 | 5.0 |
| 3 | Glacial Heritage | 9/15/2014 | 1014 | 20 | 20.2 | 53.3 | 1.5 | 71.1 | 8.2 | 0.18 | 2.7 | 15.0 |
| 4 | Glacial Heritage | 9/15/2014 | 1230 | 12 | 28.1 | 32.3 | 2.3 | 61.9 | 4.4 | 0.25 | 2.5 | 13.4 |
| 5 | Upper Weir | 8/15/2014 | 1238 | 28 | 23.8 | 67.0 | 1.2 | 59.4 | 30.0 | 0.49 | 2.3 | 1.5 |
| 6 | Upper Weir | 8/19/2014 | 1632 | 15 | 26.4 | 50.7 | 3.7 | 64.4 | 4.3 | 0.44 | 2.1 | 1.7 |
| 7 | Johnson Prairie | 8/7/2014 | 0804 | 27 | 14.4 | 87.9 | 1.9 | 58.8 | 13.3 | 0.56 | 2.2 | 0.7 |
| 8 | Johnson Prairie | 8/7/2014 | 1400 | 20 | 26.5 | 46.3 | 1.7 | 53.6 | 2.7 | 0.56 | 1.7 | 1.6 |
| 9 | Training Area 6 | 8/5/2014 | 0908 | 35 | 16.4 | 77.8 | 1.5 | 60.8 | 11.9 | 0.46 | 1.7 | 2.0 |
| 10 | Training Area 6 | 8/5/2014 | 1430 | 9 | 28.9 | 46.6 | 1.7 | 61.2 | 3.4 | 0.55 | 1.9 | 0.2 |
| 11 | Training Area 15 | 8/18/2014 | 0858 | 32 | 24.0 | 69.4 | 0.5 | 66.1 | 26.5 | 0.51 | 1.5 | 3.3 |
| 12 | Training Area 15 | 8/18/2014 | 1534 | 37 | 31.4 | 40.5 | 1.5 | 60.9 | 5.8 | 0.50 | 2.0 | 3.5 |
| 13 | Tenalquot Prairie | 9/18/2014 | 1331 | 53 | 19.7 | 72.6 | 2.0 | 58.6 | 30.0 | 0.48 | 2.8 | 2.7 |
| 14 | Tenalquot Prairie | 9/22/2014 | 1600 | 17 | 22.8 | 53.3 | 0.9 | 51.1 | 13.1 | 0.52 | 3.5 | 2.5 |
| 15 | Johnson Prairie | 8/7/2014 | 0920 | 20 | 15.2 | 84.3 | 2.1 | 66.4 | 12.3 | 0.63 | 3.3 | 0.8 |
| 16 | Johnson Prairie | 8/7/2014 | 1501 | 9 | 28.1 | 41.6 | 2.0 | 63.4 | 2.3 | 0.54 | 2.4 | 0.5 |
| 17 | Training Area 15 | 8/18/2014 | 1002 | 20 | 25.9 | 59.7 | 0.9 | 59.8 | 21.4 | 0.53 | 1.6 | 2.3 |
| 18 | Training Area 15 | 8/18/2014 | 1716 | 20 | 32.0 | 44.6 | 0.9 | 60.4 | 5.8 | 0.53 | 1.8 | 1.4 |
| 19 | Lower Weir | 7/22/2014 | 0942 | 33 | 15.9 | 71.2 | 0.5 | 74.7 | 14.5 | 0.52 | 2.4 | 0.6 |
| 20 | Lower Weir | 7/22/2014 | 1341 | 11 | 18.9 | 64.5 | 1.2 | 81.3 | 8.0 | 0.59 | 2.8 | 0.4 |

*Shaded plots were not included in any Chapter 2 analyses due to post-burn management interference*

## Appendix E: Measured dead fuel moisture vs. fuel modeling tables

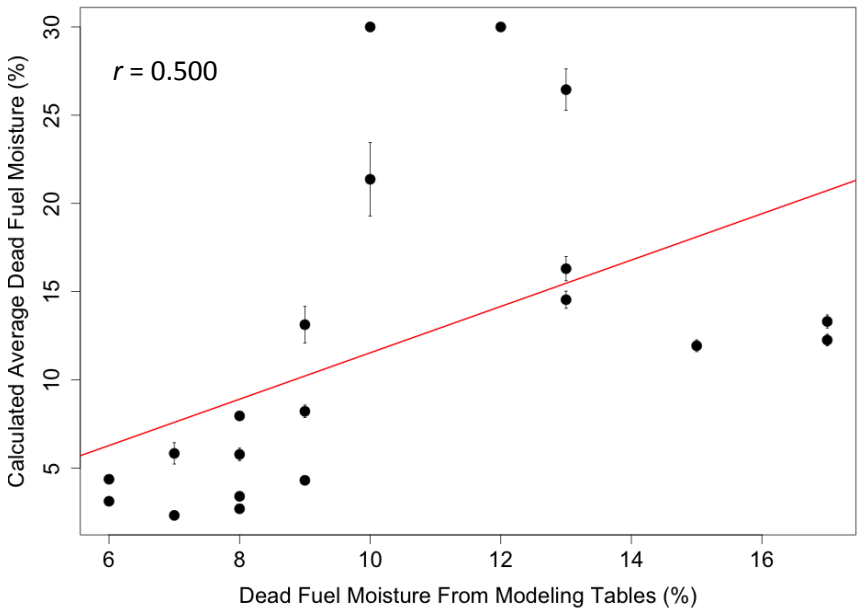


Data from all 20 plots as a function of dead fuel moisture calculated from standard fuel modeling tables using weather, slope, and time of year. Error bars represent standard error of the mean.

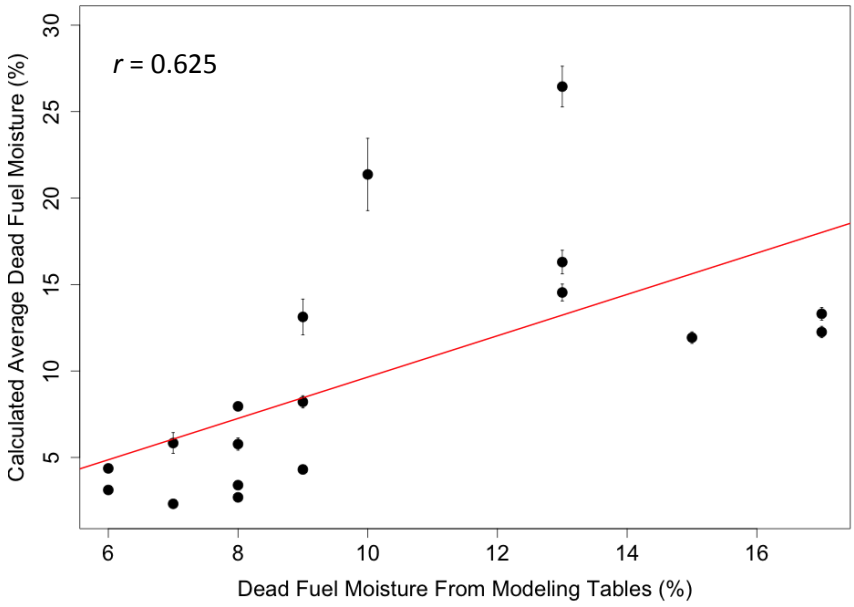


The same dataset with two plots removed due to excessively high dead fuel moistures that were calculated in the field (i.e., the maximum possible – 30%). Error bars represent standard error of the mean.

# Appendix F: Data summary tables

**Soil temperatures, heat dosages, and burn severity**

*Afternoon-burned plots are shaded*

| Plot | Burn Unit | Average peak soil temp (°C) | Total 100% lethal heat dosage (°C * log[min]) | Cover of unburned or low-severity areas (%) |
|---|---|---|---|---|
| 1 | South Weir | 24.4 | 0.0 | 18.4 |
| 2 | South Weir | 41.9 | 13.0 | 15.3 |
| 3 | Glacial Heritage | 34.5 | 4.1 | 42.9 |
| 4 | Glacial Heritage | 45.2 | 28.3 | 6.1 |
| 5 | Upper Weir | 27.6 | 0.0 | 25.5 |
| 6 | Upper Weir | 40.4 | 0.1 | 13.3 |
| 7 | Johnson Prairie | 25.1 | 0.0 | 4.1 |
| 8 | Johnson Prairie | 47.3 | 32.8 | 0.0 |
| 9 | Training Area 6 | 28.3 | 0.0 | 18.4 |
| 10 | Training Area 6 | 54.8 | 50.0 | 0.0 |
| 11 | Training Area 15 | 22.1 | 0.0 | 94.9 |
| 12 | Training Area 15 | 47.2 | 67.6 | 16.3 |
| 13 | Tenalquot Prairie | 23.4 | 0.0 | 92.9 |
| 14 | Tenalquot Prairie | N/A | N/A | 17.4 |
| 15 | Johnson Prairie | 29.3 | 0.0 | 0.0 |
| 16 | Johnson Prairie | 41.2 | 0.2 | 0.0 |
| 17 | Training Area 15 | 26.9 | 0.0 | 43.9 |
| 18 | Training Area 15 | N/A | N/A | 5.1 |
| 19 | Lower Weir | 22.7 | 0.0 | 25.5 |
| 20 | Lower Weir | 27.4 | 0.0 | 5.1 |

**Species richness, diversity, and shifts in composition**

*Afternoon-burned plots are shaded*

| Plot | Burn Unit | Average quadrat-scale species richness | | Plot-scale species richness | | Average quadrat-scale Hill's $N_1$ diversity index | | Beta richness | | Average pre- to post-burn Bray-Curtis distance (quadrat-scale) | Pre- to post-burn Bray-Curtis distance (average plot composition) |
|---|---|---|---|---|---|---|---|---|---|---|---|
| | | Pre-burn | Post-burn | Pre-burn | Post-burn | Pre-burn | Post-burn | Pre-burn | Post-burn | | |
| 1 | South Weir | 10.4 | 11.6 | 30 | 36 | 4.8 | 3.3 | 2.9 | 3.1 | 0.44 | 0.36 |
| 2 | South Weir | 12.5 | 13.2 | 34 | 34 | 6.5 | 5.5 | 2.7 | 2.6 | 0.42 | 0.36 |
| 5 | Upper Weir | 14.0 | 16.4 | 35 | 40 | 6.4 | 6.0 | 2.5 | 2.5 | 0.31 | 0.22 |
| 6 | Upper Weir | 14.6 | 14.9 | 38 | 40 | 5.5 | 5.9 | 2.6 | 2.7 | 0.42 | 0.33 |
| 7 | Johnson Prairie | 19.2 | 20.4 | 42 | 39 | 8.8 | 7.0 | 2.2 | 1.9 | 0.34 | 0.24 |
| 8 | Johnson Prairie | 17.8 | 19.0 | 37 | 36 | 8.6 | 7.4 | 2.1 | 1.9 | 0.38 | 0.31 |
| 9 | Training Area 6 | 18.9 | 21.2 | 41 | 43 | 8.6 | 10.4 | 2.2 | 2.0 | 0.38 | 0.36 |
| 10 | Training Area 6 | 19.1 | 20.3 | 41 | 41 | 9.5 | 10.5 | 2.1 | 2.0 | 0.46 | 0.39 |
| 13 | Tenalquot Prairie | 12.6 | 12.9 | 31 | 32 | 4.9 | 6.2 | 2.5 | 2.5 | 0.28 | 0.15 |
| 14 | Tenalquot Prairie | 11.4 | 12.2 | 27 | 28 | 3.7 | 6.6 | 2.4 | 2.3 | 0.40 | 0.32 |
| 15 | Johnson Prairie | 18.4 | 19.8 | 42 | 47 | 7.6 | 7.6 | 2.3 | 2.4 | 0.35 | 0.35 |
| 16 | Johnson Prairie | 22.7 | 24.7 | 52 | 50 | 11.2 | 11.7 | 2.3 | 2.0 | 0.48 | 0.44 |
| 17 | Training Area 15 | 14.9 | 15.6 | 43 | 52 | 6.4 | 6.7 | 2.9 | 3.3 | 0.32 | 0.28 |
| 18 | Training Area 15 | 16.2 | 17.6 | 48 | 48 | 7.8 | 7.7 | 3.0 | 2.7 | 0.41 | 0.34 |
| 19 | Lower Weir | 16.2 | 19.2 | 31 | 32 | 5.3 | 5.0 | 1.9 | 1.7 | 0.43 | 0.36 |
| 20 | Lower Weir | 16.4 | 17.9 | 30 | 33 | 5.3 | 5.6 | 1.8 | 1.8 | 0.30 | 0.32 |

**Vegetation structure – height**

*Afternoon-burned plots are shaded*

| Plot | Burn Unit | Average quadrat-scale CV of vegetation height | | Plot-scale CV of vegetation height | | Spatial autocorrelation of vegetation height | | | | Interspersion & Juxtaposition Index (IJI) of vegetation height (%) | |
|---|---|---|---|---|---|---|---|---|---|---|---|
| | | | | | | Range (m) | | Magnitude (%) | | | |
| | | Pre-burn | Post-burn | Pre-burn | Post-burn | Pre-burn | Post-burn | Pre-burn | Post-burn | Pre-burn | Post-burn |
| 1 | South Weir | 0.39 | 0.45 | 0.46 | 0.54 | 0.5 | <0.25 | 65.4 | 0.0 | 47.8 | 48.8 |
| 2 | South Weir | 0.45 | 0.53 | 0.56 | 0.72 | 3.0 | <0.25 | 13.7 | 0.0 | 57.9 | 50.7 |
| 5 | Upper Weir | 0.39 | 0.49 | 0.47 | 0.56 | 0.5 | 1.9 | 16.4 | 21.6 | 54.9 | 53.7 |
| 6 | Upper Weir | 0.45 | 0.50 | 0.52 | 0.55 | 0.9 | <0.25 | 1.3 | 0.0 | 53.6 | 52.3 |
| 7 | Johnson Prairie | 0.39 | 0.47 | 0.46 | 0.62 | 0.5 | <0.25 | 24.2 | 0.0 | 58.5 | 54.6 |
| 8 | Johnson Prairie | 0.40 | 0.50 | 0.49 | 0.63 | <0.25 | 3.0 | 9.2 | 18.4 | 53.7 | 50.3 |
| 9 | Training Area 6 | 0.42 | 0.46 | 0.52 | 0.53 | 0.5 | 2.2 | 10.6 | 20.6 | 56.1 | 48.1 |
| 10 | Training Area 6 | 0.37 | 0.40 | 0.44 | 0.43 | <0.25 | 0.5 | 0.0 | 6.6 | 54.6 | 48.5 |
| 13 | Tenalquot Prairie | 0.47 | 0.55 | 0.52 | 0.66 | 1.4 | 1.2 | 36.9 | 22.6 | 55.8 | 49.6 |
| 14 | Tenalquot Prairie | 0.50 | 0.63 | 0.53 | 0.70 | <0.25 | 0.5 | 0.0 | 4.2 | 53.8 | 50.7 |
| 15 | Johnson Prairie | 0.36 | 0.40 | 0.47 | 0.48 | 3.0 | 1.3 | 54.7 | 17.1 | 51.3 | 44.6 |
| 16 | Johnson Prairie | 0.36 | 0.41 | 0.45 | 0.54 | 1.1 | 1.3 | 100.0 | 100.0 | 59.6 | 50.2 |
| 17 | Training Area 15 | 0.41 | 0.48 | 0.46 | 0.53 | 0.5 | <0.25 | 46.8 | 4.1 | 52.5 | 53.9 |
| 18 | Training Area 15 | 0.41 | 0.39 | 0.49 | 0.48 | 1.6 | 0.9 | 46.0 | 15.8 | 52.8 | 54.9 |
| 19 | Lower Weir | 0.37 | 0.48 | 0.41 | 0.53 | 2.0 | <0.25 | 45.4 | 2.2 | 51.1 | 55.5 |
| 20 | Lower Weir | 0.40 | 0.45 | 0.43 | 0.48 | 3.0 | 1.2 | 18.6 | 16.6 | 52.2 | 53.2 |

Semivariogram range of <0.25 indicates a scale of spatial autocorrelation not detectable with my sample point spacing (25cm)

**Vegetation structure – bare or open ground and litter depth**

*Afternoon-burned plots are shaded*

| Plot | Burn Unit | Cover of bare or open ground (%) | | Range of spatial autocorrelation of bare or open ground (cm) | | Edge-to-area ratio of bare or open ground ($m^{-1}$) | | CV of litter depth | |
|---|---|---|---|---|---|---|---|---|---|
| | | Pre-burn | Post-burn | Pre-burn | Post-burn | Pre-burn | Post-burn | Pre-burn | Post-burn |
| 1 | South Weir | 1.6 | 9.5 | 9.5 | 13.2 | 8.0 | 12.7 | 0.43 | 0.70 |
| 2 | South Weir | 5.0 | 15.4 | 12.8 | 17.2 | 10.9 | 10.0 | 0.86 | 0.37 |
| 5 | Upper Weir | 1.5 | 5.2 | 31.6 | 17.2 | 11.9 | 6.4 | 0.44 | 0.69 |
| 6 | Upper Weir | 1.7 | 11.0 | 16.4 | 9.8 | 9.6 | 11.0 | 0.57 | 0.47 |
| 7 | Johnson Prairie | 0.7 | 4.5 | 9.5 | 14.9 | 8.8 | 12.0 | 0.61 | 0.59 |
| 8 | Johnson Prairie | 1.6 | 12.1 | 46.3 | 20.8 | 10.4 | 7.8 | 0.48 | 0.32 |
| 9 | Training Area 6 | 2.0 | 5.4 | 28.1 | 60.0 | 12.5 | 8.3 | 0.52 | 0.41 |
| 10 | Training Area 6 | 0.2 | 5.5 | 60.0 | 18.0 | 32.8 | 15.1 | 0.53 | 0.35 |
| 13 | Tenalquot Prairie | 2.7 | 4.7 | 15.6 | 11.1 | 12.4 | 16.0 | 0.37 | 0.66 |
| 14 | Tenalquot Prairie | 2.5 | 11.0 | 13.7 | 10.6 | 10.1 | 9.9 | 0.23 | 0.72 |
| 15 | Johnson Prairie | 0.8 | 7.0 | 60.0 | 15.0 | 9.0 | 10.0 | 0.41 | 0.36 |
| 16 | Johnson Prairie | 0.5 | 5.5 | 9.5 | 13.3 | 27.9 | 8.1 | 0.59 | 0.32 |
| 17 | Training Area 15 | 2.3 | 8.3 | 9.5 | 9.5 | 12.0 | 9.4 | 0.70 | 0.48 |
| 18 | Training Area 15 | 1.4 | 8.2 | 21.2 | 15.7 | 8.6 | 12.0 | 0.49 | 0.37 |
| 19 | Lower Weir | 0.6 | 6.3 | 9.5 | 10.2 | 5.9 | 5.4 | 0.59 | 0.73 |
| 20 | Lower Weir | 0.4 | 7.0 | 9.5 | 9.5 | 9.5 | 11.7 | 0.56 | 0.37 |

## Appendix G: Species list over all plots sampled for composition

*Nomenclatural authority: USDA PLANTS Database*
Most common/dominant species highlighted in bold

| Scientific Name | Common Name | Nativity | Functional Group | % of plots found in (pre-burn) | % of plots found in (post-burn) | Avg. cover in plots where present (%) (pre-burn) | Avg. cover in plots where present (%) (post-burn) |
|---|---|---|---|---|---|---|---|
| *Achillea millefolium* L. | Common yarrow | Native | Perennial forb | 50 | 56.25 | 0.29 | 0.12 |
| ***Agrostis capillaris* L.** | **Colonial bentgrass** | **Exotic** | **Perennial graminoid** | **100** | **100** | **6.56** | **10.55** |
| *Aira caryophyllea* L. | Silver hairgrass | Exotic | Annual graminoid | 31.25 | 37.5 | 0.11 | 0.42 |
| ***Aira praecox* L.** | **Yellow hairgrass** | **Exotic** | **Annual graminoid** | **93.75** | **87.5** | **0.35** | **0.37** |
| *Anthoxanthum aristatum* Boiss. | Annual vernalgrass | Exotic | Annual graminoid | 12.5 | 12.5 | 4.14 | 2.23 |
| *Anthoxanthum odoratum* L. | Sweet vernalgrass | Exotic | Perennial graminoid | 37.5 | 31.25 | 1.48 | 1.38 |
| *Apocynum androsaemifolium* L. | Spreading dogbane | Native | Perennial forb | 6.25 | 6.25 | 0.43 | 0.18 |
| *Arctostaphylos uva-ursi* (L.) Spreng. | Kinnikinnick | Native | Woody shrub | 12.5 | 12.5 | 3.39 | 3.29 |
| *Arrhenatherum elatius* (L.) P. Beauv. ex J. Presl & C. Presl | Tall oatgrass | Exotic | Perennial graminoid | 6.25 | 0 | 0.04 | N/A |
| *Balsamorhiza deltoidea* Nutt. | Deltoid balsamroot | Native | Perennial forb | 6.25 | 6.25 | 0.07 | 0.04 |
| *Brodiaea coronaria* (Salisb.) Engl. | Crown brodiaea | Native | Perennial forb | 18.75 | 25 | 0.18 | 0.16 |
| *Bromus carinatus* Hook. & Arn. | California brome | Native | Perennial graminoid | 18.75 | 25 | 0.06 | 0.13 |
| ***Camassia quamash* (Pursh) Greene** | **Small camas** | **Native** | **Perennial forb** | **87.5** | **87.5** | **1.36** | **1.45** |
| *Campanula rotundifolia* L. | Bluebell bellflower | Native | Perennial forb | 6.25 | 6.25 | 0.29 | 0.11 |
| *Cardamine hirsuta* L. | Hairy bittercress | Exotic | Annual forb | 0 | 12.5 | N/A | 0.04 |
| ***Carex inops* L.H. Bailey** | **Long-stolon sedge** | **Native** | **Perennial graminoid** | **100** | **100** | **0.86** | **0.57** |
| *Castilleja hispida* Benth. | Harsh Indian paintbrush | Native | Perennial forb | 12.5 | 6.25 | 0.04 | 0.04 |
| *Cerastium arvense* L. | Field chickweed | Native | Perennial forb | 31.25 | 31.25 | 0.17 | 0.20 |
| *Cerastium glomeratum* Thuill. | Sticky chickweed | Exotic | Annual forb | 31.25 | 68.75 | 0.06 | 0.12 |
| *Claytonia perfoliata* Donn ex Willd. | Miner's lettuce | Native | Annual forb | 6.25 | 0 | 0.04 | N/A |
| *Crepis capillaris* (L.) Wallr. | Smooth hawksbeard | Exotic | Perennial forb | 68.75 | 62.5 | 0.25 | 0.10 |
| *Cytisus scoparius* (L.) Link | Scotch broom | Exotic | Woody shrub | 81.25 | 68.75 | 0.78 | 0.30 |
| *Dactylis glomerata* L. | Orchardgrass | Exotic | Perennial graminoid | 6.25 | 0 | 0.07 | N/A |
| ***Danthonia californica* Bol.** | **California oatgrass** | **Native** | **Perennial graminoid** | **93.75** | **87.5** | **0.40** | **0.31** |

| Scientific Name | Common Name | Nativity | Functional Group | % of plots found in (pre-burn) | % of plots found in (post-burn) | Avg. cover in plots where present (%) (pre-burn) | Avg. cover in plots where present (%) (post-burn) |
|---|---|---|---|---|---|---|---|
| *Danthonia spicata* (L.) P. Beauv. ex Roem. & Schult. | Poverty oatgrass | Native | Perennial graminoid | 12.5 | 6.25 | 0.05 | 0.11 |
| *Dichanthelium oligosanthes* (Schult.) Gould | Heller's rosette grass | Native | Perennial graminoid | 31.25 | 25 | 0.21 | 0.25 |
| *Epilobium minutum* Lindl. ex Lehm. | Chaparral willowherb | Native | Annual forb | 6.25 | 6.25 | 0.04 | 0.04 |
| *Erigeron speciosus* (Lindl.) DC. | Aspen fleabane | Native | Perennial forb | 6.25 | 0 | 0.04 | N/A |
| ***Eriophyllum lanatum* (Pursh) Forbes** | **Common woolly sunflower** | **Native** | **Perennial forb** | **93.75** | **87.5** | **2.18** | **1.00** |
| ***Festuca idahoensis* Elmer subsp. *roemeri* (Pavlick) S. Aiken** | **Roemer's fescue** | **Native** | **Perennial graminoid** | **100** | **93.75** | **4.88** | **4.36** |
| *Festuca rubra* L. | Red fescue | Exotic | Perennial graminoid | 0 | 12.5 | N/A | 0.09 |
| *Fragaria virginiana* Duchesne | Virginia strawberry | Native | Perennial forb | 31.25 | 31.25 | 0.49 | 0.21 |
| *Fritillaria affinis* (Schult.) Sealy | Checker lily | Native | Perennial forb | 50 | 50 | 0.06 | 0.12 |
| *Galium parisiense* L. | Wall bedstraw | Exotic | Annual forb | 81.25 | 81.25 | 0.48 | 0.43 |
| *Gamochaeta ustulata* (Nutt.)G.L.Nesom | Featherweed | Native | Perennial forb | 6.25 | 0 | 0.04 | N/A |
| *Holcus lanatus* L. | Common velvetgrass | Exotic | Perennial graminoid | 56.25 | 43.75 | 0.71 | 0.39 |
| ***Hypericum perforatum* L.** | **Common St. Johnswort** | **Exotic** | **Perennial forb** | **100** | **100** | **0.37** | **0.31** |
| ***Hypochaeris radicata* L.** | **Hairy cat's ear** | **Exotic** | **Perennial forb** | **100** | **100** | **15.54** | **12.99** |
| *Koeleria macrantha* (Ledeb.) Schult. | Prairie Junegrass | Native | Perennial graminoid | 6.25 | 25 | 0.04 | 0.05 |
| ***Leucanthemum vulgare* Lam.** | **Oxeye daisy** | **Exotic** | **Perennial forb** | **87.5** | **100** | **2.01** | **0.54** |
| *Logfia minima* (Sm.) Dumort. | Little cottonrose | Exotic | Annual forb | 12.5 | 25 | 0.04 | 0.09 |
| *Lomatium triternatum* (Pursh) J.M. Coult. & Rose | Nineleaf biscuitroot | Native | Perennial forb | 12.5 | 18.75 | 0.13 | 0.10 |
| *Lomatium utriculatum* (Nutt. ex Torr. & A. Gray) J.M. Coult & Rose | Common lomatium | Native | Perennial forb | 62.5 | 68.75 | 0.34 | 0.40 |
| ***Lotus micranthus* Benth.** | **Desert deervetch** | **Native** | **Annual forb** | **93.75** | **100** | **0.21** | **0.36** |
| *Lupinus albicaulis* Douglas | Sicklekeel lupine | Native | Perennial forb | 18.75 | 18.75 | 0.44 | 0.31 |
| *Lupinus bicolor* Lindl. | Miniature lupine | Native | Annual forb | 0 | 12.5 | N/A | 0.29 |
| *Lupinus lepidus* Douglas ex Lindl. | Pacific lupine | Native | Perennial forb | 50 | 68.75 | 0.37 | 0.16 |
| ***Luzula comosa* E. Mey.** | **Pacific woodrush** | **Native** | **Perennial graminoid** | **93.75** | **93.75** | **0.71** | **1.40** |
| *Malus fusca* (Raf.) C.K. Schneid. | Oregon crab apple | Native | Woody shrub | 6.25 | 0 | 0.04 | N/A |

| Scientific Name | Common Name | Nativity | Functional Group | % of plots found in (pre-burn) | % of plots found in (post-burn) | Avg. cover in plots where present (%) (pre-burn) | Avg. cover in plots where present (%) (post-burn) |
|---|---|---|---|---|---|---|---|
| *Micranthes integrifolia* (Hook.) Small | Wholeleaf saxifrage | Native | Perennial forb | 12.5 | 12.5 | 0.05 | 0.04 |
| *Microseris laciniata* (Hook.) Sch. Bip. | Cutleaf silverpuffs | Native | Perennial forb | 62.5 | 56.25 | 0.16 | 0.13 |
| *Moenchia erecta* (L.) G. Gaertn., B. Mey. & Scherb. | Upright chickweed | Exotic | Annual forb | 56.25 | 50 | 0.27 | 0.20 |
| *Myosotis discolor* Pers. | Changing forget-me-not | Exotic | Annual forb | 12.5 | 18.75 | 0.13 | 0.19 |
| *Parentucellia viscosa* (L.) Caruel | Yellow glandweed | Exotic | Annual forb | 43.75 | 62.5 | 0.36 | 0.45 |
| ***Plantago lanceolata* L.** | **Narrowleaf plantain** | **Exotic** | **Perennial forb** | **100** | **100** | **1.86** | **1.89** |
| *Poa compressa* L. | Canada bluegrass | Exotic | Perennial graminoid | 68.75 | 62.5 | 0.10 | 0.14 |
| *Poa pratensis* L. | Kentucky bluegrass | Exotic | Perennial graminoid | 68.75 | 62.5 | 0.10 | 0.14 |
| *Potentilla gracilis* Douglas ex Hook. | Slender cinquefoil | Native | Perennial forb | 31.25 | 31.25 | 0.29 | 0.20 |
| *Primula hendersonii* (A. Gray) A.R. Mast & Reveal | Mosquito bills | Native | Perennial forb | 25 | 18.75 | 0.13 | 0.19 |
| *Prunella vulgaris* L. | Common selfheal | Native | Perennial forb | 18.75 | 12.5 | 0.10 | 0.05 |
| *Pseudotsuga menziesii* (Mirb.) Franco | Douglas-fir | Native | Tree | 12.5 | 43.75 | 0.13 | 0.11 |
| *Pteridium aquilinum* (L.) Kuhn | Western brackenfern | Native | Perennial forb | 6.25 | 0 | 0.07 | N/A |
| *Quercus garryana* Douglas ex Hook. | Oregon white oak | Native | Tree | 6.25 | 0 | 0.07 | N/A |
| *Ranunculus occidentalis* Nutt. | Western buttercup | Native | Perennial forb | 62.5 | 56.25 | 0.21 | 0.22 |
| *Rubus armeniacus* Focke | Himalayan blackberry | Exotic | Woody shrub | 6.25 | 0 | 0.04 | N/A |
| ***Rumex acetosella* L.** | **Common sheep sorrel** | **Exotic** | **Perennial forb** | **100** | **100** | **0.94** | **0.76** |
| *Senecio vulgaris* L. | Common groundsel | Exotic | Annual forb | 12.5 | 25 | 0.04 | 0.04 |
| *Sericocarpus rigidus* Lindl. | Columbian whitetop aster | Native | Perennial forb | 56.25 | 50 | 0.19 | 0.16 |
| *Silene antirrhina* L. | Sleepy silene | Native | Annual forb | 0 | 31.25 | N/A | 0.31 |
| *Sisyrinchium idahoense* E.P. Bicknell | Idaho blue-eyed grass | Native | Perennial forb | 0 | 12.5 | N/A | 0.04 |
| *Solidago simplex* Kunth | Mt. Albert goldenrod | Native | Perennial forb | 18.75 | 25 | 0.04 | 0.04 |
| *Spiranthes romanzoffiana* Cham. | Hooded lady's tresses | Native | Perennial forb | 62.5 | 87.5 | 0.06 | 0.12 |
| *Symphoricarpos albus* (L.) S.F. Blake | Common snowberry | Native | Woody shrub | 12.5 | 6.25 | 0.14 | 0.04 |
| *Taraxacum officinale* F.H. Wigg. | Common dandelion | Exotic | Perennial forb | 68.75 | 62.5 | 0.25 | 0.10 |
| ***Teesdalia nudicaulis* (L.) W.T. Aiton** | **Barestem teesdalia** | **Exotic** | **Annual forb** | **100** | **100** | **0.52** | **0.59** |

| Scientific Name | Common Name | Nativity | Functional Group | % of plots found in (pre-burn) | % of plots found in (post-burn) | Avg. cover in plots where present (%) (pre-burn) | Avg. cover in plots where present (%) (post-burn) |
|---|---|---|---|---|---|---|---|
| *Toxicoscordion venenosum* (S. Watson) Rydb. | Meadow deathcamas | Native | Perennial forb | 31.25 | 56.25 | 0.09 | 0.18 |
| *Tragopogon dubius* Scop. | Yellow salsify | Exotic | Annual forb | 6.25 | 6.25 | 0.04 | 0.04 |
| ***Trifolium dubium* Sibth.** | **Suckling clover** | **Exotic** | **Annual forb** | **93.75** | **100** | **1.27** | **0.82** |
| *Trifolium oliganthum* Steud. | Fewflower clover | Native | Annual forb | 6.25 | 25 | 0.11 | 0.08 |
| *Trifolium pratense* L. | Red clover | Exotic | Perennial forb | 6.25 | 0 | 0.18 | N/A |
| *Triphysaria pusilla* (Benth.) T.I. Chuang & Heckard | Dwarf owl's-clover | Native | Annual forb | 18.75 | 18.75 | 0.08 | 0.11 |
| *Veronica arvensis* L. | Corn speedwell | Exotic | Annual forb | 62.5 | 81.25 | 0.13 | 0.17 |
| *Vicia hirsuta* (L.) Gray | Tiny vetch | Exotic | Annual forb | 6.25 | 0 | 0.04 | N/A |
| *Vicia sativa* L. | Garden vetch | Exotic | Annual forb | 56.25 | 50 | 0.37 | 0.34 |
| *Viola adunca* Sm. | Hookedspur violet | Native | Perennial forb | 18.75 | 12.5 | 0.10 | 0.07 |
| *Viola praemorsa* Douglas ex Lindl. | Canary violet | Native | Perennial forb | 6.25 | 12.5 | 0.07 | 0.20 |
| *Vulpia bromoides* (L.) Gray | Brome fescue | Exotic | Annual graminoid | 12.5 | 0 | 0.05 | N/A |

## Appendix H: Stresses for NMDS ordinations

Final stresses of non-metric multidimensional scaling (NMDS) ordinations of quadrat-scale species abundance data at each site for dimensions of k = 1, 2, and 3. Chosen dimensions for ordinations shown in bold.

| Site (Burn Unit) | k = 1 stress | k = 2 stress | k = 3 stress |
|---|---|---|---|
| Lower Weir | 0.346 | 0.179 | **0.128** |
| Upper Weir | 0.375 | 0.238 | **0.170** |
| Training Area 6 | 0.386 | 0.246 | **0.165** |
| Johnson #1 | 0.327 | 0.184 | **0.129** |
| Training Area 15 | 0.443 | 0.260 | **0.178** |
| Tenalquot | 0.378 | 0.206 | **0.148** |
| South Weir | 0.400 | 0.253 | **0.172** |
| Johnson #2 | 0.305 | 0.201 | **0.140** |

## Appendix I: Semivariogram curves for vegetation height analysis

Semivariance (γ) plotted against spatial lag (h)

*Parameters in shaded boxes indicate a model with a pure nugget effect (no autocorrelation detected to the finest spatial scale sampled)*

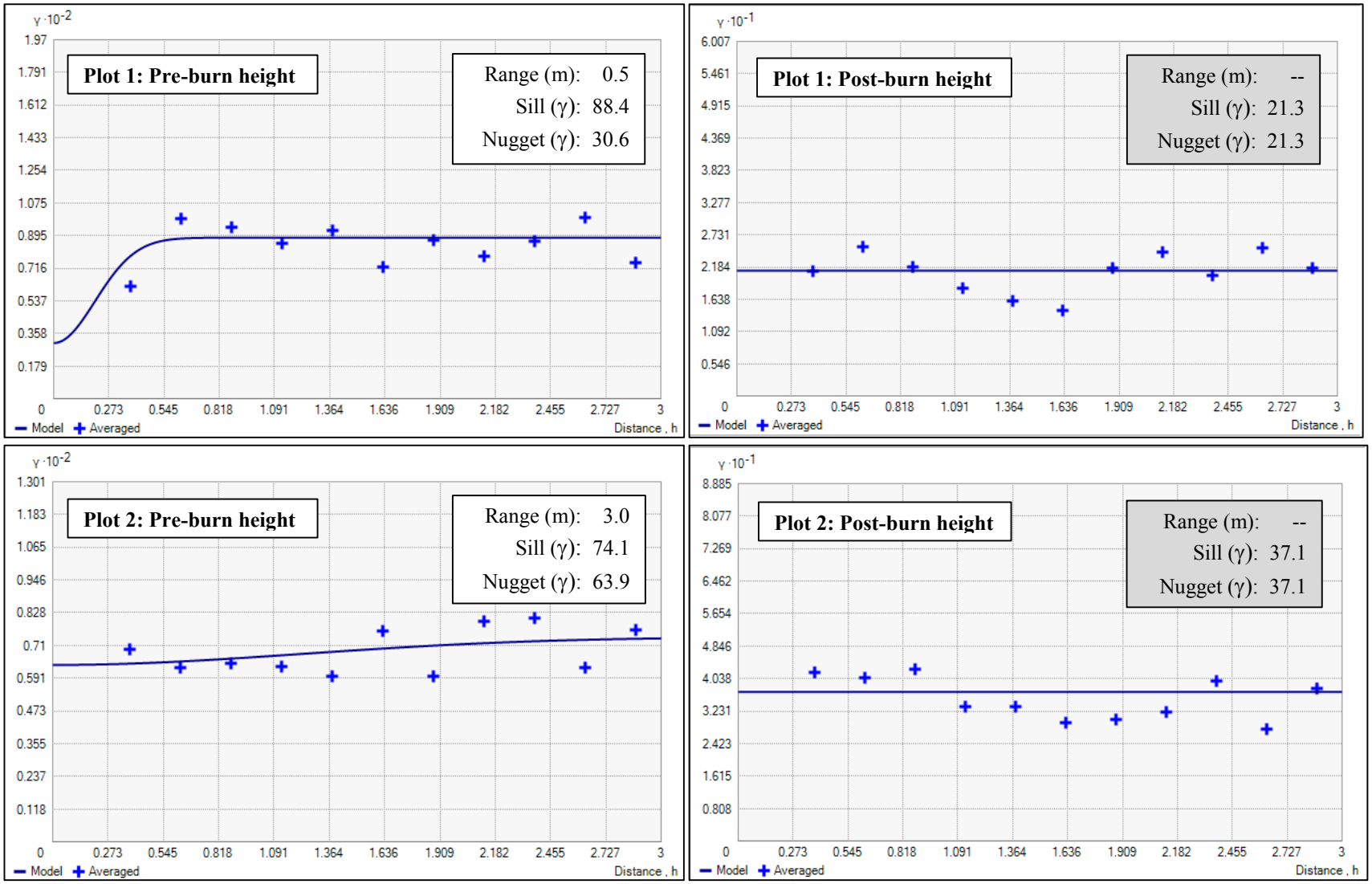

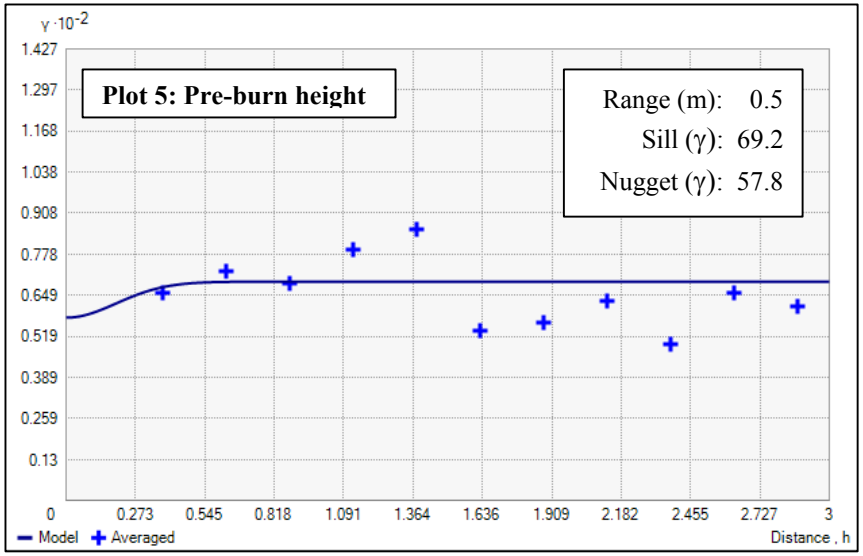
γ ·10-2
1.427
1.297
1.168
1.038
0.908
0.778
0.649
0.519
0.389
0.259
0.13
Plot 5: Pre-burn height
Range (m): 0.5
Sill (γ): 69.2
Nugget (γ): 57.8
0
0.273
0.545
0.818
1.091
1.364
1.636
1.909
2.182
2.455
2.727
3
Model
Averaged
Distance , h

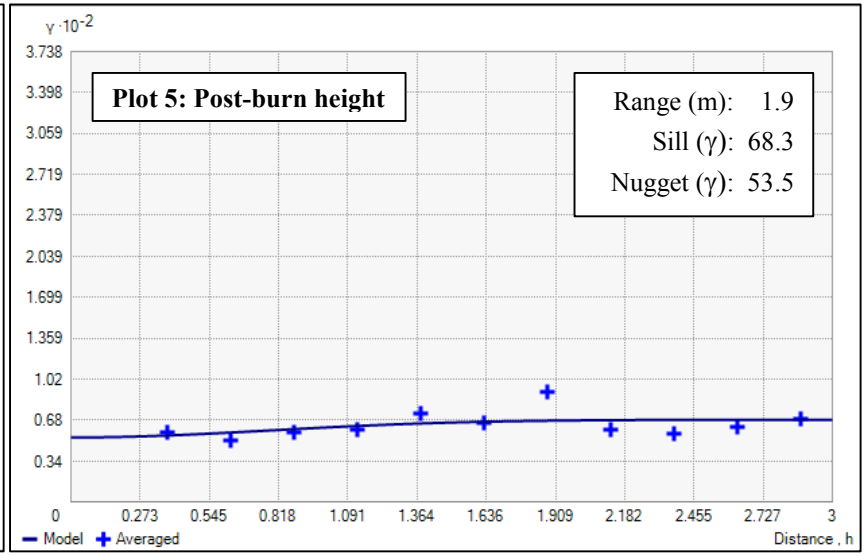
γ ·10-2
3.738
3.398
3.059
2.719
2.379
2.039
1.699
1.359
1.02
0.68
0.34
Plot 5: Post-burn height
Range (m): 1.9
Sill (γ): 68.3
Nugget (γ): 53.5
0
0.273
0.545
0.818
1.091
1.364
1.636
1.909
2.182
2.455
2.727
3
Model
Averaged
Distance , h

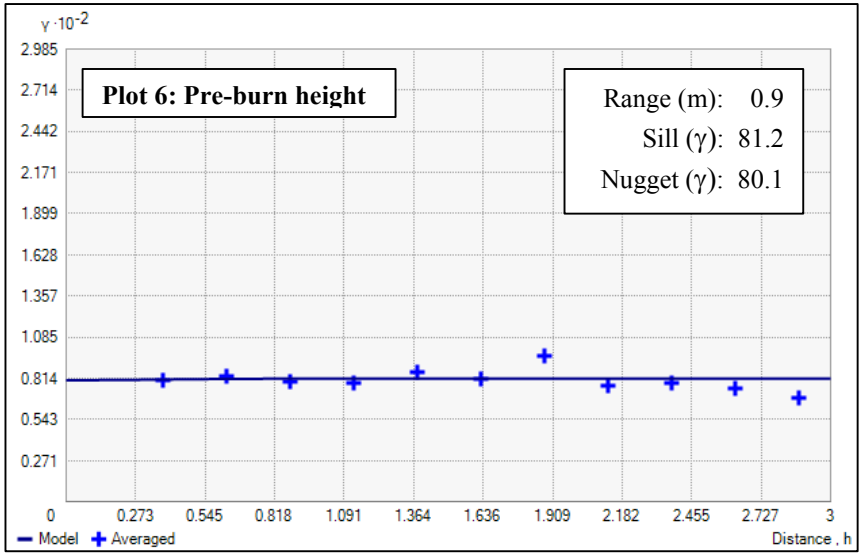
γ ·10-2
2.985
2.714
2.442
2.171
1.899
1.628
1.357
1.085
0.814
0.543
0.271
Plot 6: Pre-burn height
Range (m): 0.9
Sill (γ): 81.2
Nugget (γ): 80.1
0
0.273
0.545
0.818
1.091
1.364
1.636
1.909
2.182
2.455
2.727
3
Model
Averaged
Distance , h

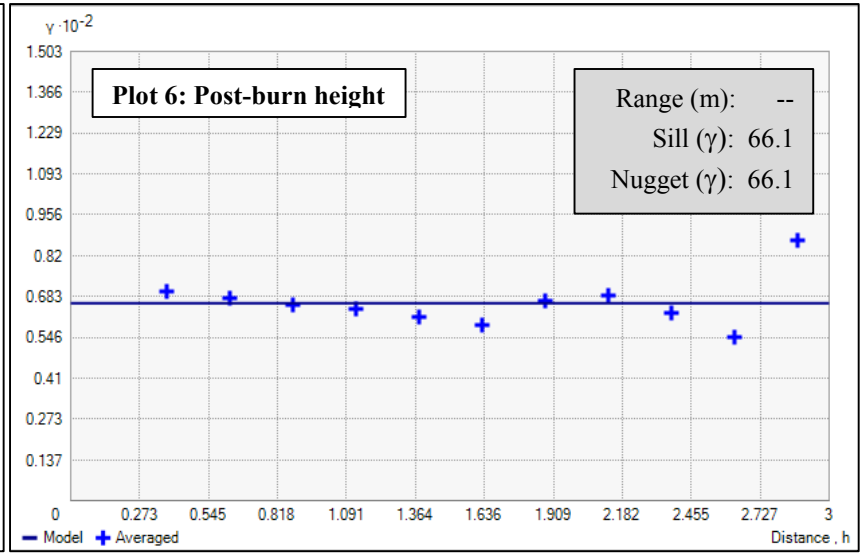
γ ·10-2
1.503
1.366
1.229
1.093
0.956
0.82
0.683
0.546
0.41
0.273
0.137
Plot 6: Post-burn height
Range (m): --
Sill (γ): 66.1
Nugget (γ): 66.1
0
0.273
0.545
0.818
1.091
1.364
1.636
1.909
2.182
2.455
2.727
3
Model
Averaged
Distance , h

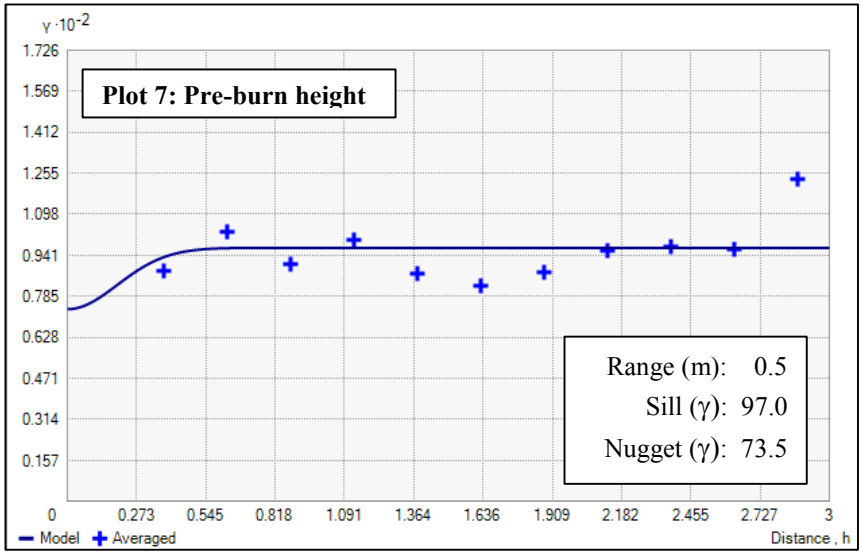
γ ·10-2
1.726
1.569
1.412
1.255
1.098
0.941
0.785
0.628
0.471
0.314
0.157
Plot 7: Pre-burn height
Range (m): 0.5
Sill (γ): 97.0
Nugget (γ): 73.5
0 0.273 0.545 0.818 1.091 1.364 1.636 1.909 2.182 2.455 2.727 3
Model Averaged
Distance , h

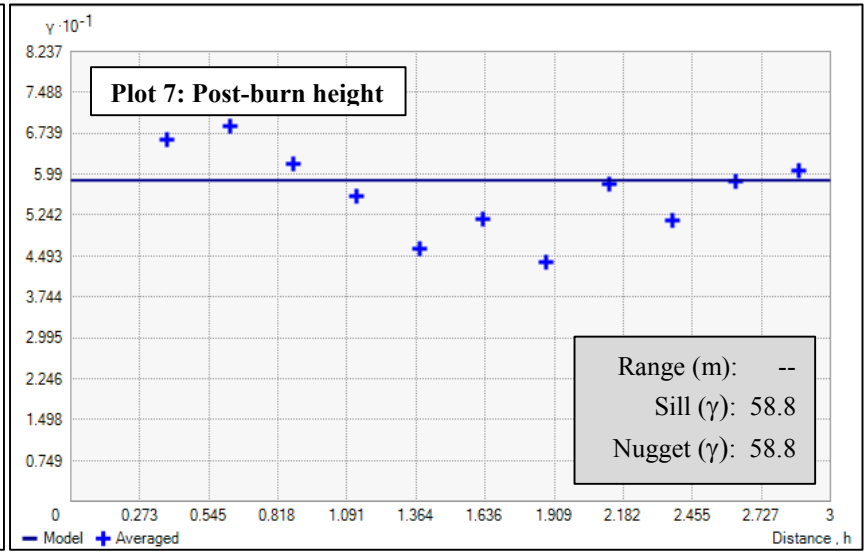
γ ·10-1
8.237
7.488
6.739
5.99
5.242
4.493
3.744
2.995
2.246
1.498
0.749
Plot 7: Post-burn height
Range (m): --
Sill (γ): 58.8
Nugget (γ): 58.8
0 0.273 0.545 0.818 1.091 1.364 1.636 1.909 2.182 2.455 2.727 3
Model Averaged
Distance , h

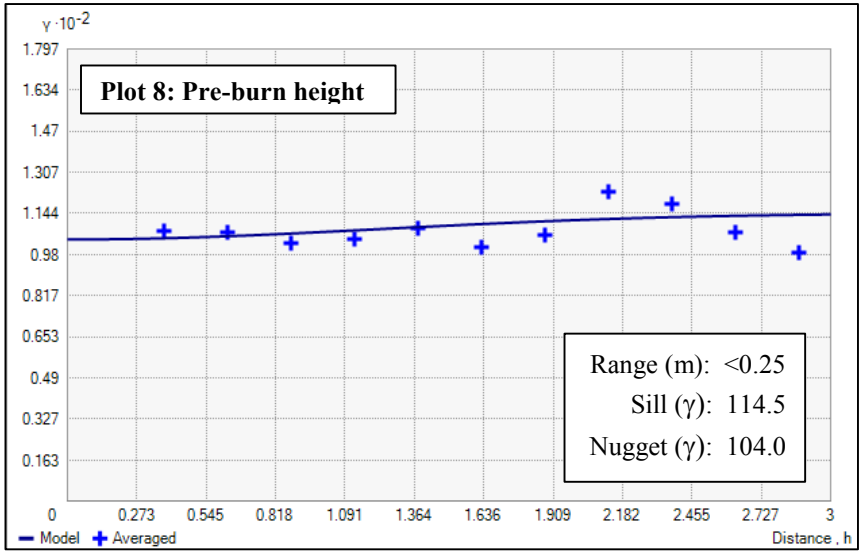
γ ·10-2
1.797
1.634
1.47
1.307
1.144
0.98
0.817
0.653
0.49
0.327
0.163
Plot 8: Pre-burn height
Range (m): <0.25
Sill (γ): 114.5
Nugget (γ): 104.0
0 0.273 0.545 0.818 1.091 1.364 1.636 1.909 2.182 2.455 2.727 3
Model Averaged
Distance , h

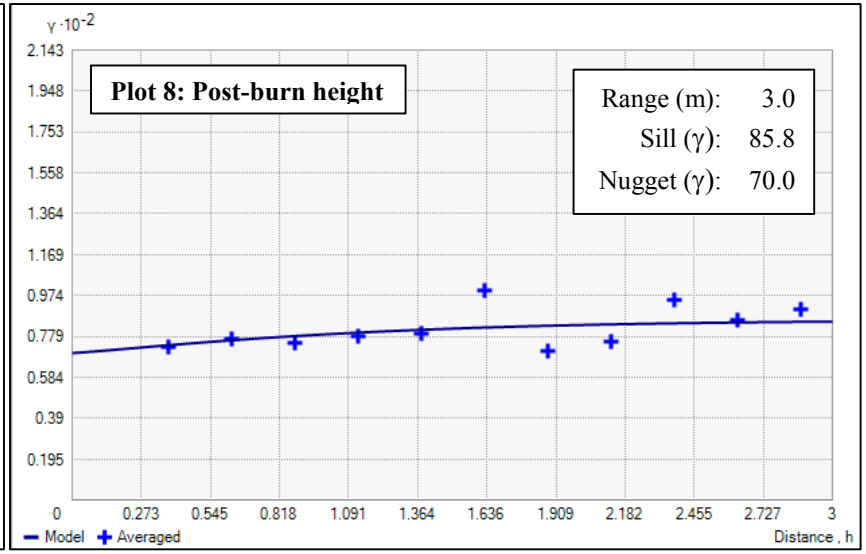
γ ·10-2
2.143
1.948
1.753
1.558
1.364
1.169
0.974
0.779
0.584
0.39
0.195
Plot 8: Post-burn height
Range (m): 3.0
Sill (γ): 85.8
Nugget (γ): 70.0
0 0.273 0.545 0.818 1.091 1.364 1.636 1.909 2.182 2.455 2.727 3
Model Averaged
Distance , h

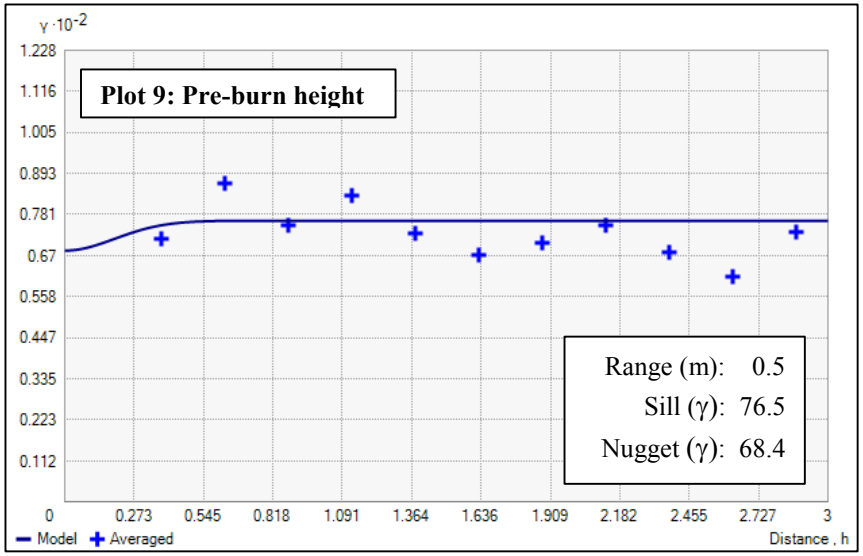
γ ·10-2
1.228
1.116
1.005
0.893
0.781
0.67
0.558
0.447
0.335
0.223
0.112
Plot 9: Pre-burn height
Range (m): 0.5
Sill (γ): 76.5
Nugget (γ): 68.4
0
0.273
0.545
0.818
1.091
1.364
1.636
1.909
2.182
2.455
2.727
3
Model
Averaged
Distance , h

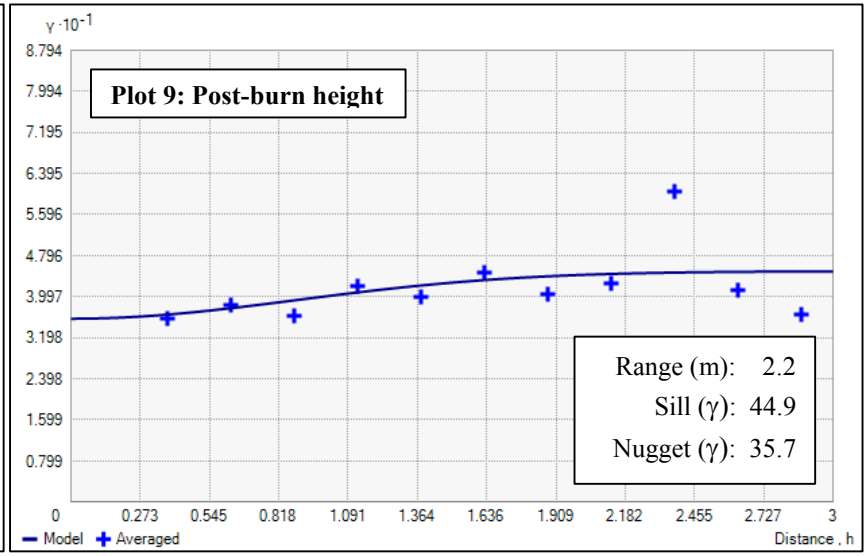
γ ·10-1
8.794
7.994
7.195
6.395
5.596
4.796
3.997
3.198
2.398
1.599
0.799
Plot 9: Post-burn height
Range (m): 2.2
Sill (γ): 44.9
Nugget (γ): 35.7
0
0.273
0.545
0.818
1.091
1.364
1.636
1.909
2.182
2.455
2.727
3
Model
Averaged
Distance , h

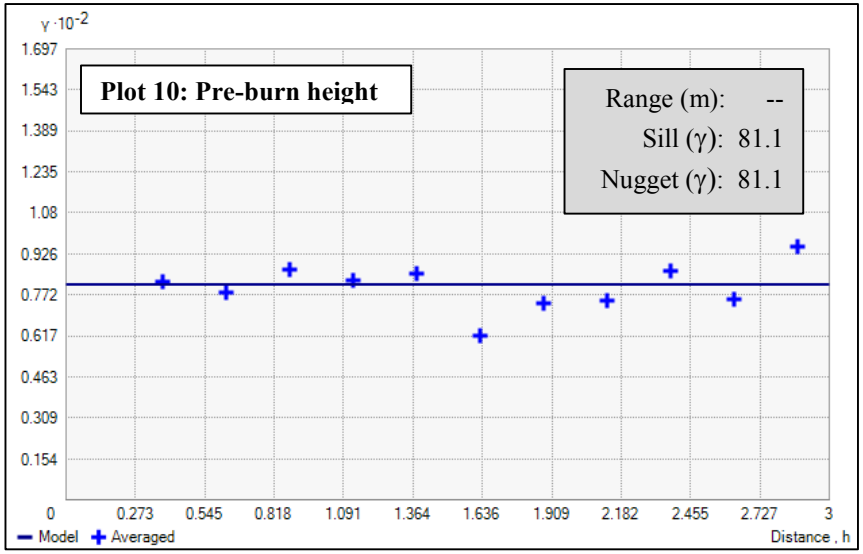
γ ·10-2
1.697
1.543
1.389
1.235
1.08
0.926
0.772
0.617
0.463
0.309
0.154
Plot 10: Pre-burn height
Range (m): --
Sill (γ): 81.1
Nugget (γ): 81.1
0
0.273
0.545
0.818
1.091
1.364
1.636
1.909
2.182
2.455
2.727
3
Model
Averaged
Distance , h

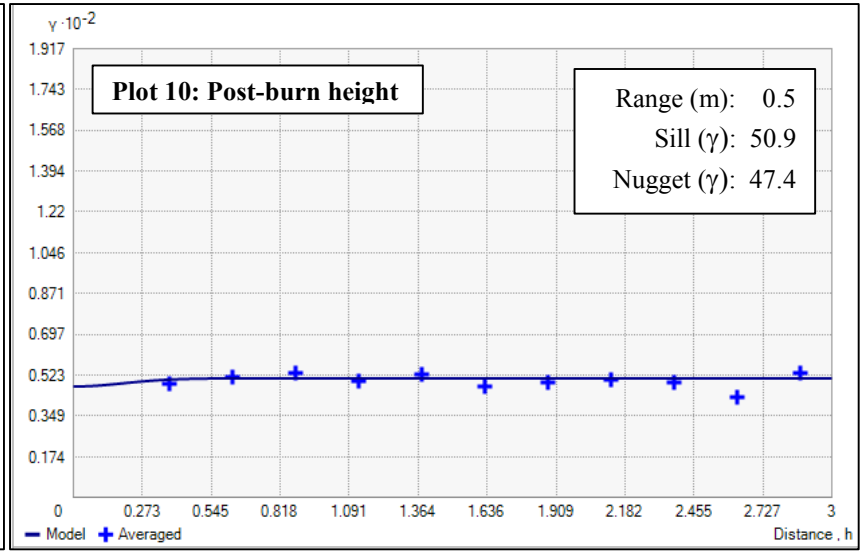
γ ·10-2
1.917
1.743
1.568
1.394
1.22
1.046
0.871
0.697
0.523
0.349
0.174
Plot 10: Post-burn height
Range (m): 0.5
Sill (γ): 50.9
Nugget (γ): 47.4
0
0.273
0.545
0.818
1.091
1.364
1.636
1.909
2.182
2.455
2.727
3
Model
Averaged
Distance , h

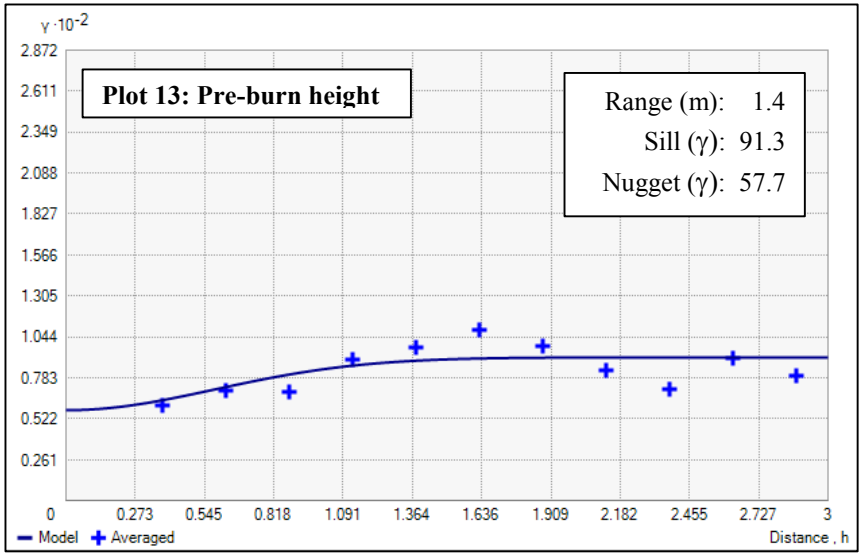
γ ·10-2
2.872
2.611
2.349
2.088
1.827
1.566
1.305
1.044
0.783
0.522
0.261
Plot 13: Pre-burn height
Range (m): 1.4
Sill (γ): 91.3
Nugget (γ): 57.7
0
0.273
0.545
0.818
1.091
1.364
1.636
1.909
2.182
2.455
2.727
3
Model
Averaged
Distance , h

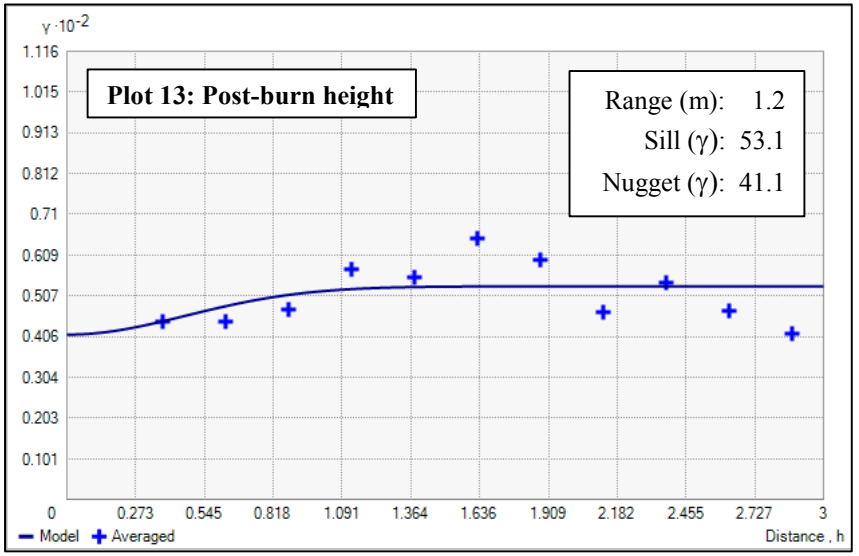
γ ·10-2
1.116
1.015
0.913
0.812
0.71
0.609
0.507
0.406
0.304
0.203
0.101
Plot 13: Post-burn height
Range (m): 1.2
Sill (γ): 53.1
Nugget (γ): 41.1
0
0.273
0.545
0.818
1.091
1.364
1.636
1.909
2.182
2.455
2.727
3
Model
Averaged
Distance , h

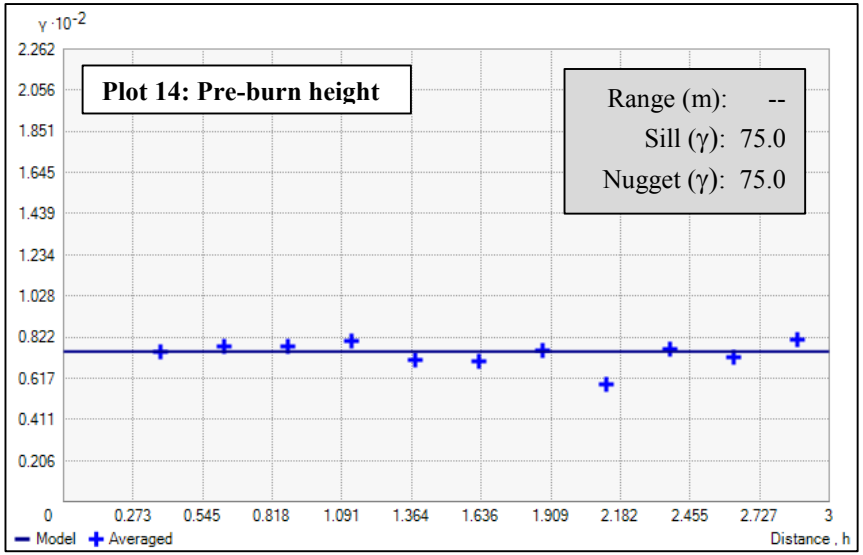
γ ·10-2
2.262
2.056
1.851
1.645
1.439
1.234
1.028
0.822
0.617
0.411
0.206
Plot 14: Pre-burn height
Range (m): --
Sill (γ): 75.0
Nugget (γ): 75.0
0
0.273
0.545
0.818
1.091
1.364
1.636
1.909
2.182
2.455
2.727
3
Model
Averaged
Distance , h

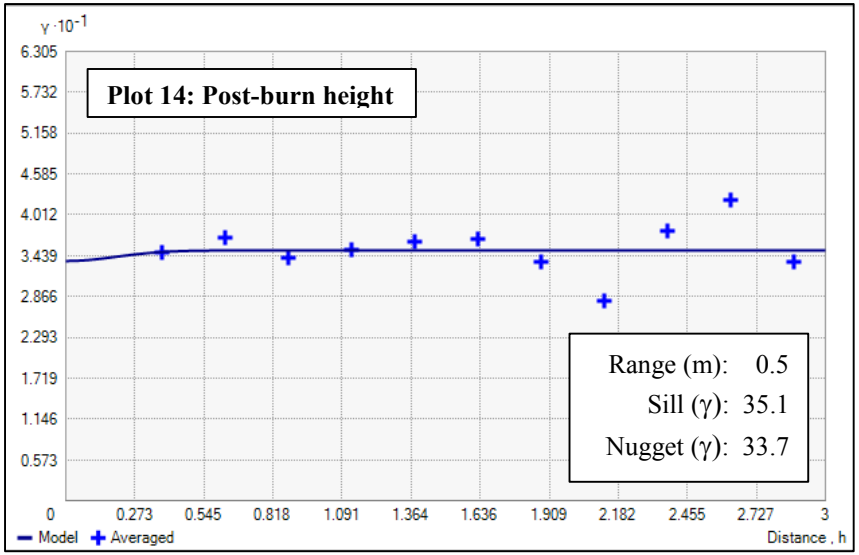
γ ·10-1
6.305
5.732
5.158
4.585
4.012
3.439
2.866
2.293
1.719
1.146
0.573
Plot 14: Post-burn height
Range (m): 0.5
Sill (γ): 35.1
Nugget (γ): 33.7
0
0.273
0.545
0.818
1.091
1.364
1.636
1.909
2.182
2.455
2.727
3
Model
Averaged
Distance , h

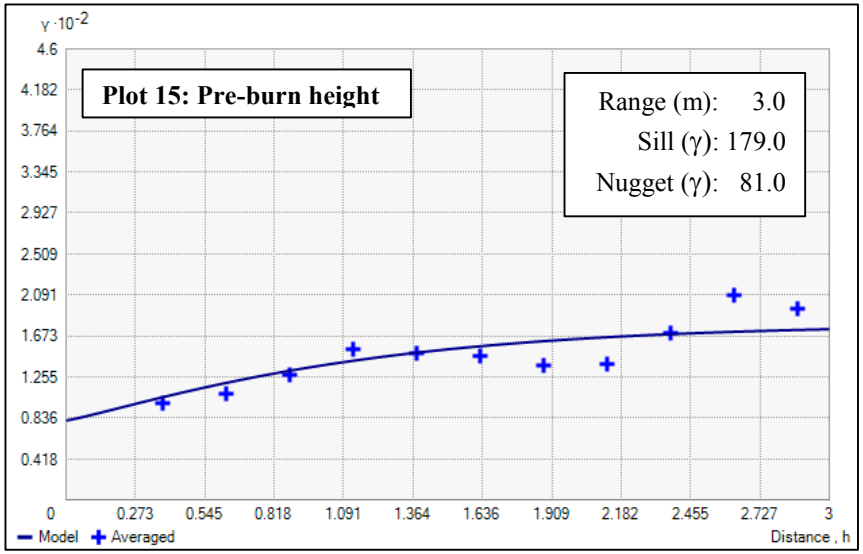
γ ·10-2
4.6
4.182
3.764
3.345
2.927
2.509
2.091
1.673
1.255
0.836
0.418
0
0.273
0.545
0.818
1.091
1.364
1.636
1.909
2.182
2.455
2.727
3
Plot 15: Pre-burn height
Range (m): 3.0
Sill (γ): 179.0
Nugget (γ): 81.0
Model
Averaged
Distance , h

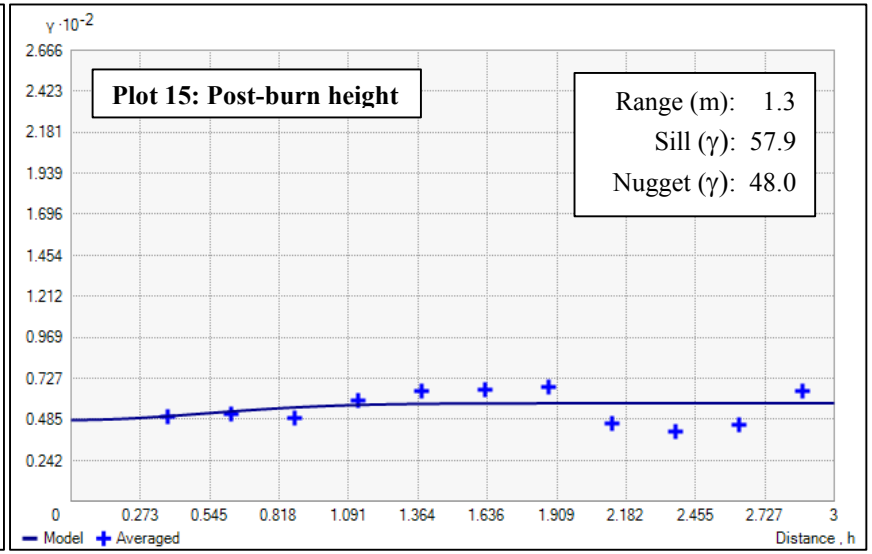
γ ·10-2
2.666
2.423
2.181
1.939
1.696
1.454
1.212
0.969
0.727
0.485
0.242
0
0.273
0.545
0.818
1.091
1.364
1.636
1.909
2.182
2.455
2.727
3
Plot 15: Post-burn height
Range (m): 1.3
Sill (γ): 57.9
Nugget (γ): 48.0
Model
Averaged
Distance , h

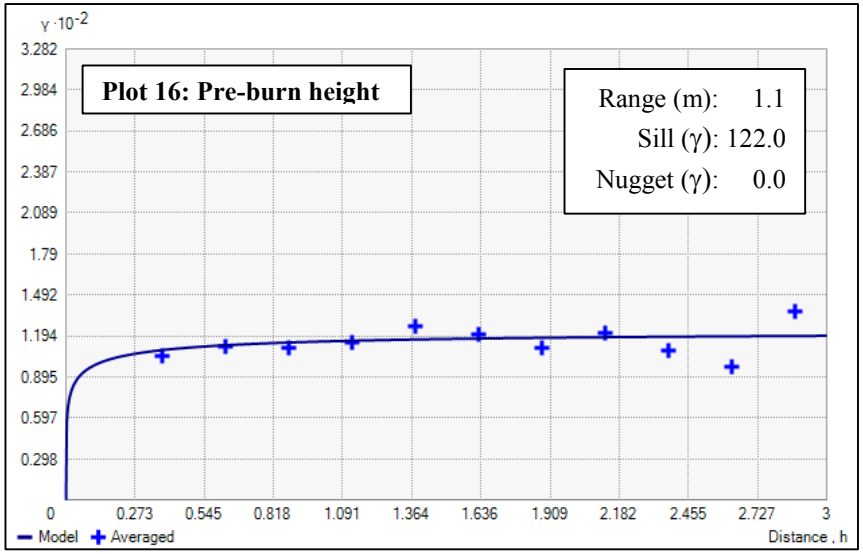
γ ·10-2
3.282
2.984
2.686
2.387
2.089
1.79
1.492
1.194
0.895
0.597
0.298
0
0.273
0.545
0.818
1.091
1.364
1.636
1.909
2.182
2.455
2.727
3
Plot 16: Pre-burn height
Range (m): 1.1
Sill (γ): 122.0
Nugget (γ): 0.0
Model
Averaged
Distance , h

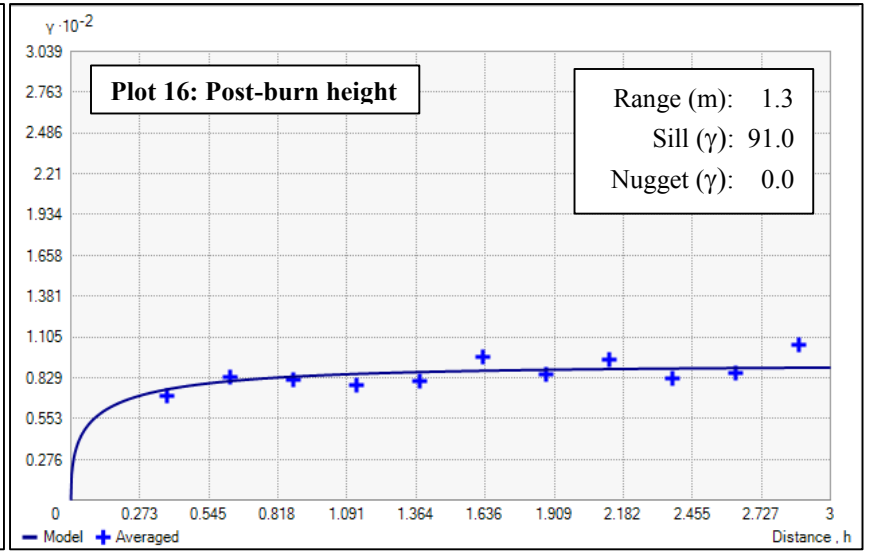
γ ·10-2
3.039
2.763
2.486
2.21
1.934
1.658
1.381
1.105
0.829
0.553
0.276
0
0.273
0.545
0.818
1.091
1.364
1.636
1.909
2.182
2.455
2.727
3
Plot 16: Post-burn height
Range (m): 1.3
Sill (γ): 91.0
Nugget (γ): 0.0
Model
Averaged
Distance , h

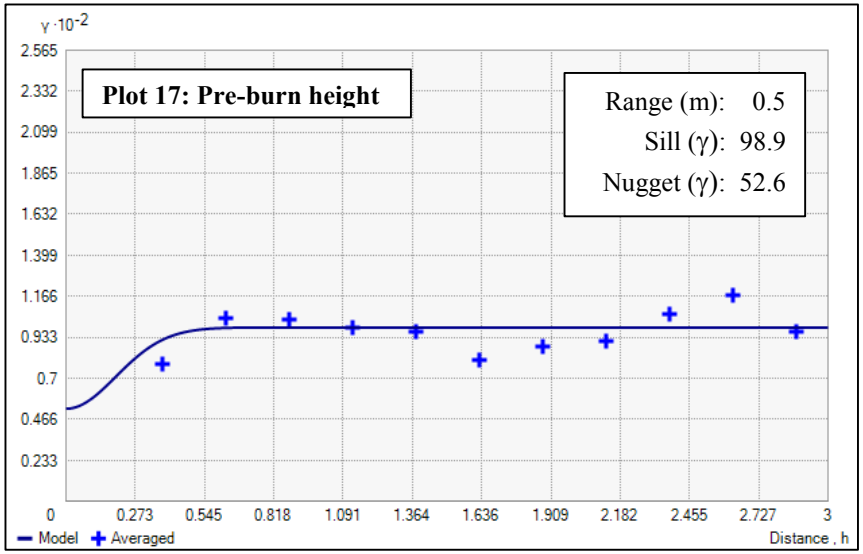
γ ·10-2
2.565
2.332
2.099
1.865
1.632
1.399
1.166
0.933
0.7
0.466
0.233
0
0.273
0.545
0.818
1.091
1.364
1.636
1.909
2.182
2.455
2.727
3
Model
Averaged
Distance , h
Plot 17: Pre-burn height
Range (m): 0.5
Sill (γ): 98.9
Nugget (γ): 52.6

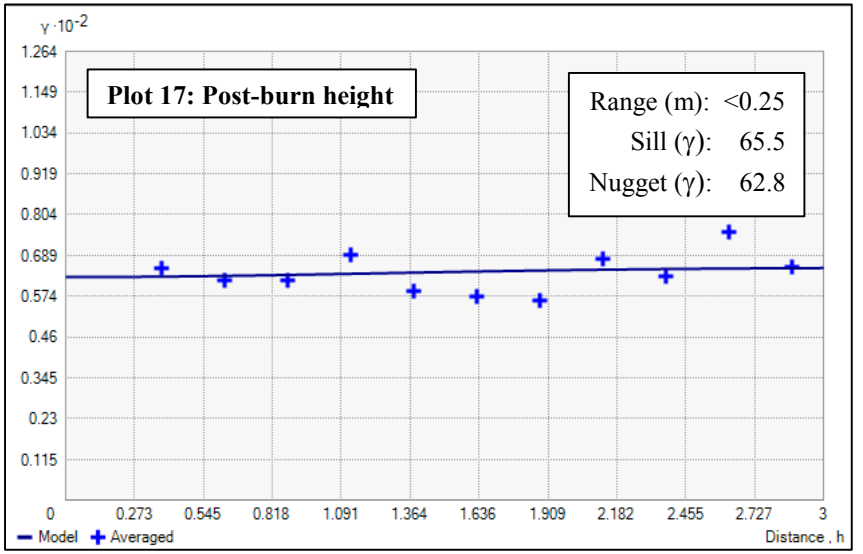
γ ·10-2
1.264
1.149
1.034
0.919
0.804
0.689
0.574
0.46
0.345
0.23
0.115
0
0.273
0.545
0.818
1.091
1.364
1.636
1.909
2.182
2.455
2.727
3
Model
Averaged
Distance , h
Plot 17: Post-burn height
Range (m): <0.25
Sill (γ): 65.5
Nugget (γ): 62.8

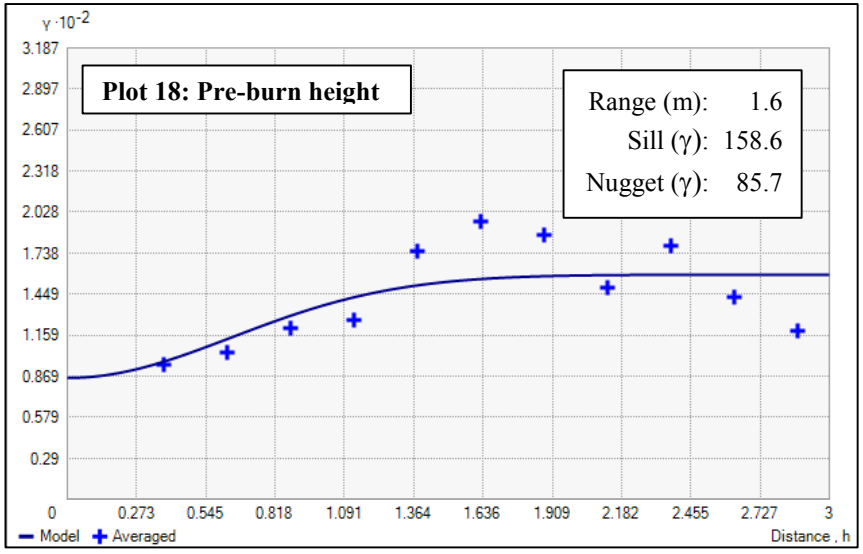
γ ·10-2
3.187
2.897
2.607
2.318
2.028
1.738
1.449
1.159
0.869
0.579
0.29
0
0.273
0.545
0.818
1.091
1.364
1.636
1.909
2.182
2.455
2.727
3
Model
Averaged
Distance , h
Plot 18: Pre-burn height
Range (m): 1.6
Sill (γ): 158.6
Nugget (γ): 85.7

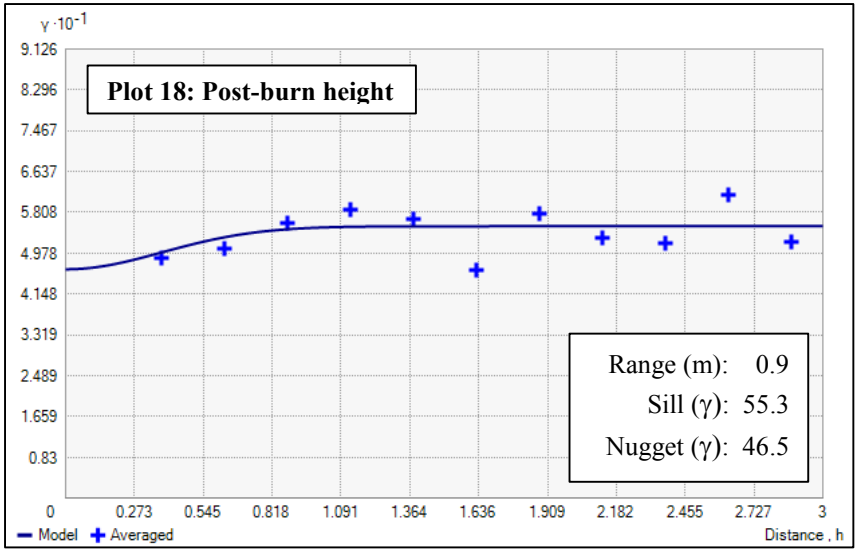
γ ·10-1
9.126
8.296
7.467
6.637
5.808
4.978
4.148
3.319
2.489
1.659
0.83
0
0.273
0.545
0.818
1.091
1.364
1.636
1.909
2.182
2.455
2.727
3
Model
Averaged
Distance , h
Plot 18: Post-burn height
Range (m): 0.9
Sill (γ): 55.3
Nugget (γ): 46.5

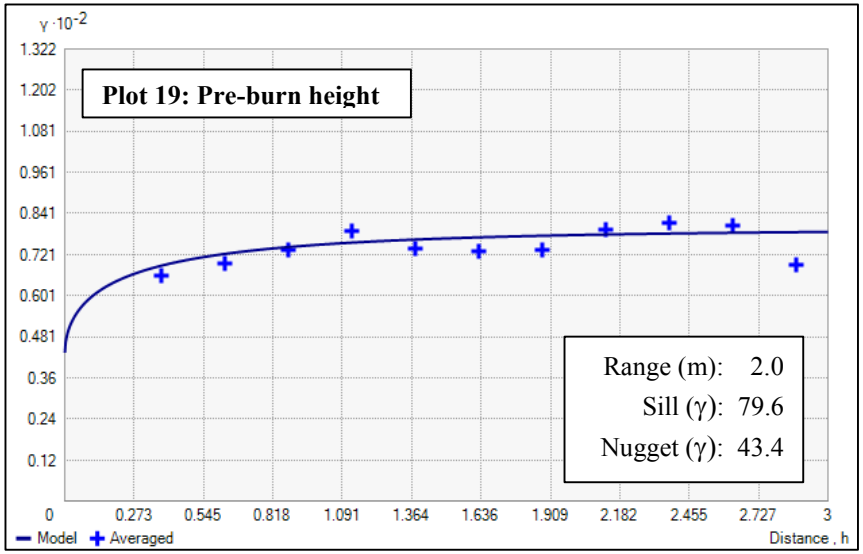
γ ·10-2
1.322
1.202
1.081
0.961
0.841
0.721
0.601
0.481
0.36
0.24
0.12
0
0.273
0.545
0.818
1.091
1.364
1.636
1.909
2.182
2.455
2.727
3
Model
Averaged
Distance , h
Plot 19: Pre-burn height
Range (m): 2.0
Sill (γ): 79.6
Nugget (γ): 43.4

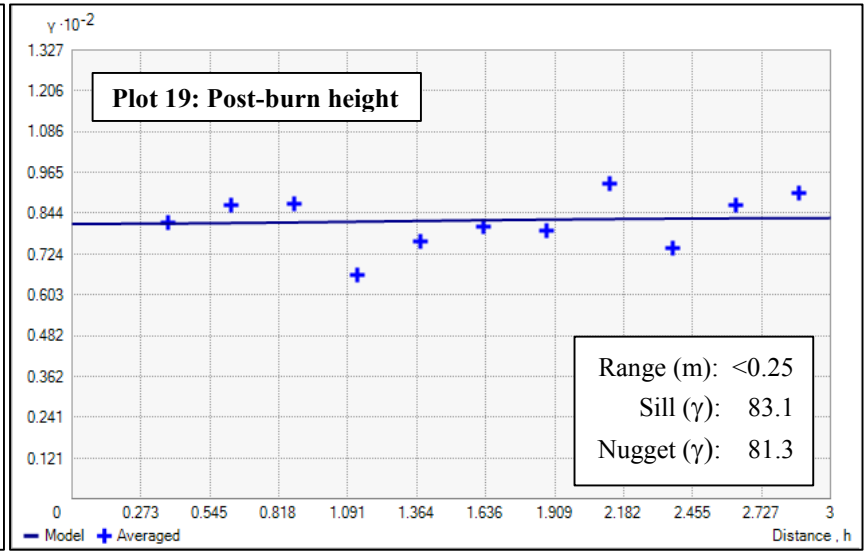
γ ·10-2
1.327
1.206
1.086
0.965
0.844
0.724
0.603
0.482
0.362
0.241
0.121
0
0.273
0.545
0.818
1.091
1.364
1.636
1.909
2.182
2.455
2.727
3
Model
Averaged
Distance , h
Plot 19: Post-burn height
Range (m): <0.25
Sill (γ): 83.1
Nugget (γ): 81.3

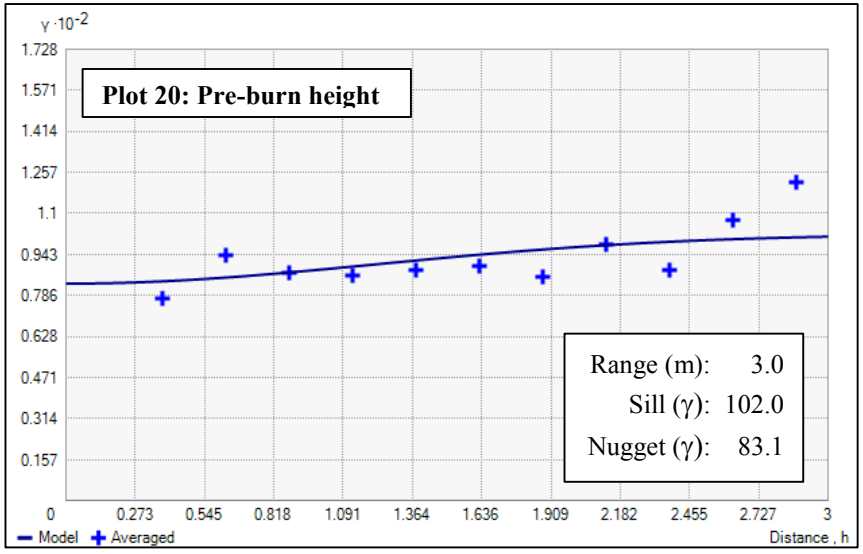
γ ·10-2
1.728
1.571
1.414
1.257
1.1
0.943
0.786
0.628
0.471
0.314
0.157
0
0.273
0.545
0.818
1.091
1.364
1.636
1.909
2.182
2.455
2.727
3
Model
Averaged
Distance , h
Plot 20: Pre-burn height
Range (m): 3.0
Sill (γ): 102.0
Nugget (γ): 83.1

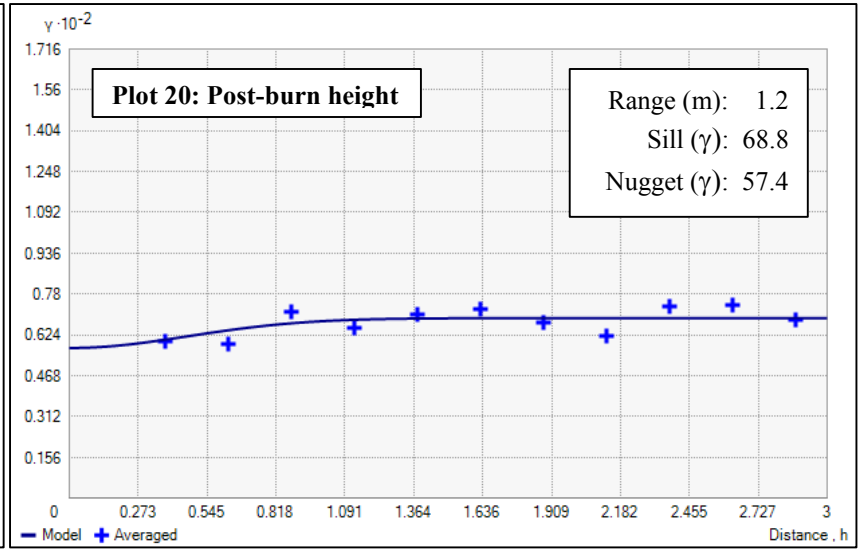
γ ·10-2
1.716
1.56
1.404
1.248
1.092
0.936
0.78
0.624
0.468
0.312
0.156
0
0.273
0.545
0.818
1.091
1.364
1.636
1.909
2.182
2.455
2.727
3
Model
Averaged
Distance , h
Plot 20: Post-burn height
Range (m): 1.2
Sill (γ): 68.8
Nugget (γ): 57.4

## Appendix J: Semivariogram curves for bare or open ground analysis

Semivariance (γ) plotted against spatial lag (h)

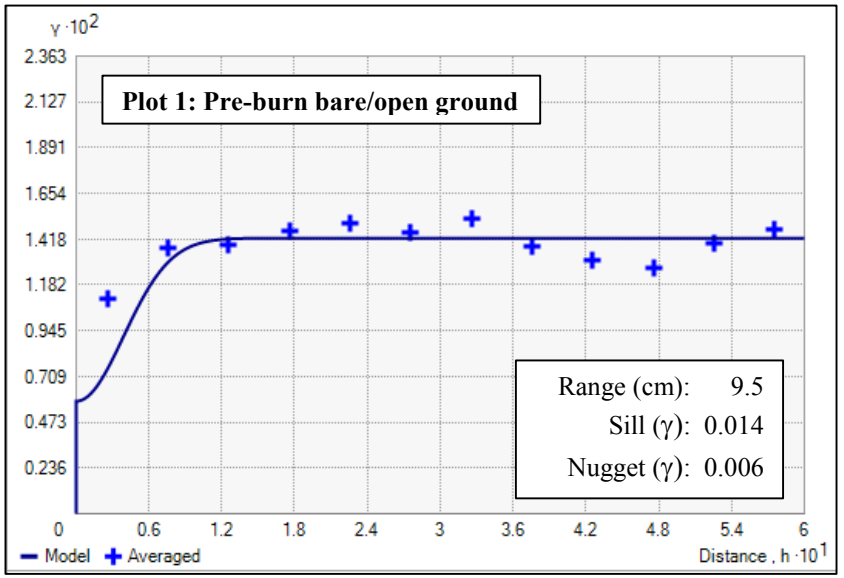


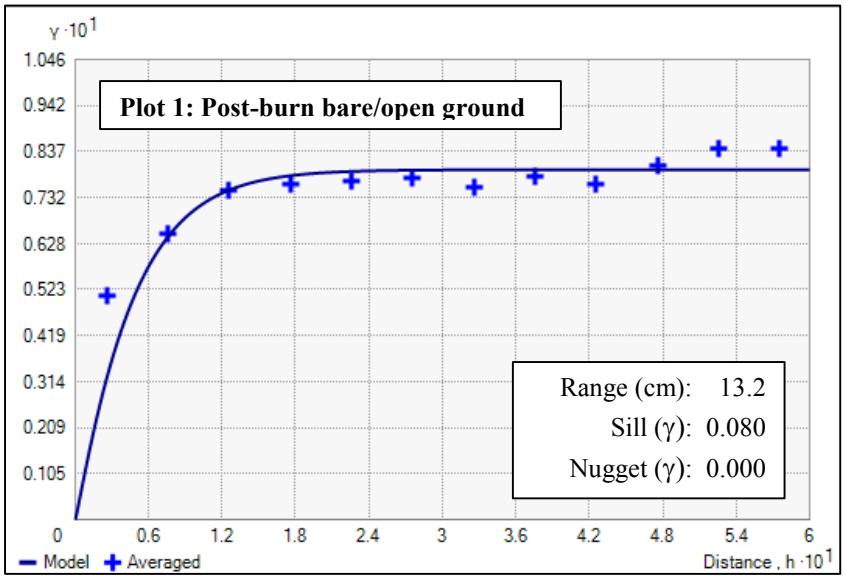


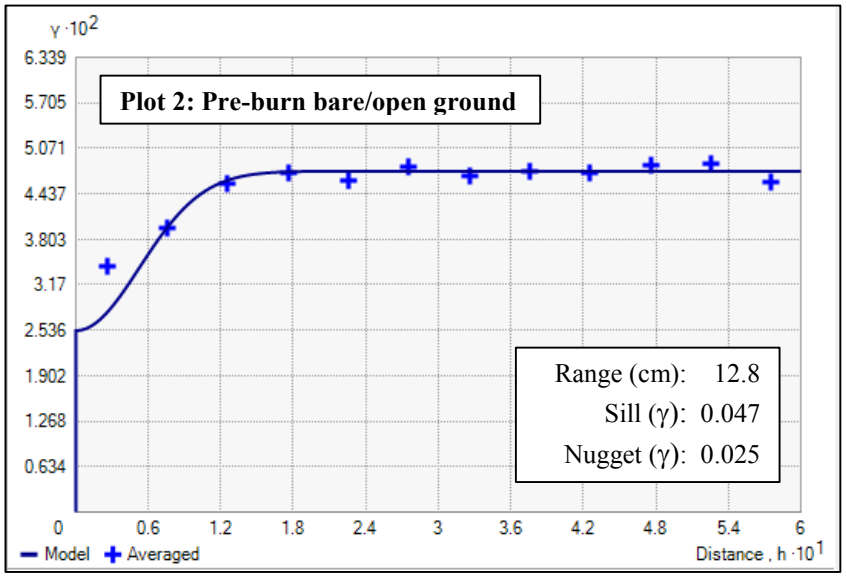


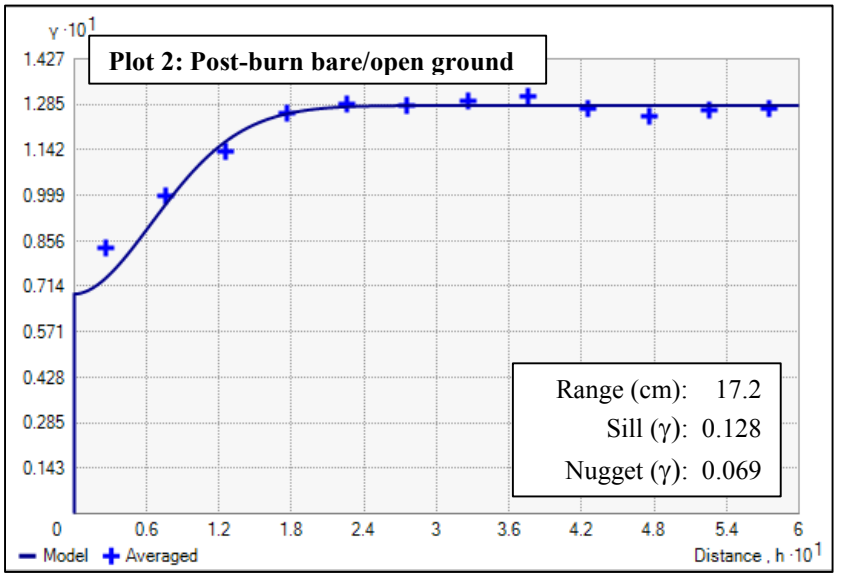

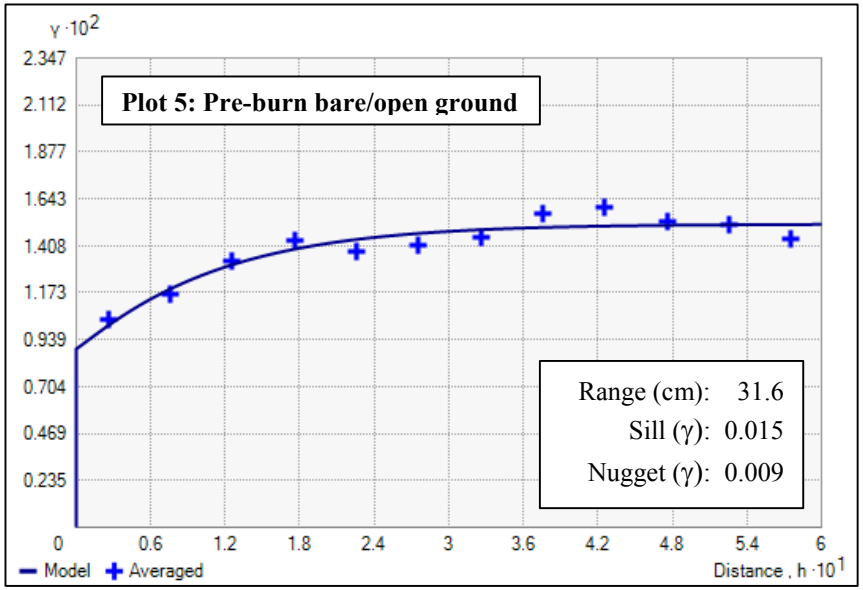
γ ·10^2
2.347
2.112
1.877
1.643
1.408
1.173
0.939
0.704
0.469
0.235
Plot 5: Pre-burn bare/open ground
Range (cm): 31.6
Sill (γ): 0.015
Nugget (γ): 0.009
0
0.6
1.2
1.8
2.4
3
3.6
4.2
4.8
5.4
6
Model
Averaged
Distance , h ·10^1

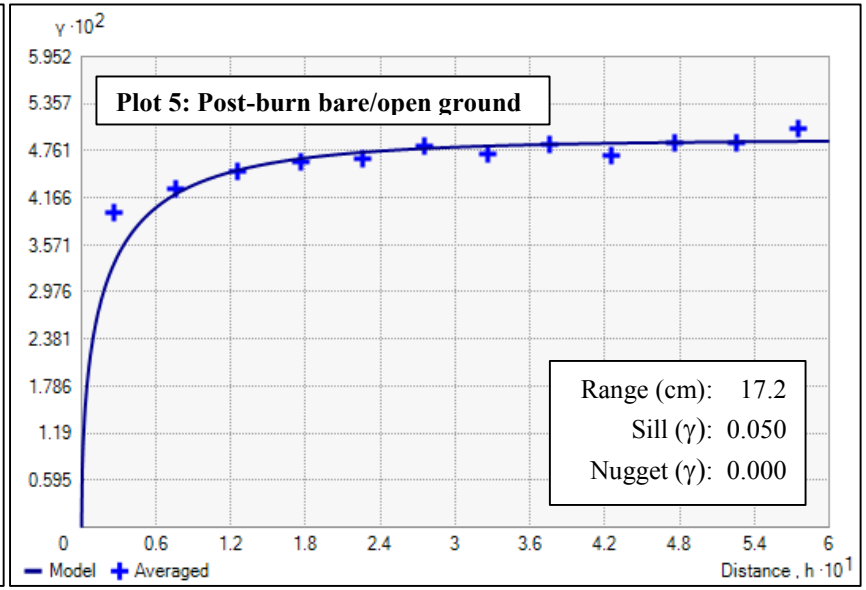
γ ·10^2
5.952
5.357
4.761
4.166
3.571
2.976
2.381
1.786
1.19
0.595
Plot 5: Post-burn bare/open ground
Range (cm): 17.2
Sill (γ): 0.050
Nugget (γ): 0.000
0
0.6
1.2
1.8
2.4
3
3.6
4.2
4.8
5.4
6
Model
Averaged
Distance , h ·10^1

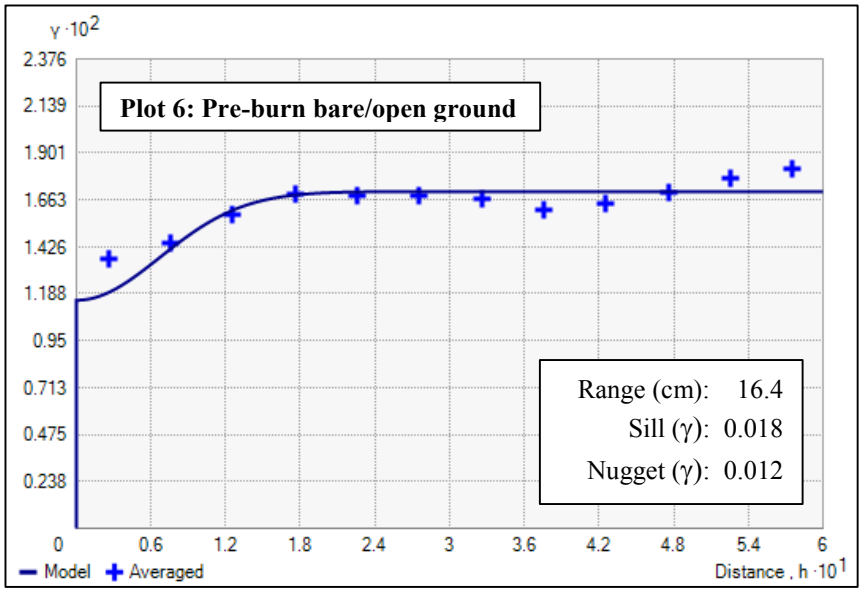
γ ·10^2
2.376
2.139
1.901
1.663
1.426
1.188
0.95
0.713
0.475
0.238
Plot 6: Pre-burn bare/open ground
Range (cm): 16.4
Sill (γ): 0.018
Nugget (γ): 0.012
0
0.6
1.2
1.8
2.4
3
3.6
4.2
4.8
5.4
6
Model
Averaged
Distance , h ·10^1

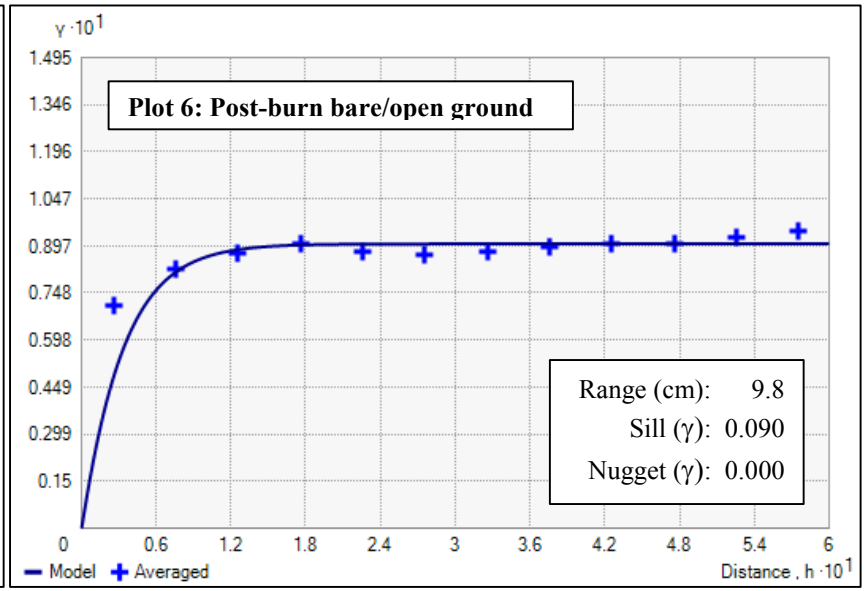
γ ·10^1
1.495
1.346
1.196
1.047
0.897
0.748
0.598
0.449
0.299
0.15
Plot 6: Post-burn bare/open ground
Range (cm): 9.8
Sill (γ): 0.090
Nugget (γ): 0.000
0
0.6
1.2
1.8
2.4
3
3.6
4.2
4.8
5.4
6
Model
Averaged
Distance , h ·10^1

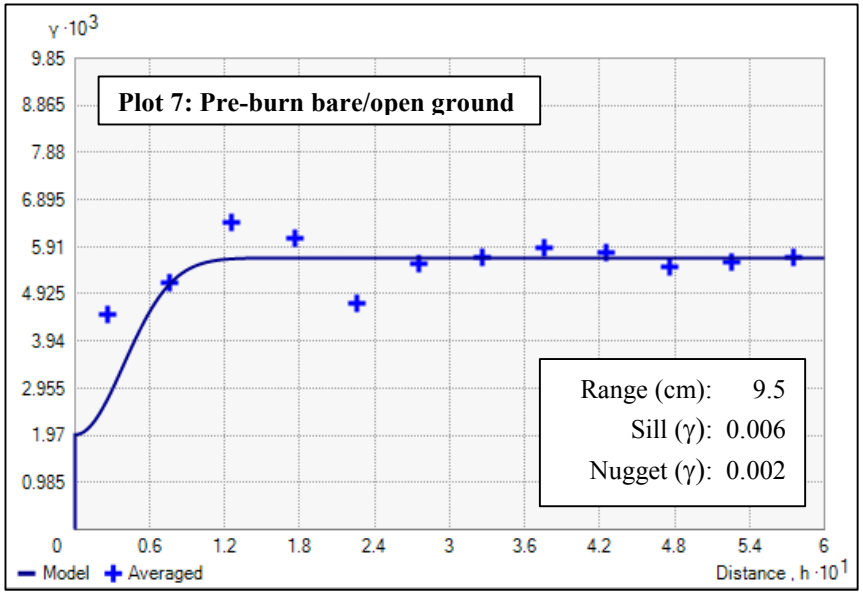
γ ·10^3
9.85
8.865
7.88
6.895
5.91
4.925
3.94
2.955
1.97
0.985
0
0.6
1.2
1.8
2.4
3
3.6
4.2
4.8
5.4
6
Plot 7: Pre-burn bare/open ground
Range (cm): 9.5
Sill (γ): 0.006
Nugget (γ): 0.002
Model
Averaged
Distance , h ·10^1

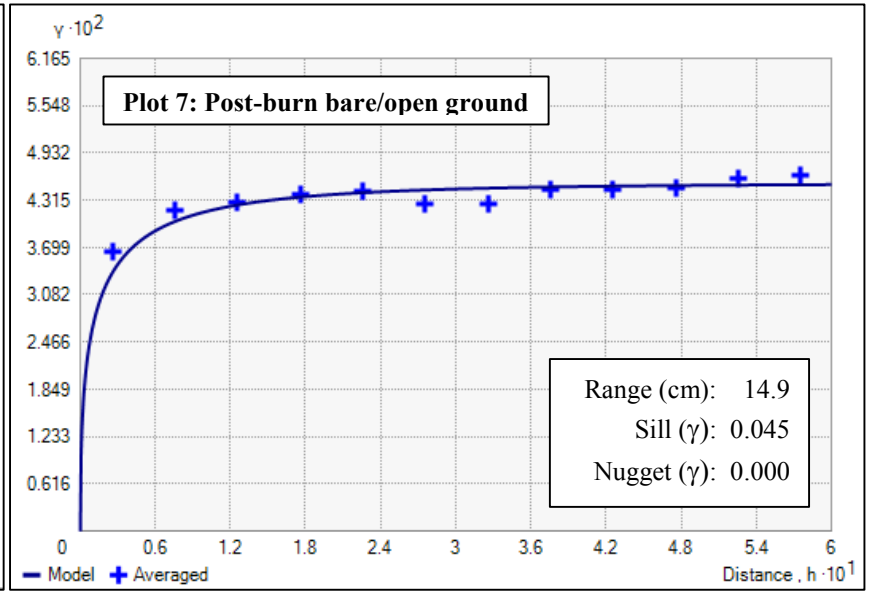
γ ·10^2
6.165
5.548
4.932
4.315
3.699
3.082
2.466
1.849
1.233
0.616
0
0.6
1.2
1.8
2.4
3
3.6
4.2
4.8
5.4
6
Plot 7: Post-burn bare/open ground
Range (cm): 14.9
Sill (γ): 0.045
Nugget (γ): 0.000
Model
Averaged
Distance , h ·10^1

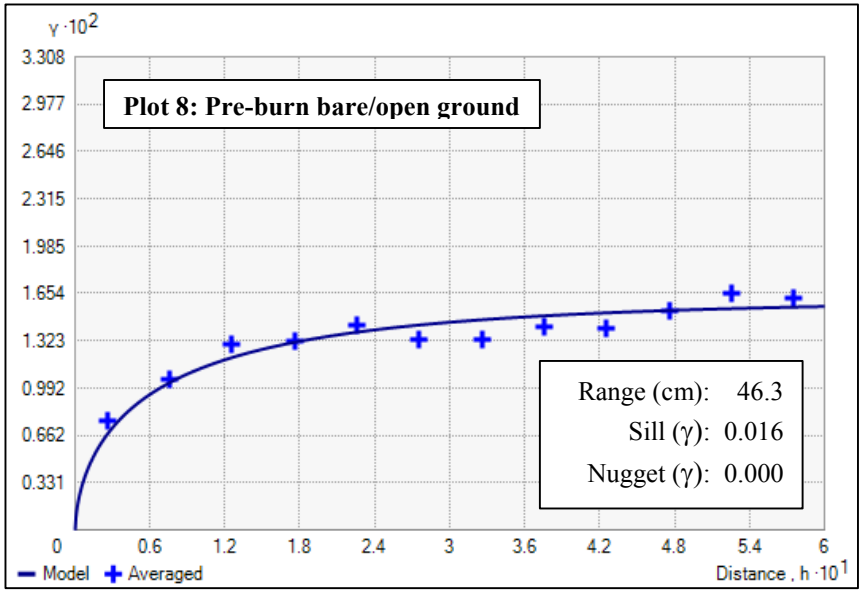
γ ·10^2
3.308
2.977
2.646
2.315
1.985
1.654
1.323
0.992
0.662
0.331
0
0.6
1.2
1.8
2.4
3
3.6
4.2
4.8
5.4
6
Plot 8: Pre-burn bare/open ground
Range (cm): 46.3
Sill (γ): 0.016
Nugget (γ): 0.000
Model
Averaged
Distance , h ·10^1

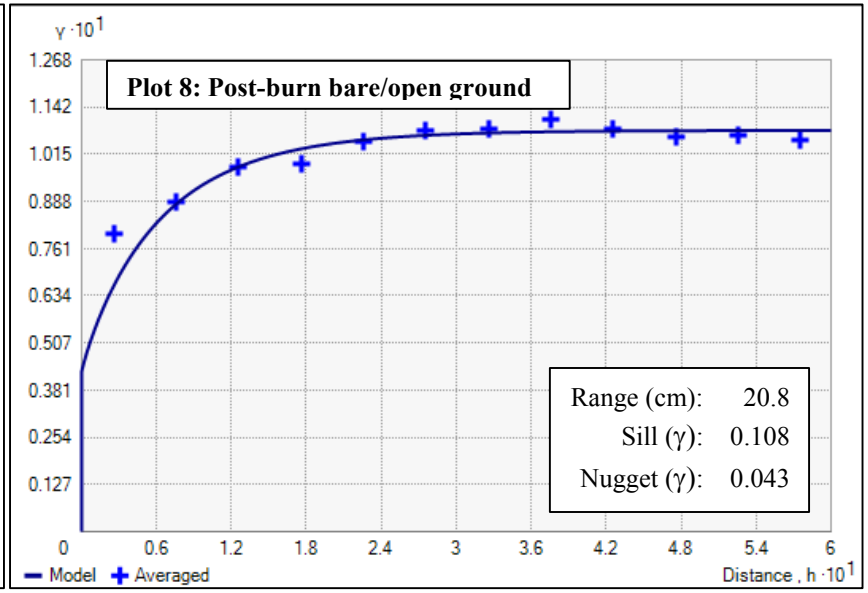
γ ·10^1
1.268
1.142
1.015
0.888
0.761
0.634
0.507
0.381
0.254
0.127
0
0.6
1.2
1.8
2.4
3
3.6
4.2
4.8
5.4
6
Plot 8: Post-burn bare/open ground
Range (cm): 20.8
Sill (γ): 0.108
Nugget (γ): 0.043
Model
Averaged
Distance , h ·10^1

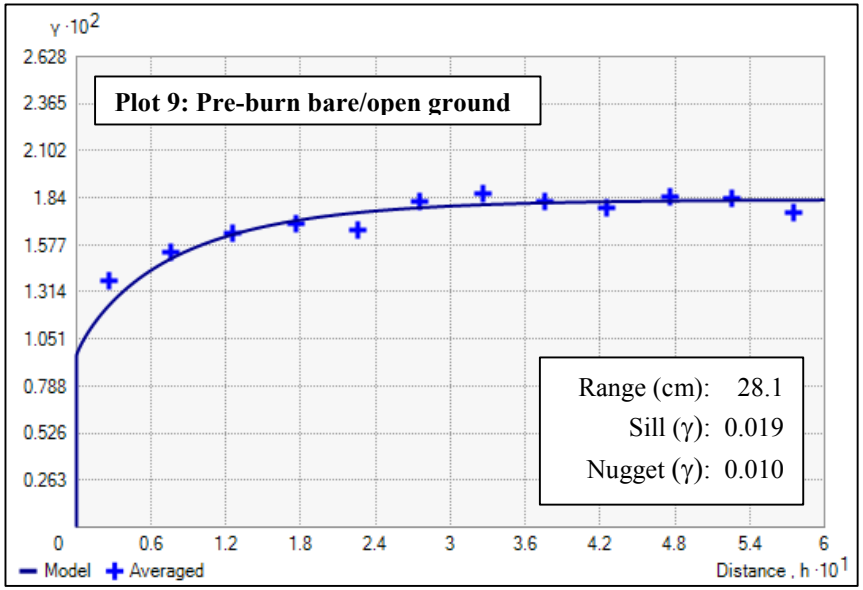
γ ·10^2
2.628
2.365
2.102
1.84
1.577
1.314
1.051
0.788
0.526
0.263
0
0.6
1.2
1.8
2.4
3
3.6
4.2
4.8
5.4
6
Plot 9: Pre-burn bare/open ground
Range (cm): 28.1
Sill (γ): 0.019
Nugget (γ): 0.010
Model
Averaged
Distance , h ·10^1

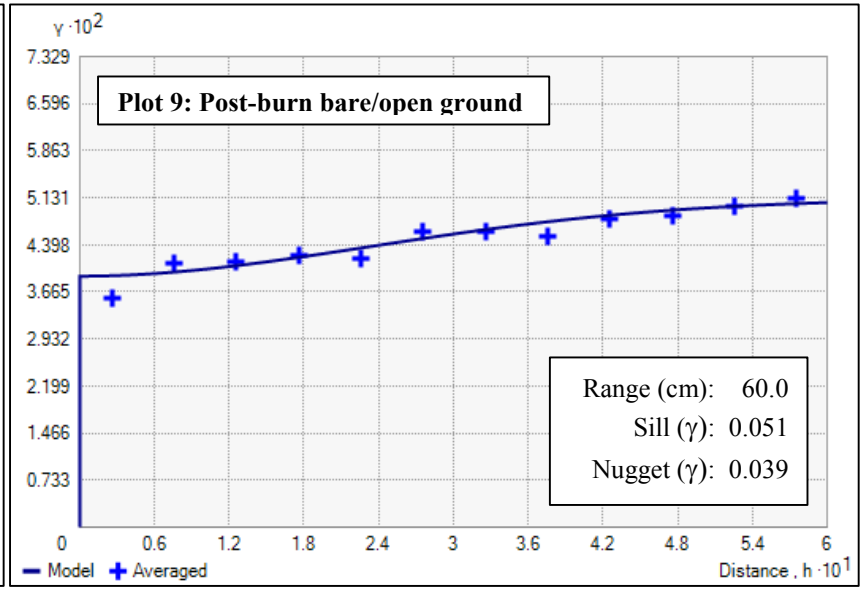
γ ·10^2
7.329
6.596
5.863
5.131
4.398
3.665
2.932
2.199
1.466
0.733
0
0.6
1.2
1.8
2.4
3
3.6
4.2
4.8
5.4
6
Plot 9: Post-burn bare/open ground
Range (cm): 60.0
Sill (γ): 0.051
Nugget (γ): 0.039
Model
Averaged
Distance , h ·10^1

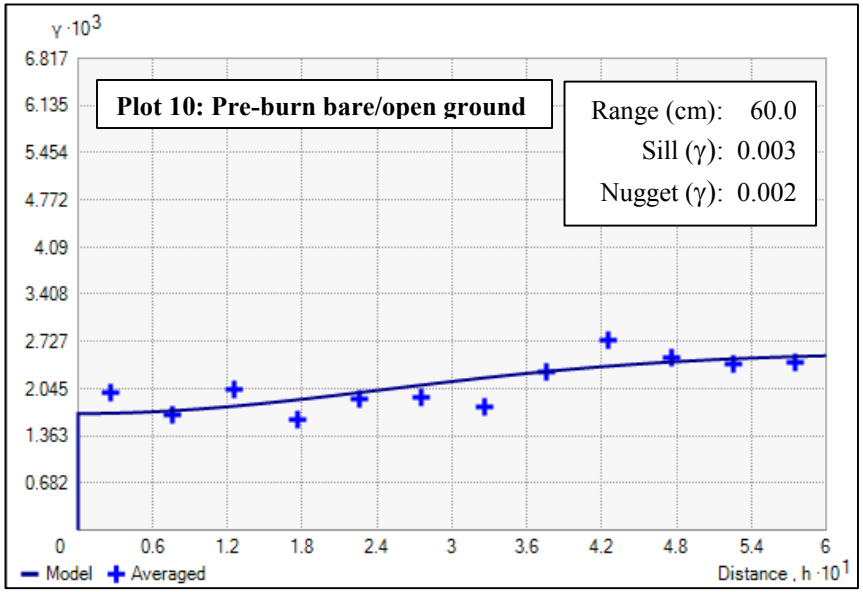
γ ·10^3
6.817
6.135
5.454
4.772
4.09
3.408
2.727
2.045
1.363
0.682
0
0.6
1.2
1.8
2.4
3
3.6
4.2
4.8
5.4
6
Plot 10: Pre-burn bare/open ground
Range (cm): 60.0
Sill (γ): 0.003
Nugget (γ): 0.002
Model
Averaged
Distance , h ·10^1

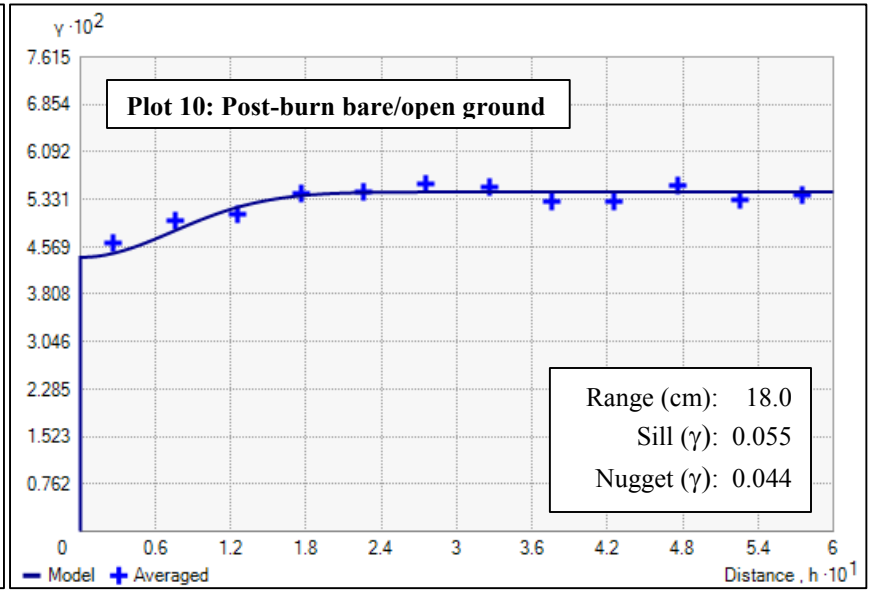
γ ·10^2
7.615
6.854
6.092
5.331
4.569
3.808
3.046
2.285
1.523
0.762
0
0.6
1.2
1.8
2.4
3
3.6
4.2
4.8
5.4
6
Plot 10: Post-burn bare/open ground
Range (cm): 18.0
Sill (γ): 0.055
Nugget (γ): 0.044
Model
Averaged
Distance , h ·10^1

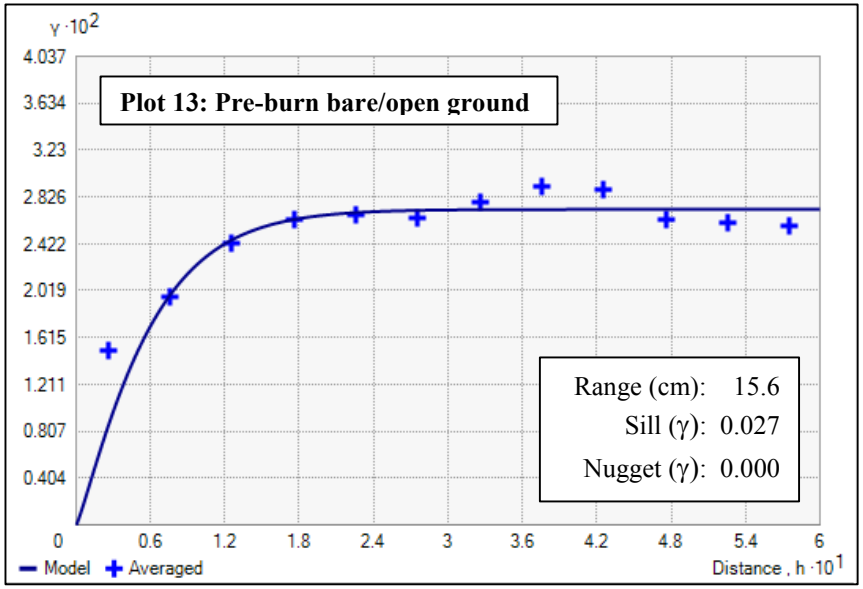
γ ·10^2
4.037
3.634
3.23
2.826
2.422
2.019
1.615
1.211
0.807
0.404
Plot 13: Pre-burn bare/open ground
Range (cm): 15.6
Sill (γ): 0.027
Nugget (γ): 0.000
0
0.6
1.2
1.8
2.4
3
3.6
4.2
4.8
5.4
6
Model
Averaged
Distance , h ·10^1

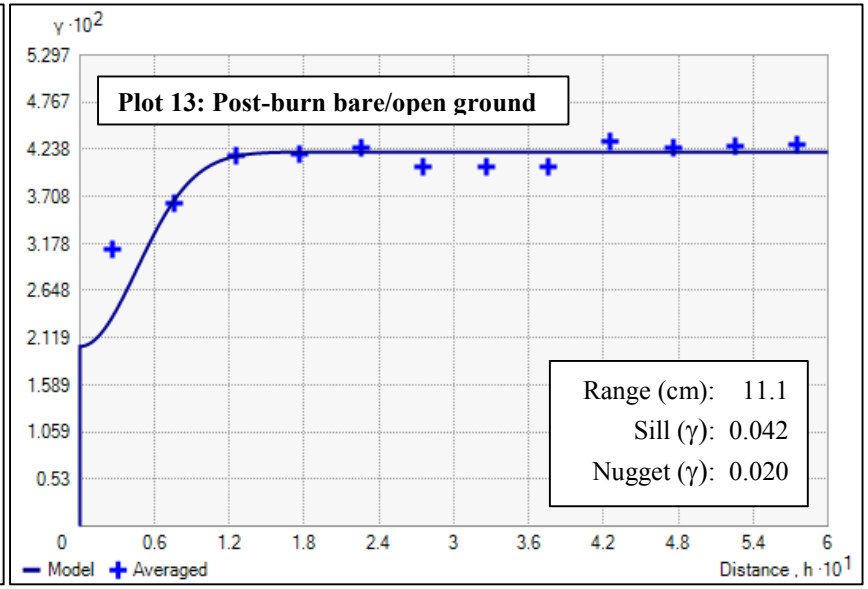
γ ·10^2
5.297
4.767
4.238
3.708
3.178
2.648
2.119
1.589
1.059
0.53
Plot 13: Post-burn bare/open ground
Range (cm): 11.1
Sill (γ): 0.042
Nugget (γ): 0.020
0
0.6
1.2
1.8
2.4
3
3.6
4.2
4.8
5.4
6
Model
Averaged
Distance , h ·10^1

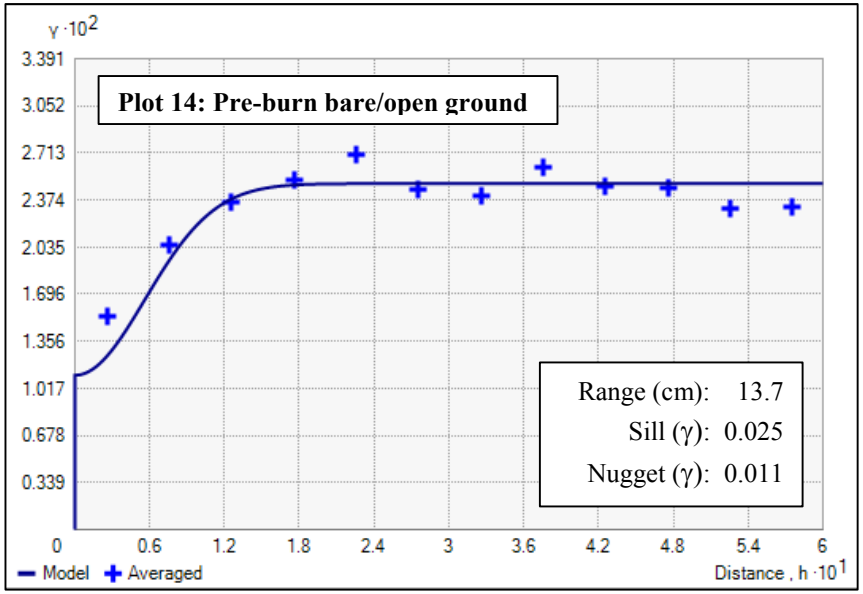
γ ·10^2
3.391
3.052
2.713
2.374
2.035
1.696
1.356
1.017
0.678
0.339
Plot 14: Pre-burn bare/open ground
Range (cm): 13.7
Sill (γ): 0.025
Nugget (γ): 0.011
0
0.6
1.2
1.8
2.4
3
3.6
4.2
4.8
5.4
6
Model
Averaged
Distance , h ·10^1

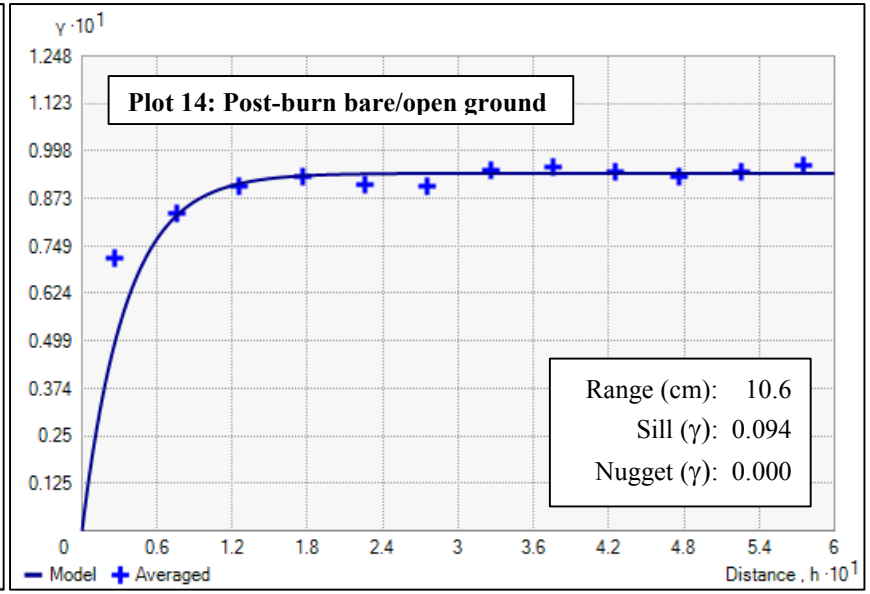
γ ·10^1
1.248
1.123
0.998
0.873
0.749
0.624
0.499
0.374
0.25
0.125
Plot 14: Post-burn bare/open ground
Range (cm): 10.6
Sill (γ): 0.094
Nugget (γ): 0.000
0
0.6
1.2
1.8
2.4
3
3.6
4.2
4.8
5.4
6
Model
Averaged
Distance , h ·10^1

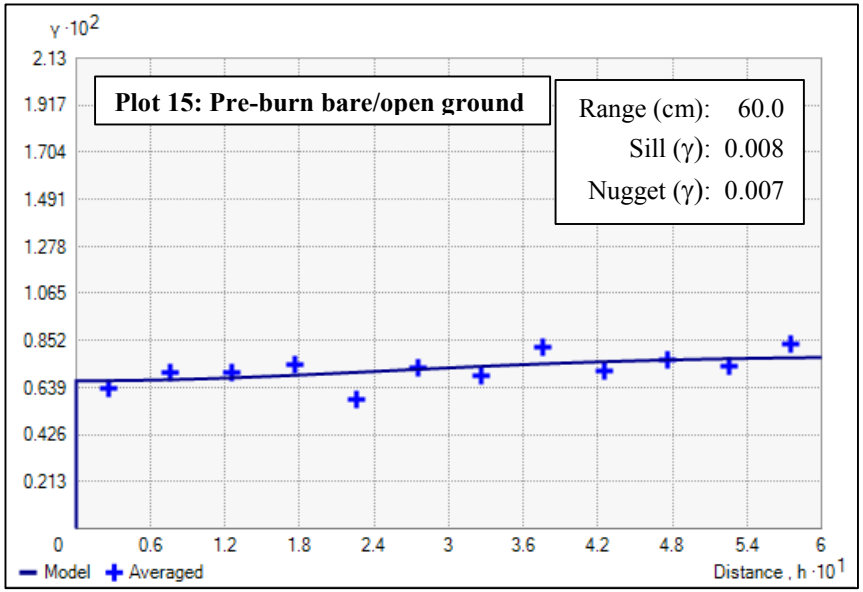
γ ·10^2
2.13
1.917
1.704
1.491
1.278
1.065
0.852
0.639
0.426
0.213
0
0.6
1.2
1.8
2.4
3
3.6
4.2
4.8
5.4
6
Model
Averaged
Distance , h ·10^1
Plot 15: Pre-burn bare/open ground
Range (cm): 60.0
Sill (γ): 0.008
Nugget (γ): 0.007

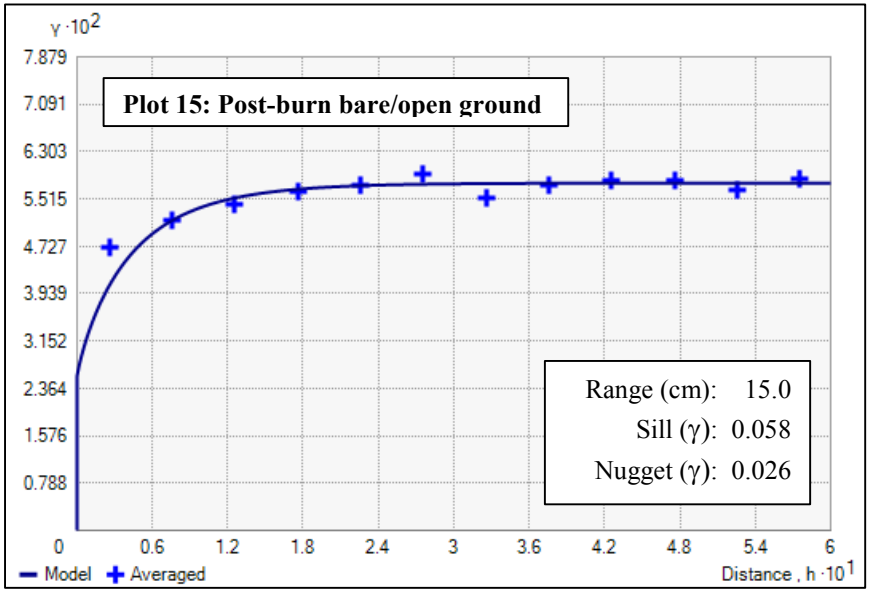
γ ·10^2
7.879
7.091
6.303
5.515
4.727
3.939
3.152
2.364
1.576
0.788
0
0.6
1.2
1.8
2.4
3
3.6
4.2
4.8
5.4
6
Model
Averaged
Distance , h ·10^1
Plot 15: Post-burn bare/open ground
Range (cm): 15.0
Sill (γ): 0.058
Nugget (γ): 0.026

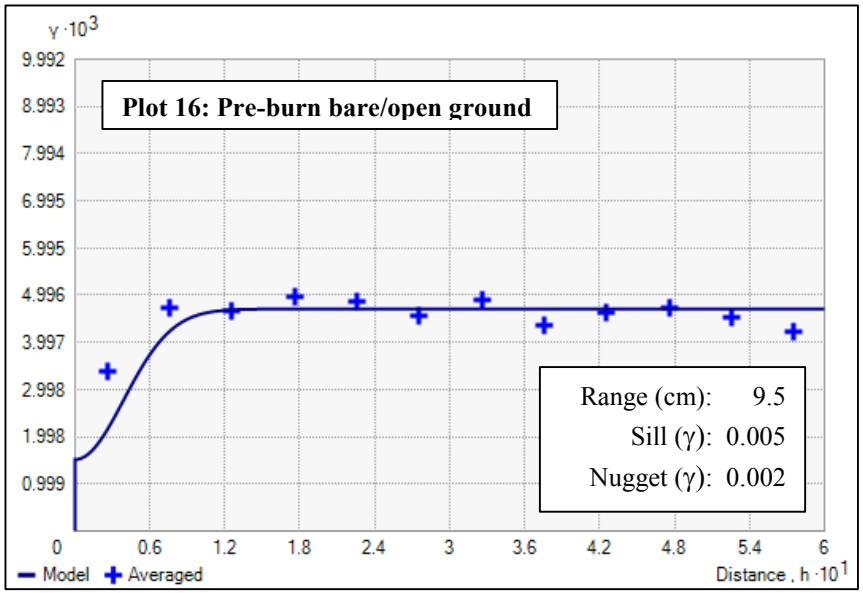
γ ·10^3
9.992
8.993
7.994
6.995
5.995
4.996
3.997
2.998
1.998
0.999
0
0.6
1.2
1.8
2.4
3
3.6
4.2
4.8
5.4
6
Model
Averaged
Distance , h ·10^1
Plot 16: Pre-burn bare/open ground
Range (cm): 9.5
Sill (γ): 0.005
Nugget (γ): 0.002

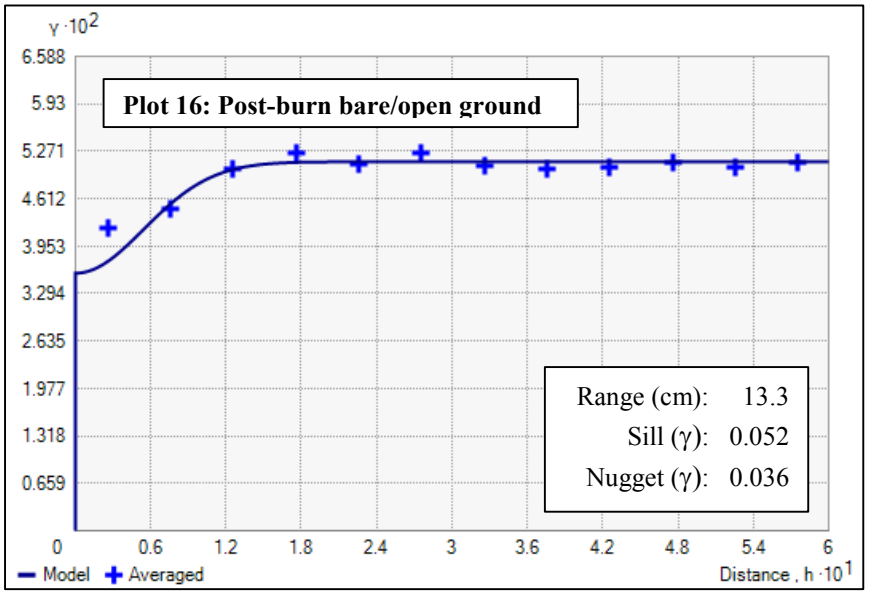
γ ·10^2
6.588
5.93
5.271
4.612
3.953
3.294
2.635
1.977
1.318
0.659
0
0.6
1.2
1.8
2.4
3
3.6
4.2
4.8
5.4
6
Model
Averaged
Distance , h ·10^1
Plot 16: Post-burn bare/open ground
Range (cm): 13.3
Sill (γ): 0.052
Nugget (γ): 0.036

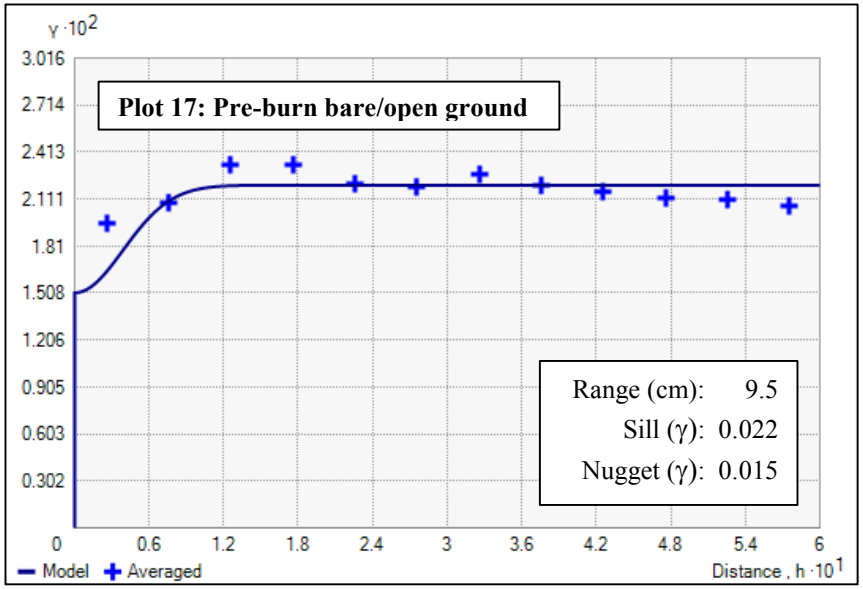
γ ·10^2
3.016
2.714
2.413
2.111
1.81
1.508
1.206
0.905
0.603
0.302
Plot 17: Pre-burn bare/open ground
Range (cm): 9.5
Sill (γ): 0.022
Nugget (γ): 0.015
0
0.6
1.2
1.8
2.4
3
3.6
4.2
4.8
5.4
6
Model
Averaged
Distance , h ·10^1

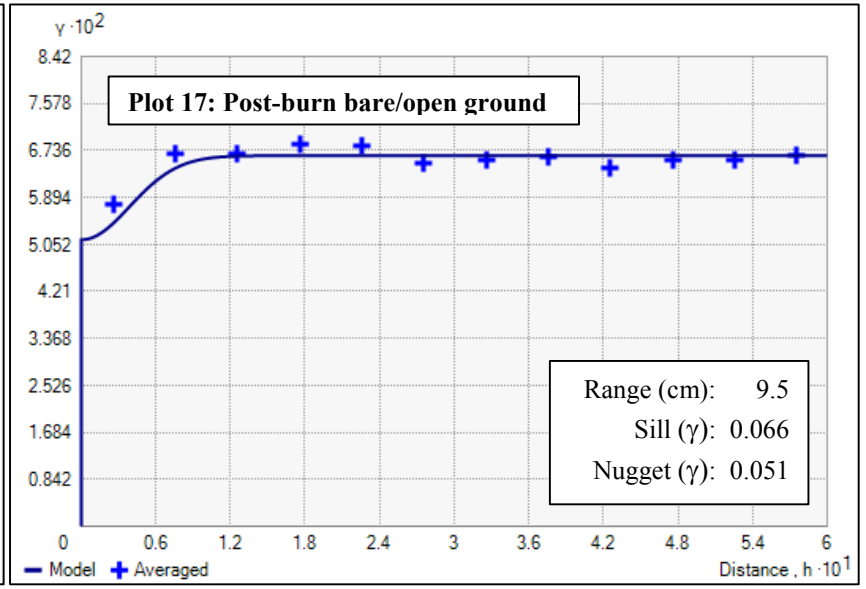
γ ·10^2
8.42
7.578
6.736
5.894
5.052
4.21
3.368
2.526
1.684
0.842
Plot 17: Post-burn bare/open ground
Range (cm): 9.5
Sill (γ): 0.066
Nugget (γ): 0.051
0
0.6
1.2
1.8
2.4
3
3.6
4.2
4.8
5.4
6
Model
Averaged
Distance , h ·10^1

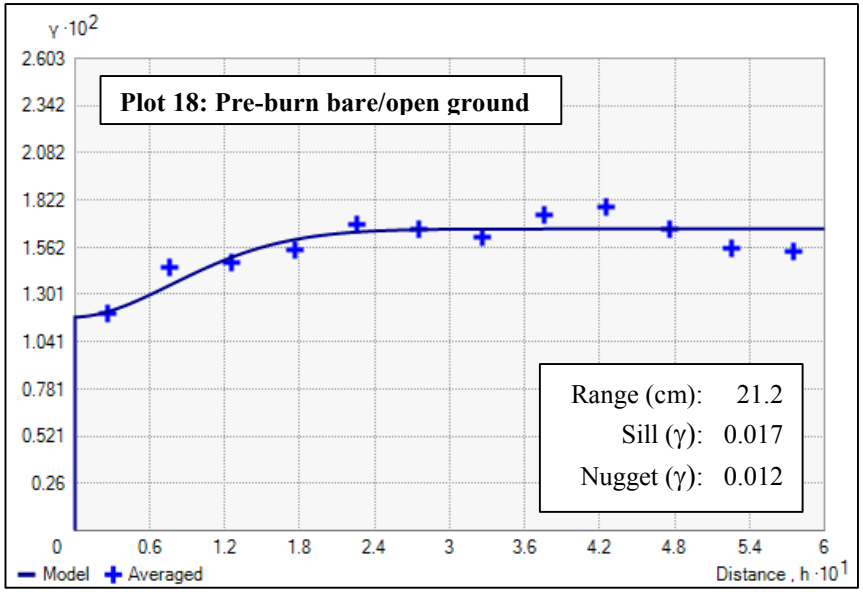
γ ·10^2
2.603
2.342
2.082
1.822
1.562
1.301
1.041
0.781
0.521
0.26
Plot 18: Pre-burn bare/open ground
Range (cm): 21.2
Sill (γ): 0.017
Nugget (γ): 0.012
0
0.6
1.2
1.8
2.4
3
3.6
4.2
4.8
5.4
6
Model
Averaged
Distance , h ·10^1

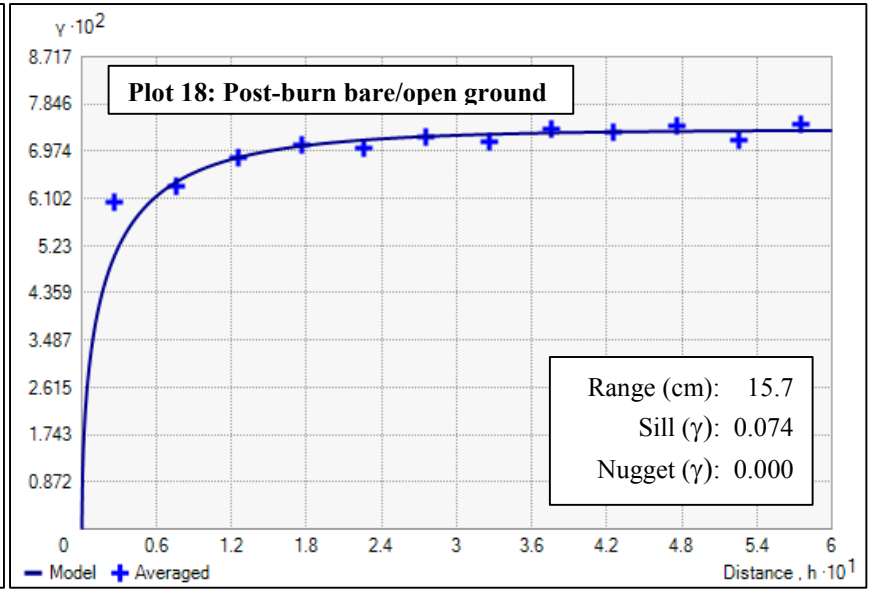
γ ·10^2
8.717
7.846
6.974
6.102
5.23
4.359
3.487
2.615
1.743
0.872
Plot 18: Post-burn bare/open ground
Range (cm): 15.7
Sill (γ): 0.074
Nugget (γ): 0.000
0
0.6
1.2
1.8
2.4
3
3.6
4.2
4.8
5.4
6
Model
Averaged
Distance , h ·10^1

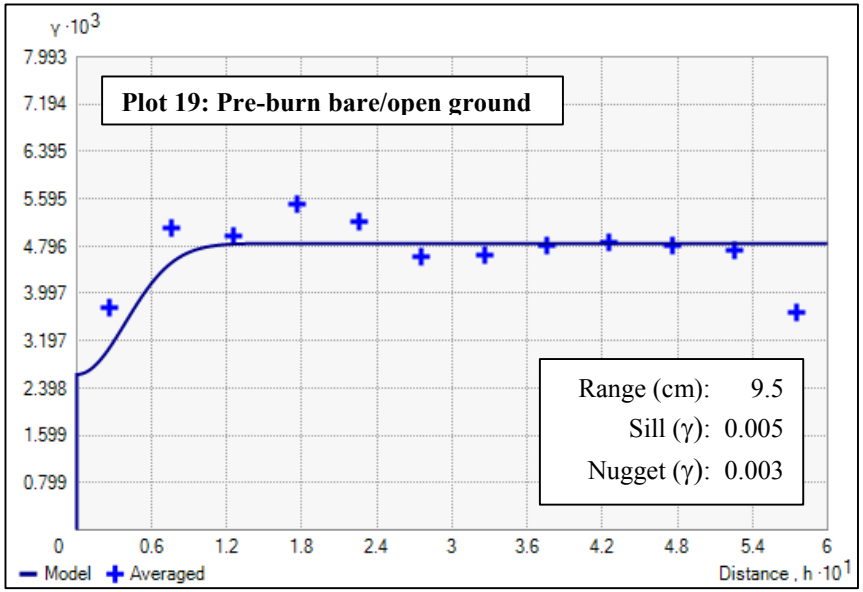
γ ·10^3
7.993
7.194
6.395
5.595
4.796
3.997
3.197
2.398
1.599
0.799
0
0.6
1.2
1.8
2.4
3
3.6
4.2
4.8
5.4
6
Model
Averaged
Distance , h ·10^1
Plot 19: Pre-burn bare/open ground
Range (cm): 9.5
Sill (γ): 0.005
Nugget (γ): 0.003

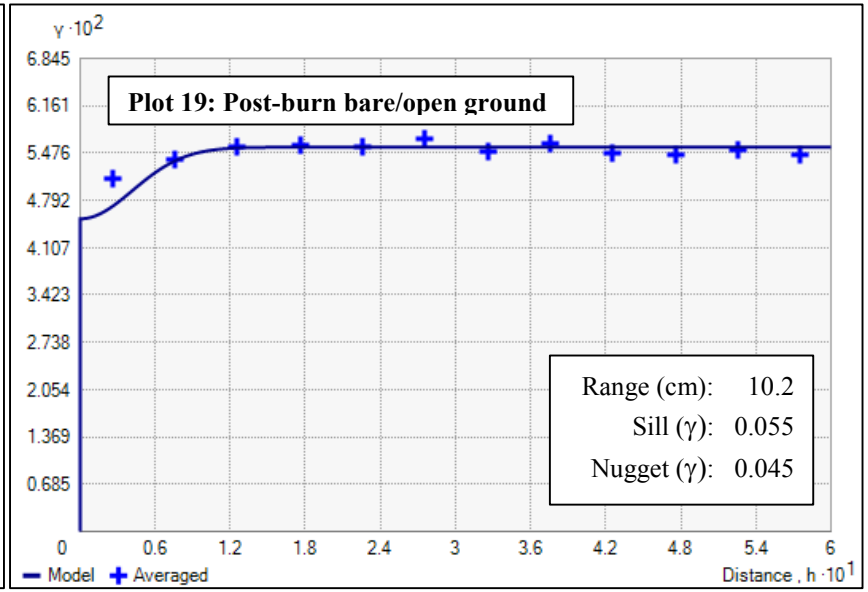
γ ·10^2
6.845
6.161
5.476
4.792
4.107
3.423
2.738
2.054
1.369
0.685
0
0.6
1.2
1.8
2.4
3
3.6
4.2
4.8
5.4
6
Model
Averaged
Distance , h ·10^1
Plot 19: Post-burn bare/open ground
Range (cm): 10.2
Sill (γ): 0.055
Nugget (γ): 0.045

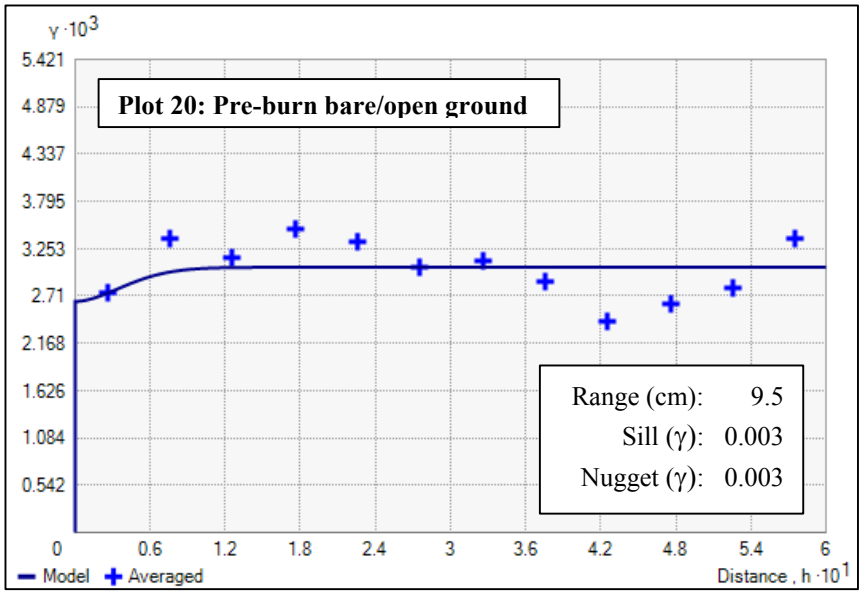
γ ·10^3
5.421
4.879
4.337
3.795
3.253
2.71
2.168
1.626
1.084
0.542
0
0.6
1.2
1.8
2.4
3
3.6
4.2
4.8
5.4
6
Model
Averaged
Distance , h ·10^1
Plot 20: Pre-burn bare/open ground
Range (cm): 9.5
Sill (γ): 0.003
Nugget (γ): 0.003

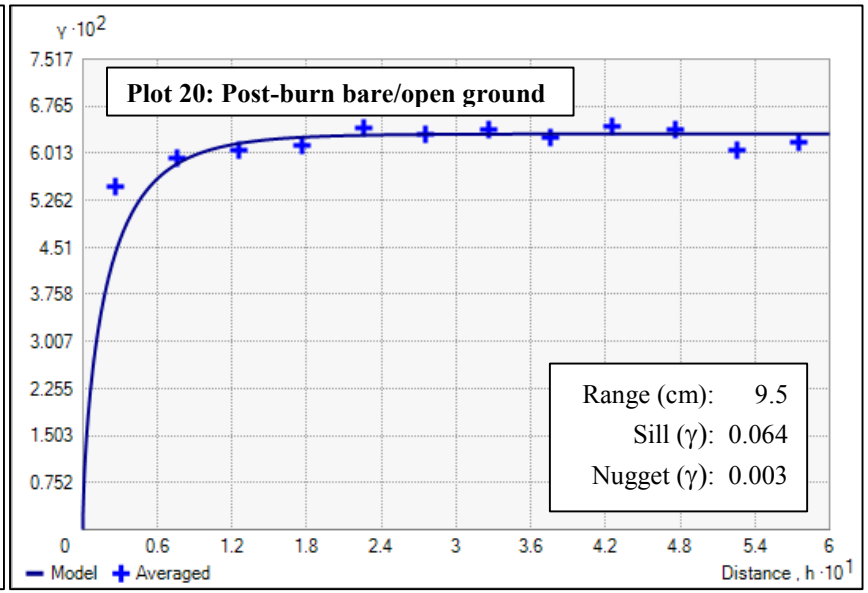
γ ·10^2
7.517
6.765
6.013
5.262
4.51
3.758
3.007
2.255
1.503
0.752
0
0.6
1.2
1.8
2.4
3
3.6
4.2
4.8
5.4
6
Model
Averaged
Distance , h ·10^1
Plot 20: Post-burn bare/open ground
Range (cm): 9.5
Sill (γ): 0.064
Nugget (γ): 0.003